LIGNIN FOR BIOENERGY & BIOMATERIALS

A Dissertation
Presented to
The Academic Faculty

By

Tyrone Wells, Jr.

In Partial Fulfillment
of the Requirements for the Degree
Doctor of Philosophy in the
School of Chemistry and Biochemistry

Georgia Institute of Technology

May 2015

LIGNIN FOR BIOENERGY & BIOMATERIALS

Approved by:

Dr. Arthur J. Ragauskas, Advisor
School of Chemistry and
Biochemistry
Georgia Institute of Technology

Dr. Julia Kubanek
School of Chemistry and
Biochemistry
Georgia Institute of Technology

Dr. Andreas S. Bommarius
School of Chemical and
Biomolecular Engineering
Georgia Institute of Technology

Dr. Lawrence A. Bottomley
School of Chemistry and
Biochemistry
Georgia Institute of Technology

Dr. Yulin Deng
School of Chemical and
Biomolecular Engineering
Georgia Institute of Technology

Dr. Preet Singh
School of Materials Science and
Engineering
Georgia Institute of Technology

Approved March 27th, 2015

ACKNOWLEDGEMENTS

This thesis is more than just a culmination of a nearly 25-year-long academic and personal journey, it's a celebration. This was a long road. But it was also brightly marked with an array of growing moments that punctuated periods of bleak self-doubt. Only by learning to *humble myself through education*, *recognizing my weaknesses and limitations*, and most importantly, *developing into a person who could effectively seek help from others* did I find the means to push myself and my boundaries. And so, I would like to thank those who helped me reach the end of this journey, who helped me find strength through their support, and who guided me onto the brilliant trajectory that I find myself on today.

Firstly, I would like to express my utmost appreciation for the guidance of Dr. Arthur J. Ragauskas. Thanks to his mentorship and standard of excellence, I have grown beyond all measures during my academic career at Georgia Tech. His straightforward and supportive demeanor and insightful teaching philosophy gave me the chance to grow ever more stronger and independent. Moreover, I would like to thank my Swedish advisor Dr. Hans Theliander for his many courtesies and thoughtful insights while hosting me during my research at Chalmers Institute of Technology.

I give thanks to my esteemed research colleagues who each taught me many valuable collaborative and interpersonal skills that continue to aid me in my endeavors: Qining Sun, Xianxhi Meng, Jonas Wetterling, Susanne Bylin, Kerstin

Most importantly, I owe my highest acknowledgements to my mother, Esther Joy Wells, who always had the utmost unshakable confidence in me, which provided me with much needed the strength to succeed during my hardest moments. Also, I give my thanks to my sister, La Vida. We're a small family, but we support each other without fail.

TABLE OF CONTENTS

LIST OF TABLES

LIST OF FIGURES

Page

LIST OF SYMBOLS AND ABBREVATIONS

β-KAP	β-ketoadipate pathway
1,2,4BTO	1,2,4-benzenetriol dioxygenase
2,6H1,2O	2,6-dichrlorhydroquinone 1,2-dioxygenase
4HSD	*cis,trans*-4-hydroxymucnoic semialdehyde dehydrogenase
4HBA	4-hydroxybenzoic acid
6H1,2O	6-Chlorohydroxquinol 1,2-dioxygenase
AAG3P	acyl-ACP:glycerol-3-phosphate acyltransferase
Ac	acetyl
ACC	acetyl-CoA carboxylase
Ac-CoA	acetyl coenzyme A
ACP	acyl carrier protein
AG3PAT	Acyl-CoA-1-acyl-glycerol-3-phosphate acyltransferase
Ara	arabinose
ASL	acid soluble lignin
BE	β-etherase
BQR	*para*-benzoquinone reductase
C1,2O	catechol 1,2-dioxygenase
CAT	catechol
CAD	Cα-dehydrogenase
CBP	consolidated bioprocessing
CMD	carboxymuconate decarboxylase
CMLE	carboxymuconate lactonizing enzyme
conc.	concentration
CP/MAS	cross polarization/magic angle spinning
CNWs	cellulose nanowhiskers
DA	diterpenoic acid
DAG	diacylglycerol
DAME	diterpenoic acid methyl ester

DCD	2,5-dichloro-2,5-cyclohexadiene-1,4-diol dehydrogenase
DGAT	diacylglycerol acyl-transferase
DH	dehydratase
DHC	dehydrochlorinase
DI	deionized (water)
DP	degree of polymerization
DTG	derivative thermogravimetric
ELH	enol lactone hydrolase
EPA	Environmental Protection Agency
EOL	ethanol organosolv lignin
EOP	ethanol organosolv pretreatment
ER	enoyl reductase
FA	fatty acid
FAME	fatty acid methyl ester
FAS	fatty acid synthase
G	guaiacyl monomer
G3PAT	glycerol-3-phosphate *O*-acyltransferase
Gal	galactose
GalA	galacturonic acid
GEN	gentisate
GK	glycerol kinase
Glc	glucose
GlcA	glucuronic acid
GPC	gel permeation chromatography
H	p-coumaryl lignin monomer
H1,2O	hydroquinone 1,2-dioxygenase
HAD	haloalkane dehalogenase
HAPL	*meta*-hydroxylaminophenol lyase
HPAE	high-performance anion-exchange
HPAEC	high-performance anion-exchange chromatography
HPLC	high performance liquid chromatography

HQD	tetrachlorohydroquinone dehalogenase
HSQC	heteronuclear single quantum coherence
HW	hardwood
KR	keto-reductase
KS	keto-synthase
LBL	Lignoboost lignin
LCC	lignin carbohydrate complex
Man	mannose
MAT	malonyl-CoA transacylase
MI	muconolactone isomerase
MLE	*cis, cis*-muconate lactonizing enzyme
MPT	malonyl-palmitoyl transacylase
Mn/M_n	number average molar mass distribution
Mw/M_w	weight average molar mass distribution
N4O	4-nitrocatechol 4-monooxygenase
OPH	organophosphate hydrolase
P3,4O	protocatechuate 3,4-dioxygenase
PAD	pulsed amperometric detection
PAP	phosphatidate phosphatase
PCA	protocatechuic acid
PCPO	PCP 4-monooxygenase
PD	polydispersity
PNP2O	*para*-nitrophenol 2-monooxygenase
PNP4O	*para*-nitrophenol 4-monooxygenase
ppm	Parts per million
PVA	polyvinyl acetate
QR	2-hydroxy-1,4-benzoquinone reductase
R. opacus	*Rhodococcus opacus*
RD	reductive dehalogenase
Rha	rhamnose
S	syringyl lignin monomer

SSF	simultaneous saccharification and fermentation
SW	softwood
SyrA	syringic acid
TAG	triacylglycerol
TCA	tri-carboxylic acid cycle
TCBQR	tetrachlorobenzoquinone reductase
TCPO	2,4,6-TCP monooxygenase
TG	thermogravimetric
TGA	Thermogravimetric analysis
TH	thiolase
TR	transferase
VanA	vanillic acid
VDH	vanillate dehydrogenase
VO	vanillate monooxygenase
WVO	waste vegetable oil

SUMMARY

Lignocellulosic (woody) biomass is a biorenewable, biodegradable, and highly abundant bioresource that has incredible potential to advance the development of green biofuels and biomaterials [41, 51, 104, 135]. Woody biomass is composed of three major organic constituents: cellulose, hemicellulose, and lignin. A detailed description of the chemical structure of these three constituents is provided in Chapter 1. In brief, cellulose and hemicellulose are two carbohydrate polymers while lignin is a complex and recalcitrant aromatic polymer [104, 136].In particular, cellulose and lignin are the most abundant of these three major lignocellulosic organic polymers, both in woody plant tissue as the terrestrial world [176]. The abundance, homogeneity, and structural properties of cellulose have made it a favorable bioresource for a variety of commercial applications such as the generation of pulp and paper-based products via the global pulp and paper industry [41, 44, 107, 117, 140, 145]. This industry specializes in biorefinery processes that may include *pretreatment*, *pulping* and *delignification* all of which are more detailed in Chapter 1 and assist in isolating cellulose from other constituents found in wood [44, 139, 145]. The kraft process is the most common industrial pulping process globally [40, 58, 182]. During kraft pulping, wood is impregnated with cooking liquor containing sulfide and hydroxide anions to principally cleave lignin-based aryl-ether linkages, resulting in the solubilization and separation of lignin fragments away from cellulose and the generation of black liquor as a byproduct[10, 106, 140, 146]. More than 50 million tons per year of lignin is industrially extracted from plant biomass by the global pulp and paper industry[117, 118]. Moreover, nearly 98% of kraft lignin solvated

in black liquor is subsequently burned within pulp mill recovery boilers in order to mediate chemical and energy costs [58, 161]. Alternatively, the capital costs associated with a recovery furnace and the desire by the pulping industry to obtain higher material yields have encouraged efforts to repurpose kraft lignin for higher utility applications, such as the generation of *bioenergy* and *biomaterials* [140, 182].

This dissertation provides a comprehensive perspective regarding the development of lignin for higher-value bioenergy and biomaterials. After a literature review provided in Chapter 2 and an experimental section supplied in Chapter 3, Chapter 4 entails the development of lignin for bioenergy while Chapters 5 and 6 discuss the optimization of lignin for biomaterials.

The *bioenergy study*, in brief, involves lignin that was sourced from an industrial waste stream and then fed to bacteria as a sole source of carbon and energy to produce microbial lipids composed of energy-rich triacylglycerols that were transesterified into fatty acid methyl esters as a fungible biodiesel. Bacterial cells accumulated a maximum of ~27% of their cellular dry weight in oils composed of oleic, palmitic, and stearic fatty acids. The results demonstrated that pretreatment waste effluent can be valorized and efficiently treated through use as a novel feedstock for microbial biofuel production. This study incorporated data interpretation from a multitude of analytical apparati to accurately determine rates of substrate depletion and to monitor the quality of bacterial growth. For example, this study describes the effective use and interpretation of UV-Visible spectroscopy (UV-Vis), gel permeation chromatography(GPC), and high pressure liquid chromatography (HPLC) data. Moreover, the proportions of fatty acids generated

during fermentation were characterized with gel chromatography-mass spectroscopy (GC/MS).

The *biomaterial study*, in brief, presents a novel lignin polymerization methodology towards the production of polymeric biomaterials. Kraft lignin has previously been demonstrated as a resource for the synthesis of high molecular weight (HMW) products such as adhesives, copolyester, and carbon fibers [25]. These applications favor the utilization of HMW lignin, and so efficient lignin polymerization strategies have gained interest [58, 94, 103, 161, 182]. Chapter 5 discusses the use of ultrasonics as a means to increase the DP of highly purified Kraft lignin. Treated samples were comprehensively analyzed with GPC, Fourier transfer infrared (FT-IR) spectroscopy, as well as ^{13}C- and ^{31}P-nuclear magnetic resonance (^{13}C- ^{31}P-NMR). In summary, ultrasonication was used to induce *cavitation*, which is a phenomenon that manifest during the rarefaction sequenced of an applied sonic wave in the form of micro-ruptures that rapidly collapse and release energy capable of forming free radicals in solution. The formation of free radicals was shown to enhance the environment for cross-coupling reactions to occur among neighboring oligomers of lignin. After 15 min of sustained cavitation, ultrasonicated lignin generated a HMW fraction (~35%) that had a weight-average molecular weight (M_w)over 450-fold greater than the initial kraft lignin sample. NMR analysis indicated that this highly-polymerized fraction was enriched with C5 condensed phenolic structures. In Chapter 6, the enhanced thermostability of sonic-treated kraft lignin precipitated from black liquor via the LignoBoost process was determined. Sonically polymerized and degraded samples exhibited improved thermal stability for temperatures as high as 500°C due to sonic-enabled enrichment of C5

condensed phenolic groups and the breakdown of aliphatic functional groups.

Conclusively, this work demonstrated an intriguing route for HMW and low molecular

weight (LMW) heat-stable biomaterials generation.

CHAPTER 1: INTRODUCTION

1.1   Green Chemistry

A major theme of the work presented here involves g*reen chemistry*, which refers

to the design of chemical products and processes that reduce or eradicate the generation

of hazardous substances. The term "green chemistry" was first used in 1991 by Paul

Anastas of the United States Environmental Protection Agency [8]. In this role, Anastas

coined the term to encapsulate a rising trend based on a philosophy of sustainable

engineering and chemical research. This philosophy outlined twelve major objectives for

improved industrial waste management, energy efficiency, and the development of

ecological products while minimizing detrimental environmental impacts [8]:

1. Prevention of Waste

   Processes should be designed to prevent the creation of waste as a more
   efficient alternative to treating, remediating, or cleaning waste after it has
   been generated.

2. Raw Material (Atom) Economy

   Synthetic methodologies should be designed to maximally incorporate all
   raw materials used in the process into the final product.

3. Less Toxic Chemical Syntheses

   Synthetic methodologies should be designed, wherever practical, to use
   and produce substances that are as minimally toxicity to humans and the
   environment as possible.

4. Development of Safer Chemicals

   Processes should be designed such that chemical products affect their intended function while minimizing their toxicity.

5. Efficient Use of Solvents and Auxiliary Substances

   Processes should be designed to implement as few auxiliary components (e.g. solvents, separation agents, etc.) as necessarily possible and environmentally harmless when used.

6. Improved Energy Efficiency

   Processes should be designed with consideration of their energy requirements and resulting environmental/economic impact. For example, synthetic methodologies should be performed as close as possible to ambient conditions as possible.

7. Use of Renewable Feedstock

   Processes should be designed to make use of renewable resources whenever technically and economically feasible.

8. Reduce Derivative Agents

   Processes should be designed to reduce superfluous derivative agents (e.g. blocking groups, protection/deprotection, etc.) in order to improve atom efficiency, reduce secondary auxiliary agents, and minimize waste.

9. Maximize Catalytic Reagents

   Processes should be designed to favor selective catalytic reagents over minimally selective catalytic reagents or stoichiometric reagents.

10. Design for Degradable Products

Synthetic methodologies should be designed such that generated products that complete their function degrade into innocuous components within a reasonable timeframe and do not persist in nature for extended durations or to the point of long-term progressive accumulation.

11. Accurate Real-Time and In-Process Monitoring for Pollution Prevention

    Analytical methodologies should be designed to provide detailed analysis and control of processes prior to the formation of hazardous components.

12. Design for Accident Prevention

    Processes should be designed to make use of substances, forms of a substance, containers holding the substance, and handling techniques that best minimize the potential for chemical accidents (e.g. spills/releases, explosions, and fires).

Over the past 30 years, green chemistry research has provided many advances in sustainable research. These benefits include solvent-less preparation techniques, advancements in the design of degradable polymers, and in-line process monitoring. Specific highlights include expanded use of hydrogen peroxide as a ecologically compatible oxidant, the development of biological insecticide Spinosad as a biologically compatible pesticide, and the energy-saving production of polyolefins polymers. A summarized timeline of green chemistry highlights in history is presented in Table 1.1.

Table 1.1. Timeline of green chemistry highlights

Year	Event
1962	Rachel Carson, environmental conversation icon, publishes *Silent Spring*, a work of

Table 1.1. Continued

	literature that directs public attention to the toxic and harmful environmental impact of pesticides (e.g. DDT). *Silent Spring* is recognized as one of the earliest and most popular cases for needed governmental environment protection [27].
1969	President Richard Nixon creates the Citizen's Advisory Committee on Environmental Quality (Executive order 11471, May 29th 1969). This was a cabinet-level council that directly informed the president on environmental matters related to science, industry, agriculture, conservation organizations, and local governments. Later that same year, Nixon appoints a committee to determine the groundwork for the development of an environmental protection agency [147].
1970	The Environmental Protection Agency (EPA) is formed [147]. (www.epa.gov)
1980	Rachael Carson is posthumously awarded the Presidential Medal of Freedom. Meanwhile, industrial waste management gradually shifts from end-of-pipeline remediation and treatment to pollution prevention strategies that can be implemented during processing (also known as *source reduction*). On the 11th of December, Congress enacts the Comprehensive Environmental Response, Compensation, and Liability Act (CERCLA), which taxed chemical and petroleum industries and authorized the federal government to directly respond to releases or potential releases of toxic substances that may endanger public health or the environment [14].
1985	CERCLA taxes collect $1.6 billion. Funds are sent to a trust fund for cleaning abandoned or unmanaged hazardous waste sites. Short and long-term removal projects are detailed in Chapter 2 [14].
1988	EPA establishes the Office of Pollution Prevention and Toxics [114].
1990	The Pollution Prevention Act is passed, enforcing ecologically compatible production of chemicals, optimized process operations, and better raw material. In addition, this act provided grants to states that adequately practiced source reduction [76].
1991	The term "green chemistry" is coined by Paul Anastas. The term quickly becomes a meme throughout environmentalism-based causes [7].
1993	EPA enacts the Green Chemistry Program that focuses on setting strict guidelines for optimizing processes and speeding adoption. United states joins the Chemical Weapons Convention (CWC). This convention aims to eliminate an entire class of weapons of mass destruction through the prohibition of developing, producing acquiring, stockpiling, retaining, transferring and use of chemical weapons by OPCW member states [39]. (http://www.opcw.org/chemical-weapons-convention/)

Table 1.1.   Continued

1995	President Bill Clinton establishes the Presidential Green Chemical Challenge Awards as a way to recognize and encourage greener industries involved with the manufacture and processing of chemicals.
1997	The Green Chemistry Institute is established [7]. (http://www.acs.org/content/acs/en/greenchemistry.html)
1998	"Twelve Principles of Green Chemistry" is published by Anastas [7].
1999	*Green Chemistry*, the monthly scientific journal begins publication (www.rsc.org/greenchem).
2000s	Research initiatives and policy advancements for green chemistry continue to develop and gain popularity (e.g. use of supercritical fluids, development of biodiesel oils from wasted plant oils, Spinosad insecticide, etc.) [6, 7].
2008	Governor Arnold Schwarzenegger signs the California Green Chemistry Initiative.
2009	President Barrack Obama nominates Paul Anastas as head of Research and Development for the EPA (http://www.brandeis.edu/now/2009/june/anastasnomination.html).

The tenets of green chemistry have and will continue to profoundly shape scientific progress. As for today, green chemistry can be applied to address challenges regarding the development of clean and sustainable energy as well as environmentally-friendly materials. These challenges stem from growing dependence and depletion of limited fossil fuel supplies, such as coal, natural gas and petroleum. For example, in 2010 the global demand for primary energy was projected to increase by ~30% before the year 2040 [183]. In addition to this, the high demand for petroleum-based products by third world countries continue to strain this unsustainable dependence [111, 144, 177]. Furthermore, the pollutants generated by these related industries are also a cause for concern [76, 114, 129, 150]. For example, the current rate of fossil fuel depletion can be correlated to rising average global temperature due to CO_2 emissions by as much as 105×10^{15} to 130×10^{15} per year [52]. It is therefore necessary to establish supplemental and

sustainable fuel platforms that better leverage limited supplies of fossil fuels and nonrenewable energy. Based on a green chemistry perspective, the use of environmentally benign and biorenewable resources as raw materials for energy and materials is more desirable than the implementation or combustion of limited nonrenewable compounds. Specifically, this condition refers to Objective #7 and also generally satisfies Objectives #3, #4, and #10 of the 12 tenets of green chemistry [8]. Accordingly, worldwide commitments have been made to support the generation of sustainable forms of energy and materials derived from renewable resources [52, 148, 150, 172]. One such renewable resource of great and growing scientific and engineering interest is lignocellulosic biomass.

1.2   Lignocellulosic Biomass

Lignocellulosic biomass is the technical term for plant tissue, which is an abundant biorenewable and biocompatible resource with a production rate of 10^{11} to 10^{12} tons per year [61]. *Wood*, for example, is a hard and fibrous form of plant tissue that enables the transportation of water and other nutrients, mechanical support, weatherproofing, microbial protection, and even the storage of food for plant life [199]. Wood is globally distributed across the Earth and has been categorized into two varieties: softwood (SW) and hardwood (HW). *Softwood* is derived from *gymnosperms*, or conifer trees with needle-like leaves that do not shed periodically and that bear uncovered seeds [141, 159]. *Hardwood* is derived from angiosperms, which refers to deciduous trees that are characterized by flat leaves that shed periodically and seeds that are protected by some form of covering such as fruit or a hard shell [13, 140, 178].

6

Examples are displayed in Figures 1.1 and 1.2. Both SW and HW are composed of constituents that can be derivatized into components compatible for biofuel and biomaterial applications [64, 109, 137, 140]. These constituents are primarily cellulose, hemicellulose and lignin and together they represent the three major organic components of woody plant biomass [13, 57, 140].

Figure 1.1. Three different types of lignocellulosic biomass. Right: A loblolly pine tree (*Pinus taeda*), characterized by needle-like leaves. Middle: a Southern sugar maple tree (*Acer barbatum*), characterized by its broad leaves. Left: A magnolia (*Mangolia gradiflora*) is an interesting exception as although it is technically a hardwood, it is also evergreen. *Photos are taken by the author, Tyrone Wells, Jr.*

Figure 1.2.   Seeds coverings typical of softwoods and hardwoods. Left: pine cones from a softwood loblolly pine (*Pinus taeda*). Right: berries from a hardwood Carolina Buckthorn (*Frangula caroliniana*).*Photos are taken by the author, Tyrone Wells, Jr.*

These components are chiefly located in the primary and secondary plant cellular walls as depicted in Figure 1.3 [3]. Although, the cellular wall thickness varies based on species, the primary and secondary cell walls are approximately 100 nm and 1 µm, respectively. The primary cell wall is a thin and flexible layer formed as the cell is growing. Within the primary cell wall, cellulose and hemicellulose are embedded in a matrix with a structural heteropolysaccharide known as pectin. The secondary cell wall is a rigid and thick layer formed between the primary cell wall and the cellular lumen after the cell has fully grown. In the secondary wall, cellulose and hemicellulose complex with lignin, forming the *lignocellulosic matrix*. What is particularly interesting

is that aspects of the lignocellulosic matrix greatly influence the properties and chemical nature of plant biomass [3, 56]. Accordingly, a detailed understanding of cellulose, hemicellulose, and lignin and their physical interactions with one another is imperative to best develop biorefinery processes where specific lignocellulosic constituents can be derivatized into energy and materials.
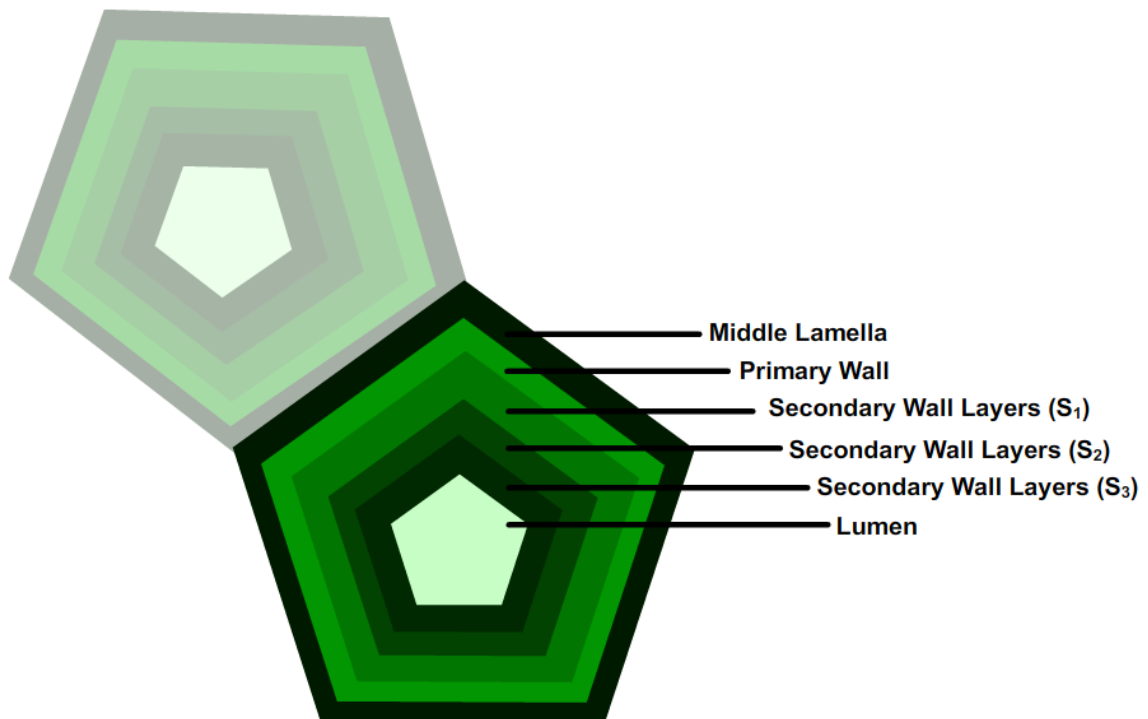
Figure 1.3.   Diagram of two adjacent plant cells. Illustration principally shows the order of layering of the primary and secondary cellular walls[12].

1.3   Cellulose

Cellulose is a polysaccharide $(C_6H_{10}O_5)_n$ and the most abundant organic polymer on Earth. Cellulose exists as a linear polymer composed of tightly packed chains of glucosyl monomer units linked by β-(1→4) glycosidic linkages. Noteworthy, *cellobiose*,

a glucose dimer, is the repeating motif in cellulose due to the stereochemistry of the glycosidic bond as show in Figure 1.3. Regardless, the dense network of intra- and intermolecular hydrogen bonding among neighboring chains allow cellulose to function as a chief structural polymer in plants [38].
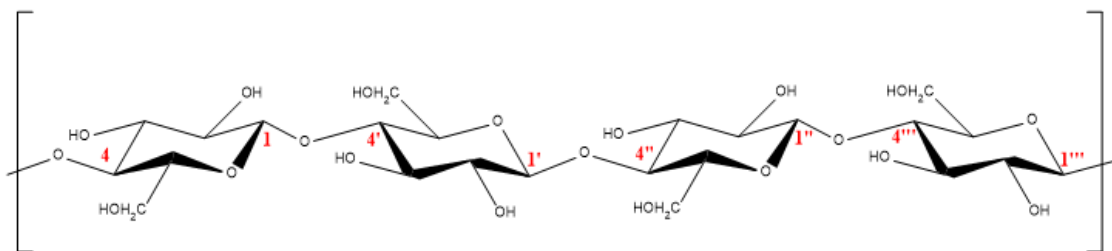
Figure 1.4. The chemical structure of cellulose.

Cellulose is located in both the primary and secondary cell walls. Cellulose accounts for ~20-30% of the dry mass in the primary cell wall and nearly 50% of the mass in the secondary cellular wall. The degree of polymerization (DP) of cellulose in the primary cellular wall is ~250-500 [71]. Meanwhile, the DP of cellulose from the secondary cellular wall generally ranges from 10^3-10^4 [71]. However, this value is dependent on how the cellulose is sourced with highest echelons of DP resulting from virgin wood and lowest ranges resulting from post-mechanical, biological, and/or chemical treatments [38, 139]. The DPs of prominent softwood and hardwood celluloses are summarized in Table 1.1.

Table 1.2. Summary of prominent hemicelluloses in softwoods and hardwoods

SW	DP
White birch	5500 [a]
Jack pine	5000 [a]
Balsam fir	4400 [a]
Eastern white cedar	4250 [a]
White spruce	4000 [a]

Table 1.2.   Continued

Eastern hemlock	3900 [a]
Pinus radiata	3063 [a]
Southern Pine	1450[b]
HW	
Trembling aspen	5000
Red maple	4450
Beech	4050
Eucalyptus regnans	1510

a Denotes samples measured after nitration using a viscometric method [63]. b Denotes samples measured via GPC analysis of cellulose tricarbanilate (CTC) derivatives [63].

Cellulose contains both crystalline and amorphous forms. In crystalline regions, hydrogen bonds and Van der Waals forces conserve a specific superstructure, whereas amorphous regions are characterized by twists and torsions that alter the ordered arrangement of cellulose as illustrated in Figure 1.5. Microfibrils are generally interspersed with regions of amorphous cellulose, and may account for 5-20% of the total composition for both SW and HW. These regions along with the surfaces of crystalline regions are firstly affected by chemical and enzymatic treatments along with reactive and adsorptive substances [38, 138]. In detail, cellulose exists in multiple crystalline forms:

- **Cellulose I**: This is the native form of cellulose and is only found in nature. Chains in cellulose I lie parallel to each other in the unit cell. Noteworthy, cellulose I is a mixture of two crystalline forms of cellulose I, **Iα** and **Iβ**. Iα is *meta*-stable with only one chain per triclinic cell and Iβ is considerably more stable and less reactive as a result of having two conformational distinct chains in a monoclinic unit cell. Accordingly, Cellulose Iβ is more common in nature and is predominant in higher

plants such as trees and cotton. Higher proportions of Iα is more prevalent in bacterial cellulose. Cellulose I can be converted to cellulose II.

- **Cellulose II**: This is the most thermodynamically stable form of cellulose. Chains in cellulose II lie antiparallel in the unit cell and have a monoclinic crystal structure. Cellulose II cannot be converted to cellulose I. Cellulose I and II are the two most studied forms of cellulose.

- **Cellulose III**: This form of cellulose is generated by the treatment of cellulose I with liquid ammonia. During treatment, amines react with cellulose to form amine-cellulose I complexes. After the amines are removed, the resulting form is cellulose III.

- **Cellulose IV**: This form of cellulose is formed by heating cellulose in a polar liquid and is structurally very similar to Cellulose I.
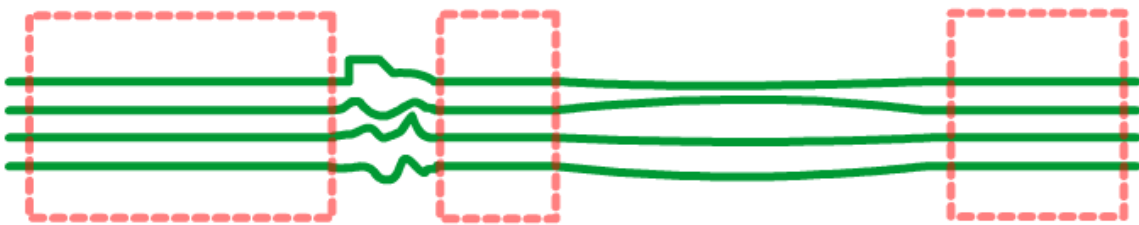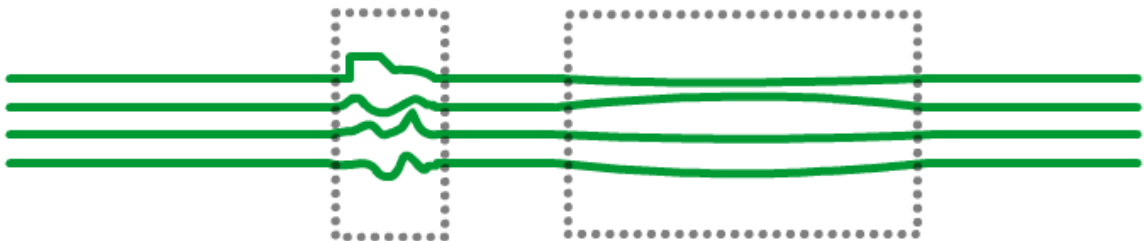
Figure 1.5. Simple representation of crystalline and amorphous regions of cellulose. Top: Regions of crystalline cellulose are boxed and labeled. Bottom: Regions of amorphous cellulose are boxed and labeled[71].

1.4   Hemicellulose

The second-most prevalent polysaccharide in plants is *hemicellulose*, a variety heteropolymers that are generally composed of varying proportions of pentose and hexose sugars. Representative pentose sugars include xylose and arabinose while common hexose sugars include glucose, mannose, galactose, rhamnose, and their corresponding uronic acids. Hemicelluloses constitute approximately 25-35% of the dry mass of plant biomass. In SW, the most common type of hemicelluloses found are galactoglucomannans (Figure 1.6) and arabinoglucuronoxylan (Figure 1.7) while in HWs such it is glucuronoxylan (Figure 1.8). Noteworthy, unlike SW xylan, HW xylan is frequently acetylated, specifically at the C_2- and C_3-positions at a ratio of ~3.5-7 acetyl groups per 10 units of xylose [188].
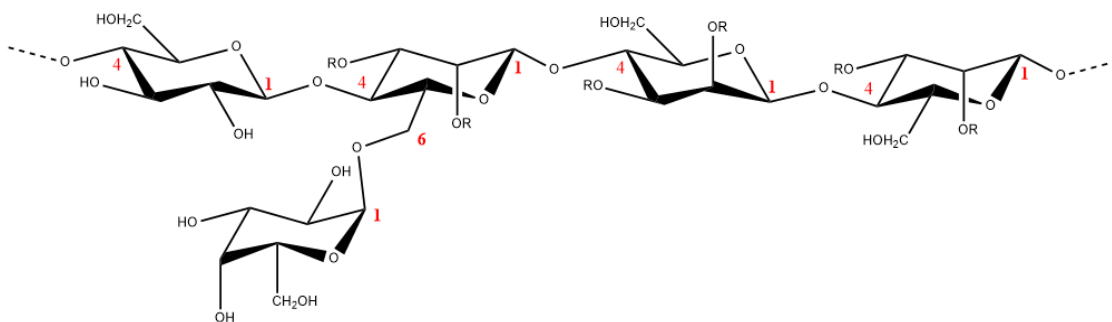
Figure 1.6. Exemplary structure of galactoglucomannans in softwood. Sugar units: β-D-glucopyranose (Glc*p*), β-D-mannopyranose (Man*p*), and β-D-galactopyranose (Gal*p*). Represented is a 4-β-Glc*p*-1→4-β-D-Man*p*1-

13

1→4-β-D-Manp_2-1→4-β-D-Manp_3-1→ backbone with a α-D-Gal$p$-1→6-β-D-Manp_1 side chain and acetylated β-D-Manp_2.
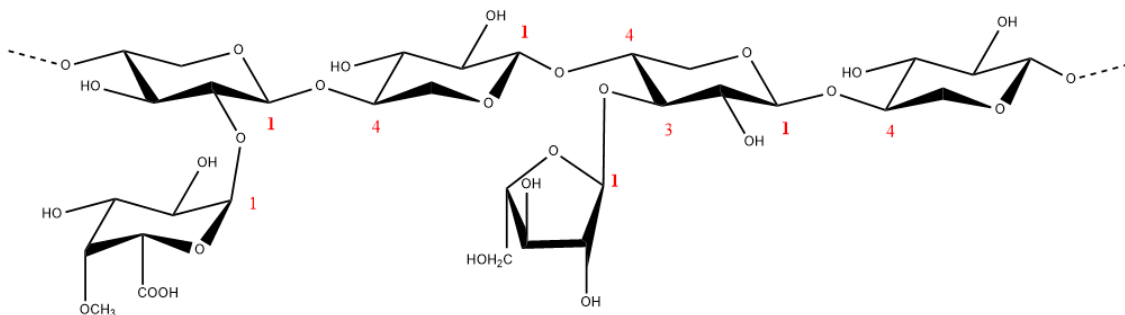
Figure 1.7.   Exemplary structure of arabinoglucuronoxylan in softwood. Sugar units: β-D-xylopyranose (Xyl$p$), 4-O-methyl-α-D-glucopyrnosyluronic acid (4-O-Met-Glc$p$A), α-L-arabinofuranose (Ara$f$). Depicted is a 1→4-β-D-Xylp_{1-4} backbone with a 4-O-Met-Glc$p$A-1→2-β-D-Xyl$p_2$and α-L-Ara$f$-1→3-β-D-Xylp_4 branch.
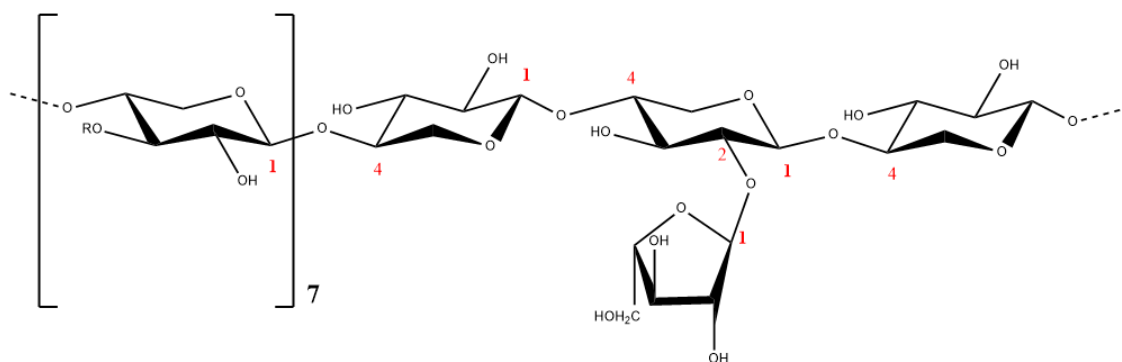
Figure 1.8.   Exemplary structure of glucuronoxylan in hardwood. Illustrated is a 1→4-β-D-Xylp_{1-10} backbone with a 4-O-Met-Glc$p$A-1→2-β-D-Xylp_2 branch.

Hemicelluloses derived from SW pine are a primary interest in this dissertation and are principally composed of *O*-acetyl-galactoglucomannan on the order of 20% based on dry weight. The glucose:mannose ratio of this heteropolymer is roughly 1:3.

Moreover, the ratio of glucose:galactose can vary from 1:1 to 10:1. The DP of SW hemicellulose is generally 100-150 monomer units, which is equivalent to ~20,000 g/mol. The second most abundant heteropolysaccharide in pine hemicellulose is xylan, specifically arabino-(4-O-methylglucurono)xylan, which accounts for 7-15% of the dry weight. The most prominent sugar monomer in xylan in xylose, for example, the arabinose:xylose ratio is 1.3:10 on average, whereas the uronic acid: xylose ratio can vary from 1:4 to 1:9 [3, 12].

Hemicellulose functions as a supporting material in the cell wall and interfaces covalently with lignin via lignin carbohydrate complexes (LCC). The most common LCC linkages are benzyl ester, benzyl ether, and glycosidic linkages [139, 168, 169]. Summarized and detailed compositions of hemicellulose are provided in Tables 1.2 and 1.3.

Table 1.2. Summary of prominent hemicelluloses in softwoods and hardwoods [168]

Wood Type	Hemicellulose Type	Composition			DP
		Units	Molar ratios	Linkages	
SW	Galactoglucomannan	β-D-Man$p$	4	1→4	100
		β-D-Glc$p$	1	1→4	
		β-D-Gal$p$	0.1	1→6	
		Acetyl	1	n/a	
	Arabinoglucurono-xylan	β-D-Xyl$p$	10	1→4	100
		4-O-Met-Glc$p$A	1	1→4	
		Acetyl	7	1→6	
HW	Glucuronoxylan	β-D-Xyl$p$	10	1→4	200
		4-O-Met-Glc$p$A	1	1→2	
		β-D-Glc$p$	n/a	n/a	
		Acetyl	7	n/a	

Table 1.3. Compositions of hemicellulose in specific species[188]

Wood	Species	Hemicellulose	Amount (% of wood)
SW	Loblolly pine	Galactoglucomannan	15-20
	(*Pinus taeda*)	Arabinoglucuronoxylan	5-10
HW	Birch	Glucuronoxylan	15-30
		Glucomannan	2-5

1.5   Lignin

The final major constituent of lignocellulose is *lignin*, which is the second most abundant organic molecule on the planet after cellulose. Structurally, lignin is a complex, three-dimensional, polyaromatic polymer composed of variously linked coniferyl (G), sinapyl (S), and *para*-coumaryl (H) alcohol phenylpropenoid units (Figure 1.9). SW The typical G:S:H ratios of various lignocellulosic biomasses are provided in Table 1.4. Meanwhile, the mechanism for lignin polymerization from these monolignol units is discussed in detail in Chapter 5. In brief, lignin polymerization is initiated by the enzymatic oxidation of a monolignol phenolic hydroxy group as illustrated in Figure 1.10. The result of this enzymatic dehydrogenation is a monolignol species with a free radical that may couple to other neighboring units. This form of radical coupling forms interlocked oligomer units and ultimately a considerably complex, highly-branched, and heterogeneous macromolecule lacking of any distinct regularity or extended repeating motifs. As a result, structure elucidation of lignin has been limited to the detection of specific substructures of lignin oligomers such as β-O-4, α-O-4, β-β, β-5, 5-5, β-1, and 4-O-5 aryl linked monolignol units as shown in Figure 1.11 and detailed in Table 1.5. For example, in the early 90's a dibenzodixocin, new sub-unit in lignin, was detected at a level of 10-15% in SW. This discovery encouraged further research towards the elucidation of new lignin sub-units, such as spirodienone in 2006,and an overall improved understanding of this intricate polymer [202].

16
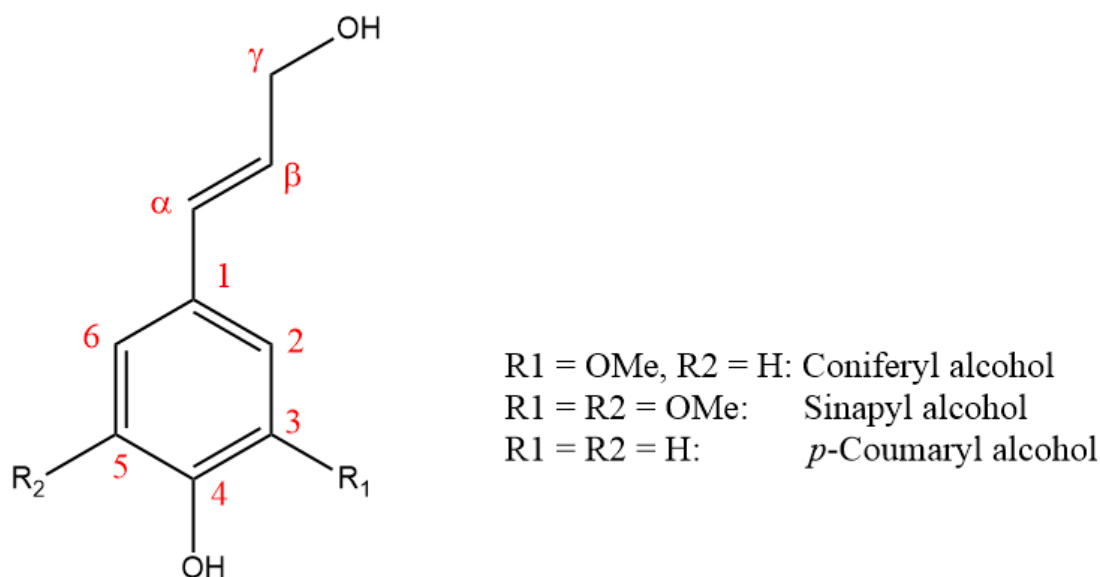
Figure 1.9. The phenylpropenoid monolignol units of lignin[140]. OMe refers to methoxyl groups, -OCH₃.

Table 1.4. Lignin Composition Ratios for select SW and HW biomass [36, 55, 60, 131]

Biomass	% Amt. Lignin	G	S	H
SW Loblolly Pine	29	86	2	12
SW Loblolly Pine Compression Wood	29	87	0	13
SW Spruce (*Picea abies*)	28	94	1	5
HW Beech	26	56	40	4
HW Acacia	28	48	49	3
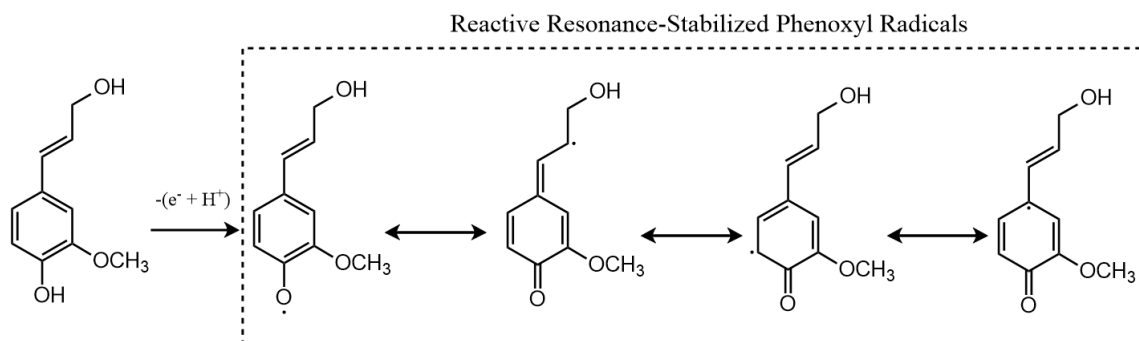
Figure 1.10. Formation of resonance-stabilized phenoxyl radical intermediates via enzymatic dehydrogenation of coniferyl alcohol [3].

17
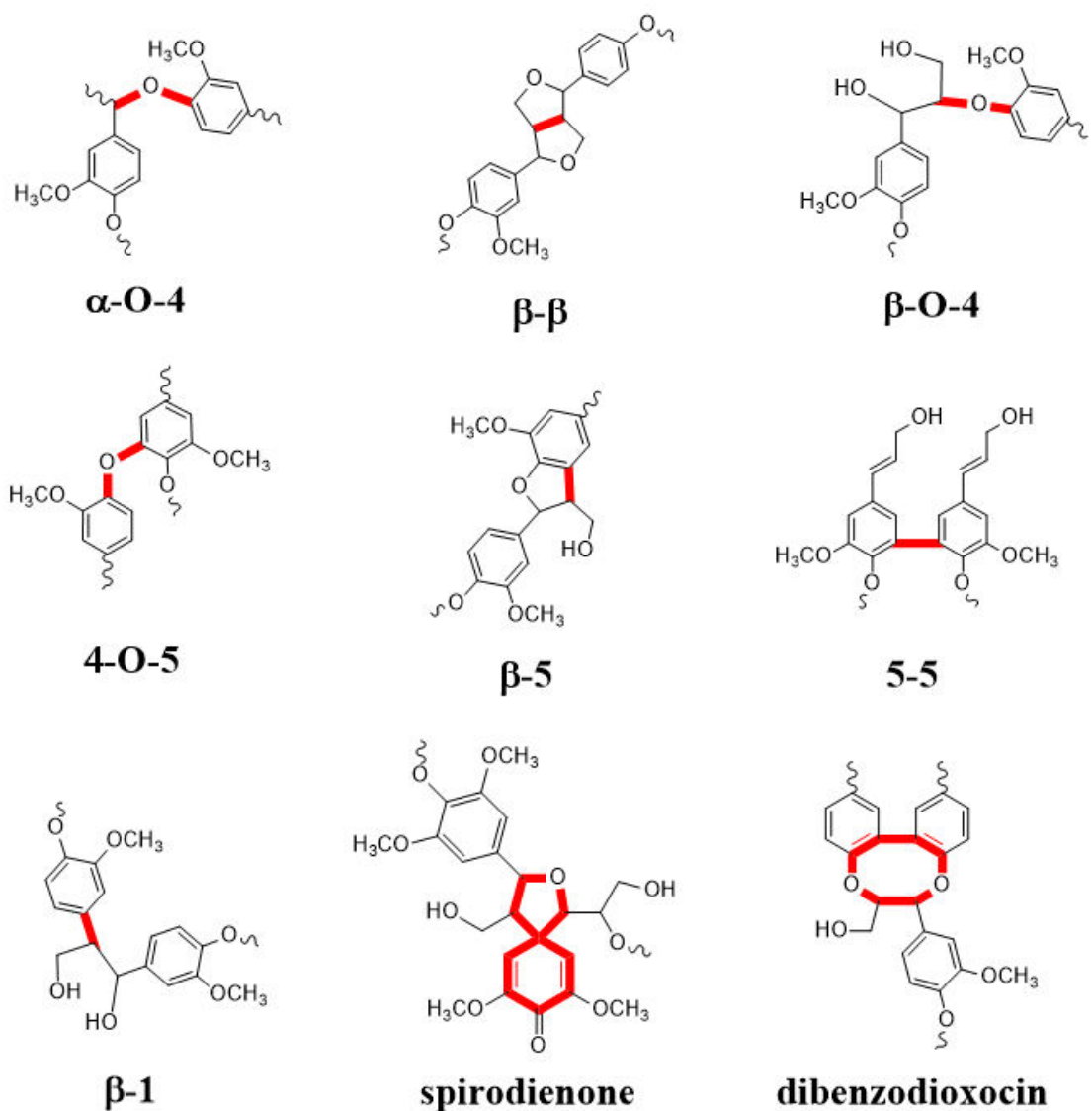
Figure 1.11. Illustrated assortment of lignin substructures. The bolded and red chemical bonds denote titular inter-unit linkage referenced by the systematic naming [140].

Table 1.5. Linkage composition in softwoods and hardwood [29, 62, 116, 117]. "Not reported" = n.p.

Linkage Type	Dimer structure	Avg. % in SW lignin	% in SW spruce
β-O-4	Phenylpropane β-aryl ether	45-50	45
5-5	Biphenyl and Dibenzodioxocin	18-25	24-27
β-5	Phenylcoumaran	9-12	9
β-1	1,2-Diaryl propane	7-10	1

Table 1.5. Continued

α-O-4	Phenylpropane α-aryl ether	6-8	16
4-O-5	Diaryl ether	4-8	n.p.
β-β	β-β-linked structures	3	2

In nature, lignin serves several vital physiological roles such as imparts rigidity and hydrophobicity to the cellular wall.   Furthermore, the complex and recalcitrant nature of lignin protects plant sugars in thelignocellulose matrix from bacterial degradation.   However, for the kraft pulp industry, the presence of lignin is largely undesirable and is removed via pulping and bleaching processes at a rate of >50 million tons per year by the global pulp and paper industry alone [204]. Delignification on an industrial scale encompasses an extensive variety of methodologies e.g., the sulfate "kraft" process, which is the most widely practiced pulping methodology, or ethanol organosolv pulping, which is practiced on a smaller scale [117]. Delignification strategies are implemented in order to primarily degrade, solubilize and reduce the overall recalcitrance of the lignin-hemicellulose-cellulose matrix and can be used to provide greater access to cellulose fibers for subsequent chemical processes. These methods result in an isolated lignin byproduct with unique properties and potentials for biofuel and biomaterial applications [135].

For example, ethanol organosolv pretreatment (EOP) is a current process that is being further optimized for industrial biorefineries [143]. An exemplary parameter EOP set can be heating at 160-170ºC for 0.5-1 h with a biomass: solvent ratio ofapproximately1:8 with a 65% EtOH aqueous solution with a catalytic amount of H_2SO_4 on the order of 0.70-0.80% of dry biomass mass. Other parameter sets for EOP experiments are summarized in Appendix A. Continuing, during this process, wood is cooked in a organic: aqueous solvent with a catalytic amount of acid in order to degrade

lignin ether linkages and solubilize the polymer away from cellulose. Hence, EOP

generates a secondary aqueous effluent that is predominantly enriched with degraded

lignin oligomers among other components such as deteriorated units of hemicellulose,

amorphous cellulose, and furans.

Alternatively, kraft lignin is a fragmented and alkaline-soluble version of lignin

produced during the kraft (sulfate) pulping process. During this procedure, wood chips

are cooked at ~170°C for ~2 h with NaSH and NaOH in order to cleave lignin alpha- and

beta-aryl ether linkages thereby solubilizing lignin fragments [73]. A sample range of

kraft cooking conditions is presented in Appendix A. Additionally, the molecular

weights of kraft lignin and other varieties is presented in Appendix A. Currently, an

estimated 98% of Kraft lignin is burned as a non-optimized energy resource within the

pulp mill recovery boiler in order to recover energy and pulping chemicals [112, 118].

This low-value use of kraft lignin and the capital costs associated with a recovery furnace

has spurred research to repurpose the polymer for higher-utility functions; and while kraft

lignin can be upgraded as a biofuel [21], alternative enhancements may significantly

broaden the range of new and value-added bioenergy and biomaterial applications.

Table 1.6.   Molecular weights and polydispersity (PD) of different variety of lignins
obtained during assorted extractions from biomass [29, 62, 116, 117].

Lignin extraction	Approx. M_w (g/mol)	PD
SW Kraft lignin	9700	3.5
SW Pine EOP	2400	1.7
HW Sulfite pulping	4300	2.0
HW EOP	4000	7.7

1.6   Characterization of Biomass

This dissertation primarily involves the characterization of lignin. Accordingly, the following is a brief background of the various instruments used to characterize lignin along with other apparati implemented to determine qualities of non-lignin biomass along with their respective recent advances:

1.6.1   *Spectroscopic Analysis of Lignin*

Fourier Transform Infra-Red (FT-IR): FT-IR is one of the most widely applied techniques for lignin structure analysis used as early as 1948 [77]. In brief, FT-IR is an absorption spectroscopy technique used to elucidate the structure of molecules via the molecules' characteristic absorption of infrared radiation The infrared spectrum (12800 to 10 cm^{-1}) correlates to a *molecular vibrational spectrum*. During exposure to infrared radiation, molecules may selectively absorb radiation of specific wavelengths. This absorption changes the dipole moment of the sample molecule thusly transferring the vibrational energy levels from a ground state to an excited state.   The vibrational energy gap determines the frequency of the absorption peak. Moreover, the number and intensity of the absorption peak(s) is dependent on the vibrational freedom and dipole moment changes of the sample molecule, respectively. Hence, by analyzing an infrared spectrum that relates the percentage of absorbed or transmitted infrared radiation to a wavelength frequency (wave number) one can readily elucidate a wealth of structural information concerning a molecule.

Most fundamental lignin molecular vibrations fall within the frequency range of 4000 to 400 cm^{-1}(2.5 to 25 µm), which is also referred to as mid-infrared spectral region. FT-IR studies discussed in this dissertation refers to mid-infrared spectroscopy [68, 72,

165, 185]. However, prominent studies within the last decade have also used near-infrared spectroscopy (12800-400 cm^{-1}) to study lignin [67, 132, 158].

Nuclear Magnetic Resonance (NMR): NMR interpretation plays a pivotal role in the elucidation of molecular structures. NMR is an analytical method through which the *spin* of certain atomic nuclei is manipulated via an external magnetic field and short radio frequency pulses in order to determine information of the chemical environment surrounding the *spin*. In a simplified sense, *spin* is a type of angular momentum characteristic of subatomic particles that provides a *magnetic dipole moment*. In the absence of a magnetic field, the magnetic dipole is oriented randomly. However, in the presence of a magnetic field, magnetic dipole moment can align with or against the magnetic field. Low energy spin will line with the magnetic field in what is referred to as the base energy. Spin at higher energy will align in the opposite direction to the magnetic field. The energy gap between these two states can be crossed by the absorption or emittence of a wavelength that corresponds to a specific radio frequency. The signal that matches the transfer is measured by the NMR, and a spectrum can be acquired [20, 83].

In this dissertation, NMR experiments based on ^{13}C, and ^{31}P isotopes were experimentally studied. While, ^{1}H-NMR can and has be used to characterize lignin, ^{13}C-NMR is generally better suited as an experiment as it provides greater resolution for quantitative studies [50, 75]. For example, ^{1}H-NMR spectra is generally measured over a spectral width of 10-15 ppm while ^{13}C-NMR is measured with a spectral width of 0-200 ppm [19, 43, 49, 50, 68, 75, 99, 152]. However, there are comparative disadvantages with ^{13}C-NMR such as low isotope sensitivity and low natural presence of the ^{13}C

isotope, which results in long time delays. Historically, carbon NMR has been used to characterize lignin as early as the 1980's, and after decades of model compound analysis, several modern and detailed chemical shift assignment tables are available to characterize lignin [19, 43, 49, 50, 68, 75, 99, 152].   Meanwhile, the features and chemical nature of lignin phenolics can be elucidated with ^{31}P-NMR. The basis of ^{31}P-NMR experimentation involves the derivatization of lignin phenolic structures with 2-chrlor-4,4,5,5-tetramethyl-1,3,2-dioxaphospholane (TMDP), as exemplified in Fig. 5.5 [133]. This process allows for the phenolic hydroxyl contents to be calculated based on the integrated region of an endo-N-hydroxy-5-norbornene-2,3-dicarboximide (NHND) internal standard.

  Gas Chromatography-Mass Spectroscopy (GC-MS): GC-MS is an analytical method that combines the aspects of gas chromatography with mass spectrometry. Gas chromatography (GC) is a analytical separation technique used to characterize volatile substances in the gas phase. During experimentation, samples that have been dissolved in a solvent are vaporized without decomposition and are passed through a heated column by an inert carrier gas. The carrier gas serves as a mobile phase and the interior surface of the column is coated with a stationary phase that interacts with the analytes resulting in characteristic elution times. A mass spectrometer ionizes sample molecules, usually to cations, and separates them by external electric and magnetic fields based on their mass and charge. A GC-MS combines the analytical benefits of both of these apparati. For example, a GC-MS provides identification of sample molecules by not only their respective retention time to an internal standard, as is conventional with GC, but also by

their mass spectrum. This allows for the identification of unknown samples.

Furthermore, in GC-MS a capillary column (~0.25 mm diameter) is utilized as opposed

to a column packed with a stationary phase [15, 69].

1.6.2   *Chromatographic Analysis of Lignin*

Gel permeation chromatography (GPC): GPC is a chromatographic method

that utilizes size exclusion chromatography to separate analytes on the basis of molecular

weight distribution. Samples are first dissolved in a solvent that serves as the mobile

phase. The mobile phase flows through a stationary phase made up of millions of porous,

rigid particles that are tightly packed in a column. Different flow rates result for analytes

based on their "effective size," in other words, molecules of various sizes will elute from

the column at different speeds resulting in different retention times. Core components of

a GPC include a pump that moves the sample through the system, an injector that

introduces the sample to the mobile phase, a column set used to separate sample

components from one another, a detector that monitors the separation and recognizes

eluted sample, and data processing software that automatically calculates, records and

reports quantitative values for molecular weight [162, 176, 191].

1.6.3   *Additional Analysis of Lignin*

Thermogravimetric Analysis (TGA): TGA is a means of determining the rate

of degradation of a material as a function of escalating temperature. During the

experiments discussed in this dissertation, a sample mass is heated at a constant rate

under an inert gas flow. As the sample degrades, components become more volatile and

leave the system (sample pan), reducing the residual mass. Changes in mass are recorded by a sensitive balance that holds the sample pan and provides the data necessary for a computer to track residual mass vs. temperature thermograms. This thermograms can be derived with respect to temperature to yield the *rate of degradation* as a function of escalating temperature [32, 37, 160].

1.6.4   *Analysis of Non-Lignin Biomass*

High Pressure Liquid Chromatography (HPLC): HPLC is an analytical and chromatographic chemistry technique that was used in this dissertation to identify and quantify the presence of specific sugar monomers. The mechanical concepts of HPLC are similar to GPC with the two major exceptions. Firstly, HPLC runs at a significantly higher pressure (50-350 bar), which provides superior resolving power when separating mixtures. Secondly, unlike size exclusion chromatography, HPLC separates analytes based on ion-exchange chromatography. An example of this is *high-performance anion exchange chromatography* (HPAEC). In this dissertation, HPAE was used with a high pH and hydroxide-based eluent to produce analyte anions. These ions were then passed through a column packed with a nonporous cation-exchange resin powder, resulting in highly effective separation of a wide variety of carbohydrates. In order to detect these separated underivatized analytes, pulsed amperometric detection (PAD) implemented in tandem (HPAEC-PAD). During PAD, a series of voltage steps in a waveform are implemented to charge a gold electrode, detect the analytes, and then clean and restore the electrode surface. This cycle of preparation, detection, and cleaning occurs on an

order of milliseconds and allows for a high-quality analytical analysis of carbohydrate concentrations [53, 74, 97].

1.7   Objectives and Hypotheses

The objective of the first half of this thesis is to describe the utilization of lignin and degraded lignocellulose polysaccharides sourced from industrial-based pretreatment waste stream towards the development of bioenergy and biochemicals. Certain heterotrophic bacterial species are capable of utilizing enzymatic aromatic-degradation sequences that are capable of converting lignin into metabolites for lipid synthesis. These processes incorporate an enzymatic degradation sequence known as the *β-ketoadipate pathway* (β-KAP). This metabolic pathway and its several-fold green technology applications are discussed thoroughly in the Chapter 2. Continuing, certain species of bacteria that use the β-KAP are also capable of accumulating single cell oils that can processed into biodiesel[183]. One such species is *Rhodococcus opacus*, as initial work demonstrated that various strains of *R. opacus* exhibited considerable *oleaginicity*, which refers to a cell's ability to accumulate oil. Cells that produce over 20% of their cell dry weight (CDW) in oil are classified as *oleaginous*. For example, Alvarez et. al demonstrated that a strain of *R. opacus* generated >80% CDW using glucose as a substrate[4]. In a later study, *R. opacus* DSM 1069 utilized coniferyl alcohol and then Kraft lignin as a sole carbon and energy resource, which resulted in limited oleaginicity on the order of <5% CDW [85, 86]. In Chapter 4, the use of a biorefinery waste stream containing fragmented lignin and sugars are used as a novel substrate for microbial oil production via *R. opacus* DSM 1069in order to determine a means of producing higher

lipid production rates through the simultaneous conversion of sugars and lignin. Hence, hypothetically, the simultaneous conversion of lignin and sugars derived from pretreatment waste effluent as a novel substrate may provide improved oleaginicity, a unique and efficient approach to biodiesel production, and a new route for biorefinery waste stream optimization.

The second half of this thesis describes the development of lignin for biomaterials. HMW polymeric materials favor the use of polymerized lignin, which has increased demand for efficient lignin polymerization strategies. Notable lignin polymerization strategies have been performed using cross-linking agents such as polystyrene, acrylamide, and maleic anhydride that operate by connecting neighboring lignin oligomer units at specific functional sites[94, 103, 182]. Other polymerization methods can involve enzymes such as laccase and peroxidase that modify lignin with high coupling selectivity using benign oxidants such as molecular oxygen and hydrogen peroxide, respectively [9, 206]. In Chapter 5, a novel polymerization method that utilized ultrasonics to rapidly augment the molecular weight of lignin is demonstrated. This methodology was dependent on the generation of highly reactive free radicals that provided an environment for cross-coupling reactions to occur between nearby oligomers of lignin. Finally, Chapter 6 expands on the thermostabilization affects provided by this ultrasonic pretreatment process. Hypothetically, lignin can be rapidly polymerized and thermostabilized through the use of ultrasonics to improve aspects of its chemical nature that make the polymer more suitable for polymeric heat-stable biomaterial applications, such as carbon fiber development.

The main objectives of this dissertation are summarized as follows:

- Establish the utility of the β-KAP

- Investigate the conversion via the β-KAP of biorefinery waste streams
  that contain lignocellulosic aromatics and sugars into lipids suitable
  for biodiesel production

- Test and characterization novel ultrasonic polymerization strategies for
  lignin

- Evaluate the degree of heat stability enhancement of ultrasonic-treated
  lignin samples

CHAPTER 2: LITERATURE REVIEW

2.1   The Case for a Green Chemistry Approach to Environmental Remediation

Environmental contamination caused by toxic aromatic compounds originating from industrial, agricultural, medical, and municipal waste streams are critical ecological issues[1, 78, 84, 91, 121, 197]. Among these hazardous contaminants are priority pollutants recognized by the US Environmental Protection Agency (EPA), including nitrophenols, organophosphates (e.g., parathion and paraoxon), and polychlorinated aromatic and aliphatic cyclic hydrocarbons [16, 119, 164, 167, 201]. An improved understanding of the effects of these pollutants has spurred research into effective treatment of industrial waste streams and environmental remediation strategies [154]. Traditional physicochemical remediation methods generally rely on incineration, chemical hydrolysis, or *in situ* chemical oxidation (e.g., aeration and ozone treatment) to treat aromatic pollutants, but these strategies can be complex, inefficient, and/or expensive [34]. Biological remediation strategies are particularly challenging because the resonance energy of aromatic rings provides high stability and recalcitrance against microbial degradation [121]. Fortunately, specific heterotrophic microorganisms have evolved proficient catabolic networks that are capable of aryl-ring degradation. The intradiol (*ortho-*) cleavage of dihydroxy-substituted arenes, for example, is mediated by a catabolic route known as the β-KAP. This catabolic network offers several intriguing biotechnological opportunities for metabolic uptake of a diverse variety of toxic aromatic materials and their subsequent bioconversion into benign or even valued metabolites. Here, we review recent applications of the β-KAP as a means to reconcile environmental

niches contaminated with EPA-recognized priority pollutants, including nitrophenols, organophosphates, and chlorinated aromatics and hydrocarbons. Also discussed is a novel incorporation of the β-KAP as a means to convert lignocellulosic aromatic waste into lipids suitable for biodiesel purposes.

2.2   Basis of the β-KAP

The β-KAP is an enzyme-mediated aromatic degradation sequence that is widely distributed among soil bacteria and fungi. The nine essential enzymes and key chemical intermediates of this metabolic network were first established in Gram-negative *Pseudomonas putida* in 1966 by L. Nicholas Ornston [123]. Understanding of the β-KAP has been advanced since then, particularly among Gram-negative bacteria belonging to *Acinetobacter, Burkholderia,Cupriavidus, Flavimonas,* thermophilic *Geobacillus,* haloalkaliphilic *Halomonas, Klebsiella, Pantoeba, Serratia,* and *Sphingomonas*[54, 95, 127, 170, 189]. To a lesser extent, the β-KAP has been studied in Gram-positive bacteria, and includes insights into species belonging to *Arthrobacter, Corynebacterium, Kribbella, Mycobacterium, Nocardioides, Sarcina, Streptomyces, Nocardia,* and *Rhodococcus* genera [16, 31, 33, 66, 80, 95, 96, 197]. Exemplary representatives of the β-KAP among fungi include the maize pathogen *Cohliobolus heterostrophus* and the white rot fungi *Phanerochaete chrysosporium* and *Fusarium solani* [23, 163]. To date, utilization of the β-KAP by members of Archea has not been reported. The β-KAP is preceded by preliminary conversion of a broad range of organic compounds into one of two aromatic compounds, catechol or protocatechuate (Figure 1) [198].Protocatechuate may be derived from lignin monomers(e.g., coniferyl alcohol) and chlorinated aromatics

(e.g., 4-chlorobenzoate) among other starting materials [48, 65, 79, 81, 130]. Catechol

may be sourced from comparable molecular entities, as well as nitroaromatics (e.g., 2-

nitrophenol) and simple cyclic aromatic hydrocarbons that include the priority pollutants

benzene, toluene, and phenol [17, 65, 108, 126, 194].Both the bacterial and eukaryotic β-

KAP are largely chromosomally encoded (e.g., *pca* and *cat* genes for *P. putida*) and start

with intradiol cleavage of catechol or protocatechuate via mononuclear non-heme iron

enzymes catechol 1,2-dioxygenase (CatA) or protocatechuate 3,4-dioxygenase(PcaGH)

to produce *cis,cis*-muconate or β-carboxymuconate, respectively [54]. For bacteria, two

additional enzymatic steps join the catechol and protocatechuate branches at the

formation of β-ketoadipate enol-lactone. This molecular intermediate is then converted

via enol-lactone hydralase (PcaD or CatD) into the eponymous β-ketoadipate. The

protocatechuate branch of the eukaryotic β-KAP is distinguished by the reduction of β-

carboxymuconolactone via a hydrolase enzyme to generate β-ketoadipate. Consequently,

the point of convergence of the eukaryotic β-KAP protocatechuate and catechol branches

occurs at β-ketoadipate. Finally, two further steps convert β-ketoadipate into metabolites

of multiple anabolic pathways including the TCA cycle and fatty acid biosynthesis

(succinyl-CoA and acetyl (CoA) (Figure 2.1; Appendix A) [65, 93].
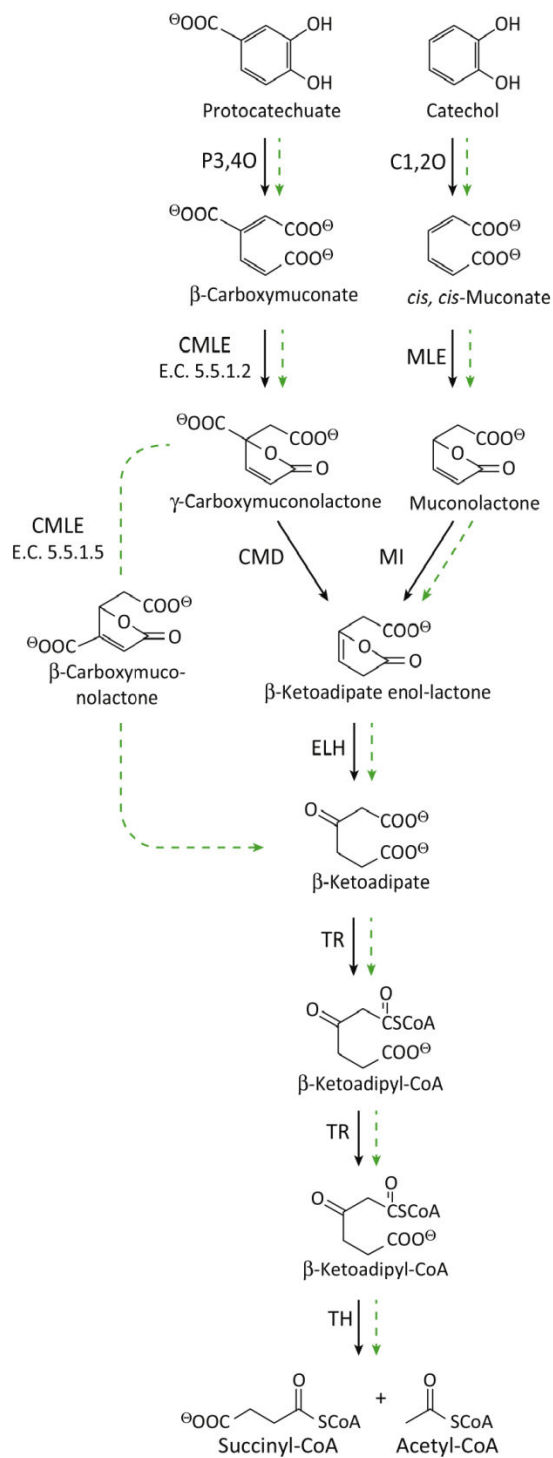
Figure 2.1. The bacterial and eukaryotic β-ketoadipate pathways. Black solid arrows show pathways in bacteria; green dotted arrows show routes in eukaryotes. Full names for enzyme abbreviations are listed in Appendix A [65, 93].

2.3 Bioremediation

2.3.1 *Biodegradation of ortho-, meta-, and para-nitrophenol*

Nitrophenols ($HOC_6H_4NO_2$) are a versatile family of organic compounds commonly used as precursors for industrial production of munitions, pigments, plasticizers, pharmaceuticals, and organophosphorus pesticides [35, 183]. In contrast to their advantageous multifaceted utility, nitrophenol isomers are especially hazardous waste products because of their persistence, acute non-target toxicity, and mutagenic potential [16]. Animal studies have demonstrated that chronic exposure to nitrophenols can cause blood disorders such as methemoglobinemia and anemia [183]. Moreover, recalcitrant nitrophenol pollutants are a threat to soil and groundwater and their contamination is already widespread, being one of 275 prevalent environmental pollutants found at sites designated under the Comprehensive Environmental Response, Compensation, and Liability Act (CERCLA) [78, 203]. This situation has spurred research into effective long-term remediation of environmental niches contaminated with these nitroaromatic compounds. Fortunately, specific heterotrophic microorganisms that survive in these contaminated niches are distinguished by nitroaromatic catabolic pathways that incorporate the β-KAPand allow thorough degradation of all three mononitrophenol isomers: *ortho-* (2-), *meta-* (3-), and *para-* (4-)nitrophenol. The bacterial degradation sequence of *ortho*-nitrophenol (ONP) determined in isolated strains of *Alcaligenes, Pseudomonas*, and *Sarcina* exhibits a comparatively simple (*onp*-encoded) degradation process before the β-KAP. This step involves direct removal of the nitro group by means of enzymatic hydroxylation via ONP monooxygenase (OnpA) to form catechol, with the release of nitrite [16, 183, 203]. When first purified from Gram-

negative *P. putida* strain B2, this monooxygenase required 2 mol of NADPH as a cofactor to complete the initial hydroxylation reaction, which supported *ortho-*benzoquinone as an intermediary, though undetected, step while ONP is converted to catechol [171]. The reactive intermediate *ortho*-benzoquinone is reduced to catechol via *ortho*-benzoquinone reductase (OnpB) (Appendix A). Recent studies have demonstrated the complete microbial breakdown of ONP by *Pseudomonas* sp. strain NyZ402 transfected with *onpAB* derived from *Alcaligenes* sp. strain NyZ215 (Figure 2.2a) [181, 184]. Once formed, catechol is degraded along the catechol branch of the β-KAP and is converted to *cis,cis*-muconate via catechol 1,2-dioxygenase and then further metabolized to muconolactone via (*catB*-encoded) *cis,cis*-muconate lactonizing enzyme; further metabolic processes ultimately generate metabolites of the TCA (Figure 2.2c) [184]. A variation of the ONP degradation pathway was reported for Gram-positive S. maxima strain MTCC 5216 that includes the catechol branch of the β-KAP up to the formation of *cis,cis*-muconate or muconolactone. This study revealed that *cis,cis*-muconate and muconolactone are converted to β-ketoadipate via intermediary metabolites γ-hydroxymuconate semialdehyde, γ-hydroxymaleyl acetate, and maleylacetate, with the latter being reduced via maleylacetate reductase to form β-ketoadipate and return to the β-KAP for further degradation (Figure 2.2b) [17].Although *meta*-nitrophenol (MNP) and *para*-nitrophenol(PNP) show less recalcitrance to biodegradation compared to ONP, their catabolic pathways are substantially more complex [184]. The MNP degradation pathway, as reported for *Cupriavidus*, *Pseudomonas*, and *Sarcina* strains, has a number of reported variations that lead to β-ketoadipate, typically involving a 1,2,4-benzenetriol (BT) intermediate.
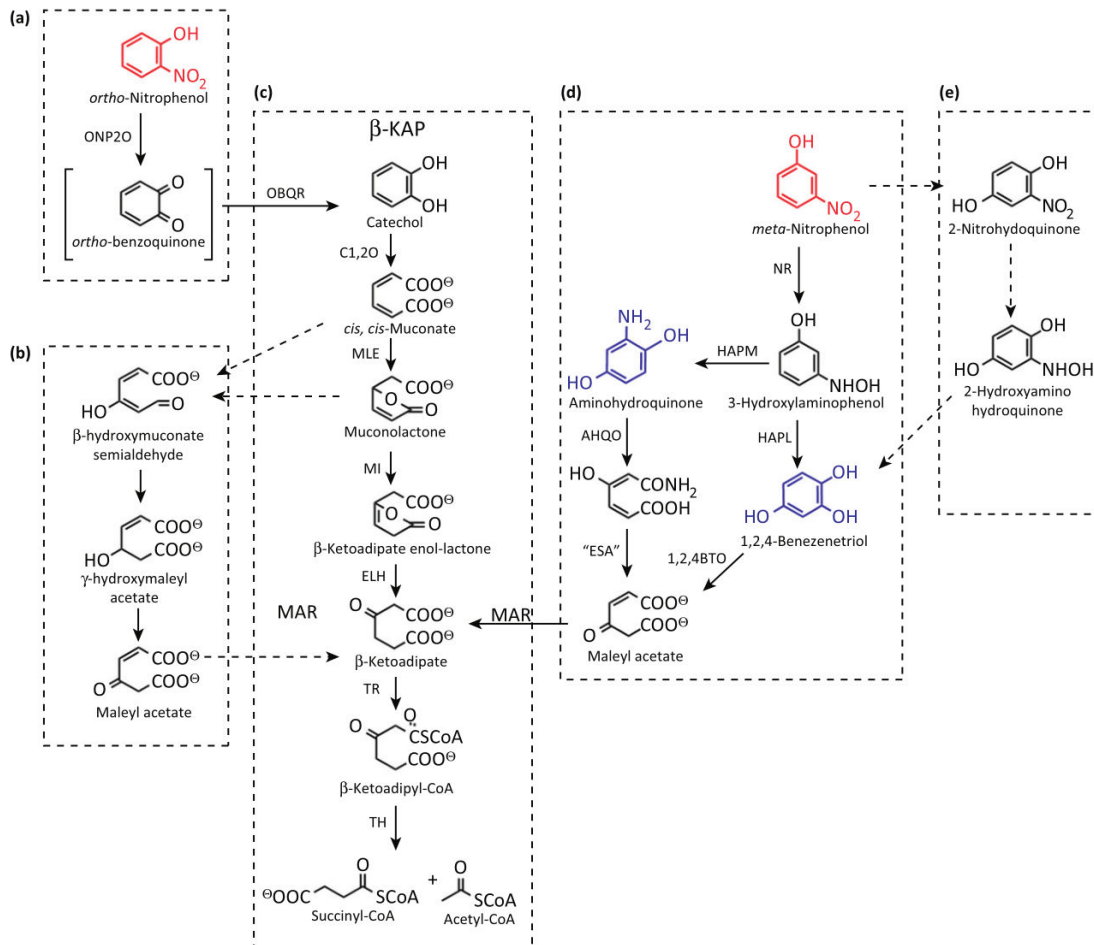
Figure 2.2. The *ortho*-nitrophenol degradation pathway in **(a)** transgenic *Pseudomonas* sp. strain NyZ402 and **(b)***S. maxima* strain MTCC 5216 (proposed), and their incorporation with **(c)** the β-ketoadipate pathway. The *meta*-nitrophenol degradation pathway in **(d)** *Cupriavidus necator* strain JMP134 (leftmost) and *P. putida* strain B2 (rightmost) and **(e)** the proposed pathway for *S. maxima* strain MTCC 5216. Priority pollutants are depicted in red, key intermediates are shown in blue, dotted arrows represent hypothetical pathways, and the full names for all enzyme abbreviations are listed in Appendix A[17, 181, 186, 203].

For *P. putida* B2 and *Cupriavidus necator* JMP134, MNP degradation begins with NADPH-dependent partial reduction of the nitro group via a nitroreductase (encoded by *mnpA*) to generate *meta*-hydroxylaminophenol (MHAP) [130]. In *P. putida*

B2, MHAP is then attacked by a lyase enzyme to yield BT with concomitant release of ammonia [171, 190]. Cleavage among the adjacent hydroxyl groups of BT via 1,2,4-benzenetriol dioxygenase generates maleylacetate, which is then reduced to form β-ketoadipate (Figure 2.2d) [17]. The BT intermediate is bypassed in *C. necator* JMP134 because MHAP undergoes Bamberger re-arrangement via MHAP mutase to yield aminohydroquinone. Further degradation of aminohydroquinone is mediated by dimeric aminohydroquinone dioxygenase (encoded by *mnpC*), which performs aryl-ring scission between the adjacent amino and hydroxyl groups. The amino group is then cleaved via an amidase encoded by *mnpD* to yield maleylacetate and, after subsequent reduction, β-ketoadipate (Figure 2.2d) [193]. A proposed intermediate sequence for MNP degradation in *S. maxima* MTCC 5216 starts with oxidation of MNP to yield 2-nitrohydroquinone. This compound is then partially reduced to form 2-hydroxyamino hydroquinone, which is converted to BT and then maleylacetate before reductive catalysis yields β-ketoadipate (Figure 2.2e) [17, 186].

Oxidative degradation of PNP is the most extensively studied among the three mononitrophenol isomers, particularly in *Pseudomonas, Flavobacterium, Moraxella, Bacillus, Rhodococcus, Nocardia, Arthrobacter*, and *Burk holderia* strains [184, 200, 203]. The PNP degradation pathway generally involves a hydroquinone (HQ) intermediate for Gram-negative bacteria or a BT intermediate for Gram-positive strains [184]. For *Pseudomonas* sp. strain WBC-3, PNP degradation begins with NADPH-dependent monooxygenase (PnpA) release of nitrite to generate *para*-benzoquinone. This intermediate is then reduced via *pnpB*-encoded *para*-benzoquinone reductase to generate HQ. The aryl ring of HQ is then targeted by hydroquinone 1,2-dioxygenase (PnpC),

which mediates oxidative *ortho*-ring fission to generate *cis,trans*-4-hydroxymuconic

semialdehyde. A final oxidizing step via a dehydrogenase (PnpD) converts this

compound to maleylacetate, which leads to the β-KAPvia a *pnpE*-encoded maleylacetate

reductase for further degradation (Figure 2.3). The PNP degradation pathway of Gram-

positive Rhodococcus opacus strain SAO101 and Rhodococcus sp. strain PN1 begins

with a hydroxylation step via *para*-nitrophenol 2-monooxygenase to generate 4-

nitrocatechol, which is then converted to BT with concomitant release of nitrite and

ultimately leads to the formation of β-ketoadipate (Figure 2.3) [184, 200, 203].
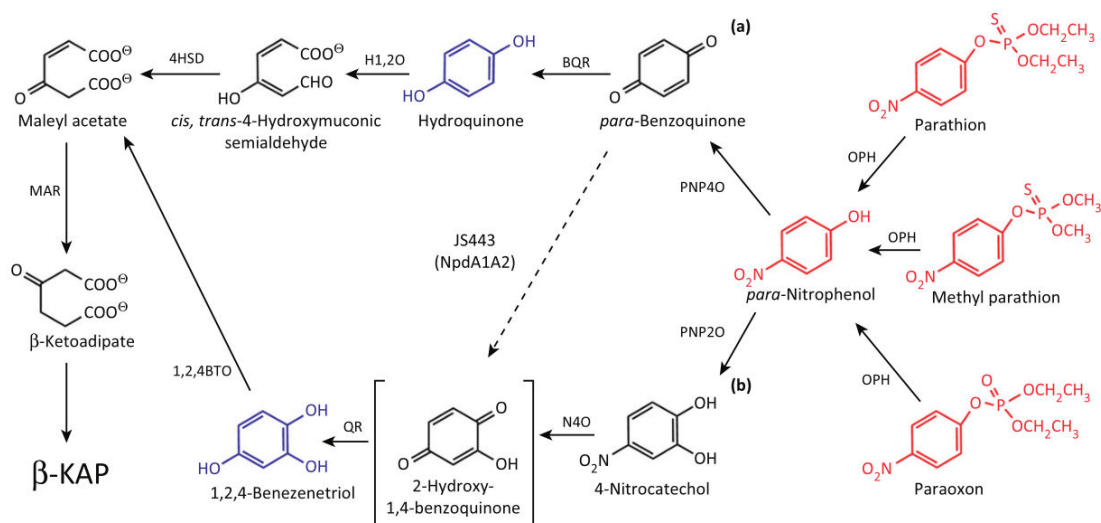
Figure 2.3.   *para*-Nitrophenol degradation pathway and the two general pathways representing **(a)** Gram-negative and **(b)** Gram-positive strains. Dotted arrows represent a pathway variation reported for *Arthrobacter* sp. strain JS443. Priority pollutants are depicted in red, key intermediates are shown in blue, and the full names for enzyme abbreviations are located in Appendix A [184, 200, 203].

Although the Gram-negative and Gram-positive PNP degradation pathways are

apparently widespread among a range of bacteria, an increasing number of reports detail

37

significant deviations to widely accepted general schemes. A notable example is exhibited by Gram-negative *Burkholderia* sp. strain SJ98, which degrades PNP via the BT pathway. Moreover, Perry and Zylstra elucidated the PNP catabolic degradation pathway of *Arthrobacter* sp. strain JS443, which proceeds via HBQ and BT without 4-nitrocatechol as an intermediate (Figure 2.3; Appendix A) [184].. Despite these variations, the routes that allow thorough biodegradation of PNP all exhibit substantial reliance on

the β-KAP [184].

2.3.2   *Parathion, methyl parathion, and paraoxon*

PNP contamination may arise as a product of hydrolysis of organophosphorus agrochemical wastes such as parathion ($C_{10}H_{14}NO_5PS$), methyl parathion ($C_8H_{10}NO_5$ PS),and paraoxon ($C_{10}H_{14}NO_6P$). These substantially more hazardous chemicals adversely affect metabolic functions of enzymes in the central nervous system, especially parathion and paraoxon, which are potent cholinesterase inhibitors [186]. As a sponsor of the Chemical Weapons Convention (1993), the USA is responsible for the treatment of over 6500 metric tons of chemical weapon stockpiles that in part comprise organophosphorus compounds (C-16/DG.18 OPCW) [186]. As an alternative to physiochemical methods, previous studies have demonstrated the potential of transgenic microbes for detoxification of these pollutants by means of initial catalytic hydrolysis via an *opd*-encoded organophosphate hydrolase and further degradation of the resulting PNP byproduct via the *pnp*-encoded PNP degradation pathway and the *pca-* and *cat*-encoded β-KAP(Appendix A).This strategy was specifically used to engineer the soil bacterium

Pseudomonas putida strain KT2442 with the PNP operon and *opd* gene to allow microbial uptake of parathion as the sole carbon and energy source. Diethylthiophosphate was the nontoxic byproduct of the initial detoxification hydrolysis of PNP, and was degraded as a source of phosphorous, sulfur, and carbon (Figure 2.3) [180]. More recently, methyl parathion degradation has been investigated using *Pseudomonas* sp. strain WBC-3. The strain was transfected with a gene that encodes methyl parathion hydrolase to mediate initial hydrolysis of methyl parathion. The hydrolysis byproduct, dimethyl thiophosphate, was converted to a source of phosphorus and thePNP generated was catabolized along the HQ branch of the PNP degradation pathway leading into the β-KAP (Figure 2.3) [200]. Paraoxon was completely mineralized with an engineered strain of *P. putida* transfected with the *pnp* operon of *Pseudomonas* sp. strain ENV2030 and the opd gene of *Flavobacterium* sp. strain ATCC 27551; the transgenic strain was also transfected with phosphodiesterase (*pde*) from *Delftia acidovorans* and alkaline phosphatase (*phoA*) from *P. aeruginosa* HN854 to degrade the diethylphosphate hydrolysis byproduct (Figure 2.3; Appendix A). This strain exhibited complete mineralization of paraoxon up to1 mM (275 mg/L) within 48 h, utilizing paraoxon as the sole source of carbon, phosphorus, and energy [186].

2.3.3   *Pentachlorophenol and 2,4,6-trichlorophenol*

Pentachlorophenol (PCP, C_6HCl_5O), the most prominent pesticide of the mid-20th century, and 2,4,6-trichlorphenol (2,4,6-TCP, $C_6H_3Cl_3O$), a common byproduct of wood pulp bleaching effluent, are two of the most acutely toxic chlorophenol isomers [154, 186]. Specific heterotrophic bacteria can achieve complete mineralization of these

priority pollutants, a fate for which physiochemical remediation methods fail [121]. A notable example of this is the *pcp*-encoded hybrid PCP degradation pathway in *Sphingobium chlorophenolicum* strain L-1 (as a result of two apparent horizontal gene transfers) and *S. chlorophenolicum* strain ATCC 39723. Degradation starts with PCP hydroxylation by PCP 4-monooxygenase (PcpB) to yield tetrachlorobenzoquinone (TCBQ). This compound is then reduced by a reductase (PcpD) to yield tetrachlorohydroquinone (TCHQ), which is then converted to 2,6-dichlorohydroquinione (2,6-DCHQ) via two dehalogenation reactions mediated by TCHQ dehalogenase (PcpC). Catalysis of 2,6-DCHQ to β-ketoadipate in *S. chlorophenolicum* strain ATCC 39723 occurs in three steps. First, 2,6-DCHQ undergoes oxidative cleavage to yield 2-chloromaleylacetate via 2,6-dichlorohydroquinone 1,2-dioxygenase (PcpA). The second and third steps involve two NADH-dependent reductive dechlorination steps mediated by maleylacetate reductase (PcpE) to generate β-ketoadipate (Figure 2.4) [186].

40
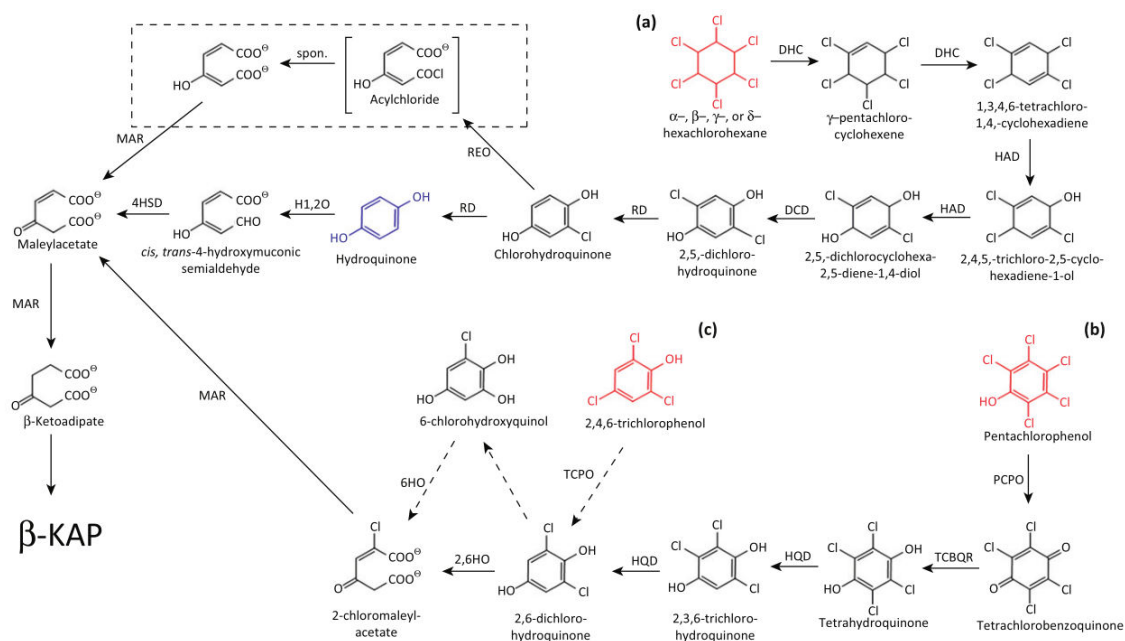
Figure 2.4. Degradation pathways for **(a)** hexachlorohexane stereoisomers and **(b)** pentachlorophenol by various sphingomonads and **(c)** 2,4,6-trichlorophenol by *Cupriavidus necator* JMP134. The dotted rectangle represents the hypothetical major catalytic route for (NADH-dependent) conversion of chlorohydroquinone to maleylacetate according to the literature [183]. Dotted arrows highlight the catalytic steps exclusive to C. necator JMP134. Pollutants are indicated in red, key intermediates are shown in blue, and the full names for enzyme abbreviations are listed in Appendix A.

The *tcp*-encoded bacterial biodegradation pathway of 2,4,6-TCP by *C. necator* JMP134, which has been described as a biodegradative agent for nitroaromatics, also involves a 2,6-DCHQ intermediate [130]. This catabolic route begins with two oxidation steps mediated by 2,4,6-TCP monooxygenase (TcpA) to yield 2,6-DCHQ and then 6-chlorohydroxyquinol. This intermediate is then cleaved between adjacent hydroxyl group moieties by 6-chlorohydroxyquinol 1,2-dioxygenase (TcpC) to yield 2-chloromaleylacetate. Finally, maleylacetate reductase (TcpD) mediates the reduction of both 2-chloromaleylacetate and the resulting maleylacetate to β-ketoadipate[186]. Variant strains expressing mutated maleylacetate reductase were still able to grow on maleylacetate, which suggests a redundant maleylacetate reductase pathway courtesy of genes such as *mnpE* (Figure 2.4; Appendix A)[130, 186].

2.3.4   *Hexachlorohexane*

Another prominent pesticide of the late 20th century is hexachlorohexane (HCH, $C_6H_6Cl_6$), which is the nonaromatic product of benzene photochlorination by UV light. Commercial production of HCH via this method generates an assortment of HCH stereoisomer byproducts, the most ubiquitous of which are α-HCH (60–70%), β-HCH (5–

12%), γ-HCH (10–12%), δ-HCH (6–10%), and ε-HCH (3–4%). Only γ-HCH (lindane) has technical biocidal properties; the remaining waste stereoisomers have similar or greater stability than γ-HCH. Many countries have prohibited the use of HCH because of the long residence times and high rates of accumulation of these waste stereoisomers. It is estimated that $4–6 \times 10^6$ tons of HCH waste exists worldwide, which equals the net amount of all other persistent organic pollutants combined [115, 166, 174]. The biodegradation pathway for α-, β-, γ, and δ-HCH stereoisomers has been studied in *Pseudomonas* strains and more recently in over 30 sphingomonads isolated from HCH-contaminated sites worldwide. For *S. japonicium* strain UT26, *S. indicum* B90A, and *Sphingobium* sp. strain BHC-A, the HCH stereoisomer degradation pathway involves an upstream series of five dehalogenation steps leading to the formation of 2,5-dichlorohydoquinione (2,5-DCHQ) and then downstream formation of HQ, with further degradation along the HQ degradation pathway and β-KAP(Figure 2.4) [130, 174].

2.3.5 *Future perspectives for biofuel synthesis*

Novel studies are currently examining the potential of the β-KAP as a means to produce bioenergy. New routes for biofuel production will abate the rising global demand for primary energy, which in 2010 was projected to increase by ~30% before 2040 [186]. Therefore, it is imperative to establish a sustainable supplemental fuel platform to better leverage reserves of limited and nonrenewable energy. Advancements in lignocellulosic pretreatment and biorefining technologies will be a key factor towards establishing this new fuel platform [26, 110, 156]. Lignin, a constituent of lignocellulosic biomass (10–35%), is a highly abundant and biorenewable 3D polyaromatic macromolecule produced

in secondary cell walls of plants. Industrial isolation of lignin by the pulp and paper industry amounts to approximately50 million tons per year, yet it is principally burnt as a non-optimized fuel in paper mill recovery boilers [183]. Industrially fragmented lignin is generally composed of distinct low-molecular-weight oligomeric polyaromatic components [196]. Theoretically, these aromatic remnants can be reused as feedstocks for catabolic degradation processes via the β-KAP in oleaginous microbes to yield acetyl-CoA, the basis for fatty acid biosynthesis, and ultimately lipids that are well suited for biodiesel applications [86].

The microbial degradation of lignin oligomers (comprising β-O-aryl ether, di-aryl propane, biphenyl, diaryl ether, phenylcoumarane, spirodienone, and resinol linkages) may involve extracellular lignin peroxidase or laccase enzymes to initiate the breakdown process [183]. Genes encoding lignin peroxidase (*dypA* and *dypB*) were recently identified in *Rhodococcus jostii* strain RHA1; along with complete sequencing of the *R. jostii* RHA1 genome and the relative speed and simplicity of growing bacteria, this finding heightens the prospect of producing lignin-degrading enzymes at an industrial scale [2]. The products of laccase and peroxidase degradation are further catabolized to metabolites of the β-KAP and typically involve a vanillate intermediate [170]. In *Sphingomonas paucimobilis* SYK-6, degradation of β-O-aryl ether-linked lignin monomers, which is the predominant linkage found in lignin derived from woody biomass (45–50% in softwood, 60% in hardwood), starts with NAD +-dependent oxidation of the α-hydroxyl functional group by a dehydrogenase (LigD). This results in a ketone product that is subject to further attack by in a unique reductive ether cleavage reaction. This unusual catalytic reduction incorporates two molecules of glutathione and

is mediated by a β-etherase (LigEFG) to yield a lignin monomer-based moiety. The resulting ketone product was detected in the lignin degradation sequences of Gram-negative and Gram-positive bacteria including *Pseudomonas putida* and *R. jostii* RHA1 and is also the product of a β-elimination reaction (Figure 2.5a). Further degradation of this intermediate may involve oxidation of the γ-hydroxyl group to generate a carboxylic acid, followed by cleavage of the aliphatic moiety in a reaction similar to fatty acid β-oxidation to yield vanillic acid. A tetrahydrofolate-dependent demethylase (LigM) mediates the conversion of vanillic acid to protocatechuic acid in *S. paucimobilis* SYK-6 for further degradation via the β-KAP pathway. In *Acinetobacter* and *Pseudomonas*, this same reaction is catalyzed by a non-heme iron-dependent demethylase enzyme. For the white rot fungus *Phanerochaete chrysosporium*, lignin peroxidase mediates the direct Cα–Cβ oxidative cleavage of β-O-aryl components to yield vanillin, which is converted to vanillic acid via vanillate dehydrogenase (Figure 2.5a; Appendix A) [183].
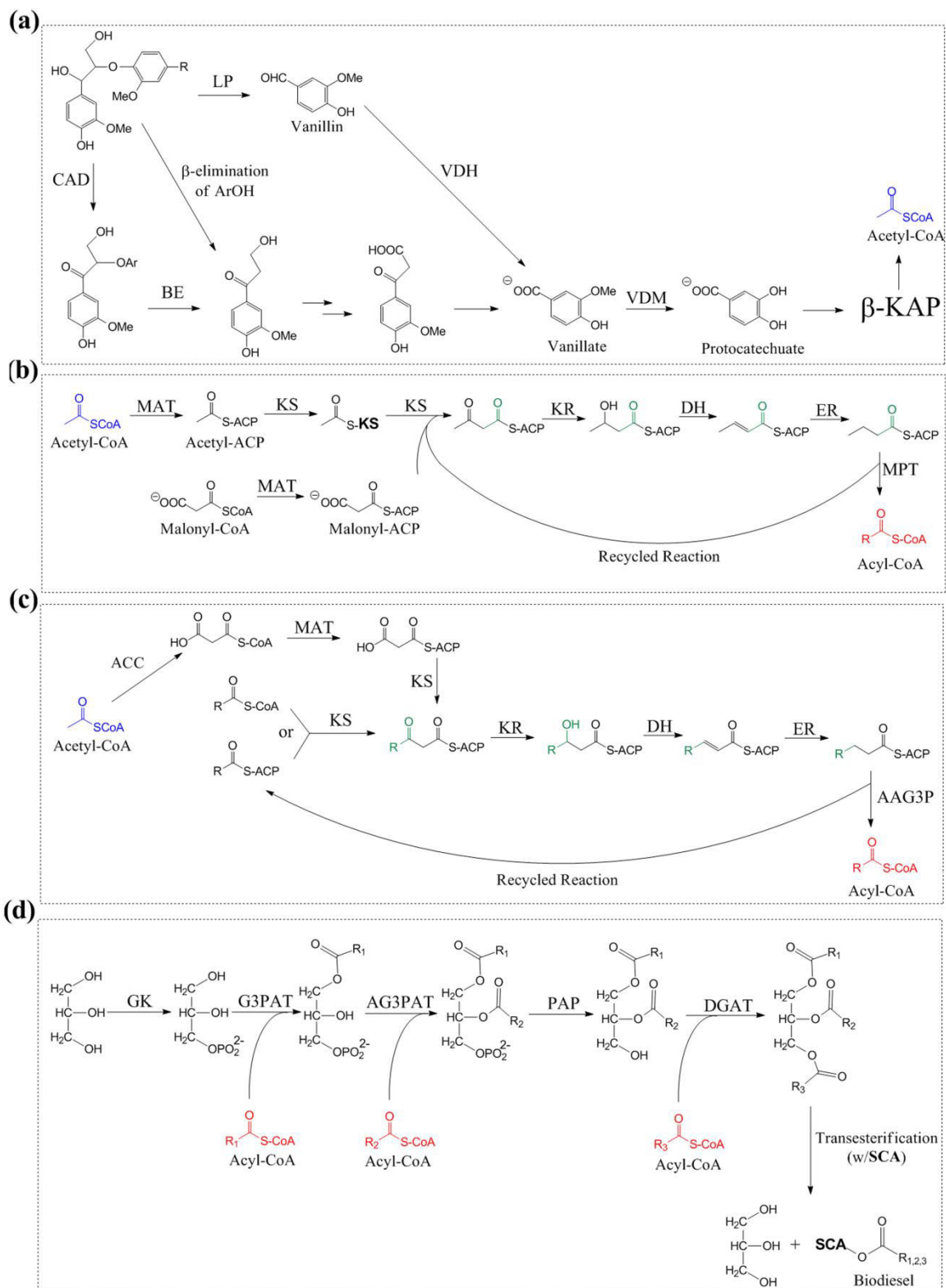
Figure 2.5. Proposed pathway for bioconversion of lignin to lipids, which can be transesterified to biodiesel, as detailed in three sequences: **(a)** conversion

of an exemplary β-O-aryl ether-linked oligomers to protocatechuate for further degradation via the b-ketoadipate pathway to yield acetyl-CoA (blue); fatty acid biosynthesis as classically understood in **(b)** yeast and **(c)** E. coli to yield acyl-CoA (red); and **(d)** generation of triacylglycerols and subsequent transesterification into biodiesel [86]. Newly incorporated atoms are highlighted in green and the full names for enzyme abbreviations are listed in Appendix A.

Acetyl-CoA generated via the β-KAP can be utilized to produce lipids via metabolic fatty acid biosynthesis, which is classically understood in yeast and *E. coli* (Figure 2.5b,c). The accumulated lipids synthesized during this process can be transesterified with short-chain alcohols (SCAs; ethanol or methanol) into fatty acid ethyl or methyl esters that are suitable for biodiesel applications (Figure 2.5d; Appendix A).

Use of the β-KAP for biofuel development was first explored by Kosa *et. al* who reported on the concept of lignin-to-lipid conversion with *R. opacus* PD 630 and DSM 1069 using aromatic compounds based on monolignol units as sole sources of carbon [86]. *Rhodococcus opacus* strains DSM 1069 and PD630 produced oleaginous levels of lipids when utilizing lignin model compounds (4-hydroxybenzoic and vanillic acids) as the sole carbon source. In a subsequent study, Kosa *et al.* demonstrated native pine lignin-to-lipid bioconversion with *R. opacus* DSM 1069 that resulted in limited accumulation of lipids (4.08% CDW) [87]. Overall, *R. opacus* has established potential for the conversion of certain lignocellulosic sugars or aromatics into microbial single cell oils [87, 92]. Lipid accumulation was stimulated during nitrogen-limiting conditions for both strains; however, DSM 1069 exhibited minimal nitrogen source dependence for adequate lipid accumulation. In addition, both strains demonstrated a preference for slightly alkaline pH (~8), which probably contributed favorably to substrate conversion

and membrane transport [86]. Fatty acid methyl esters derived from this method included

trans-palmitoleic, 10-methyl-hepatdecanoic, steric, and nonadecanoic acids, with an

overall saturated:unsaturated ratio of approximately 2:1 and no aromatic contaminants.

Overall, the lipids generated represented a composition that was deemed suitable for

biodiesel applications [86]. Future challenges in this area involve improving the

oleaginous limits of the adapted Rhodococcus strains and investigating lipid production

from alternative novel feedstocks including lignin derived from industrial pretreatment

methods.

CHAPTER 3: EXPERIMENTAL

3.1 Materials, chemicals, and bacteria

3.1.1   Reagents and microorganisms

Chemicals reagents were sourced from Sigma-Aldrich (St. Louis, MO, USA) and VWR (West Chester, PA, USA). Chemicals were used as received. Gases were purchased from Airgas (Radnor Township, PA, USA). *Rhodococcus opacus* strain DSM 1069 was purchased from the German Collection of Microorganisms and Cell Cultures (Deutsche Sammlung von Mikroorganismen und Zellkulturen, DSMZ).

3.1.2   Loblolly pine

All studies referring to Loblolly pine (*Pinus taeda*) refer to sample wood derived from a 15-year old tree from the University of Georgia plot in Baldwin Country, GA. This tree was 45-50 feet high, visually devoid of disease and compression wood. The wood was debarked manually, chipped, and then refined via Wiley mill (0.05" screen). Refined wood was measured to have a moisture content of 10.34%. Samples were stored below 0°C until implemented in experimentations.

3.1.3   EOL

Ethanol organosolv lignin was produced based on literature pertaining to an organosolv methodology for lodgepole pine (*Pinus contorta*)[124], however the feedstock in this case was loblolly pine.

3.1.4 Black liquor and kraft lignin

A table summarizing all varieties of lignin used in this study is provided in Appendix A. For Chapter 5, kraft lignin was sourced via the acidification and purification of black liquor following a previously published the method [88]. Black liquor was sourced from a commercial kraft pulp mill located in Southeaster USA. For Chapter 6, kraft lignin was sourced from black liquor via the LignoBoost process as described in literature [207], and is referred to as LignoBoost lignin (LBL) for the rest of this dissertation. This batch of black liquor was sourced from a commercial softwood kraft paper mill located in Western Sweden and provided to Chalmers University of Technology (Gothenberg, Sweden).

3.1.5 Fermentation media

Full media and minimal media solutions used for shake flask fermentations were prepared according to DSMZ recommendations[46]. The components of each solution are listed in Appendix A.

3.2 Experimental procedure

3.2.1 Soxhlet extraction of wood

Loblolly pine with an initial chemical composition of 64.3% sugars, 31.3% lignin, 3.4% extractives, and 1.0% ash on a dry weight basis was treated to Soxhlet extractions

performed with 2:1 toluene:ethanol solvent mixture for a duration of at least 48 h. Before

extraction, loblolly pine was milled into chips via a Wiley mill through a 5 mm mesh.

3.2.2   *Ethanol organosolv pretreatment (EOP) of loblolly pine*

Organosolv pretreatment of loblolly pine was performed according to Pan et al.

[124]. Parameters used in this experiment were 170 ºC, 1 h, biomass:solvent 1:8, 65%

EtOH, and 0.76 dry wt.% H_2SO_4. Exemplary and additional parameters are provided in

Appendix A for reference. Contents were cooked in a 1 gal Parr pressure reactor (Parr

Instruments, Moline, IL). Pretreatment effluent was obtained after separating the solid

cellulose-rich fraction.

3.2.3   *Preparation of pretreatment effluent for fermentation*

Pretreatment effluent separated from 3.2.2 was prepared for bacterial fermentation

by first adjusting the pH of the sample to 10.3 with NaOH. The solution was then passed

through a 0.2 µm filter and then neutralized with 2 M H_2SO_4 [87]. The resulting solution

was 1.5% w/v solids, from which 1.0 and 0.5% w/v dilutions were prepared using sterile

minimal media salt mixture, which are detailed in Appendix A. This sample was

implemented as a substrate for fermentation as detailed in Chapter 4.

3.2.4   *Fermentation parameters using R. opacus*

Fermentation experiments were performed by inoculating cells of *R. opacus* DSM

1069 into aerobic shaker tubes containing 10.00 mL of full media solution. Samples

were shook at 150 rpm at 30°C. When the optical density of the solution at 600 nm was

>0.6 (after 10 h) cells were centrifuged and washed thrice with minimal media solution. Cells were then re-suspended in 10.00 mL of minimal media and a volume of 0.10-1.50 mL was inoculated into larger shake flasks. Samples were acquired at a minimum of 12 h for at least five days.

3.2.5 *Kraft lignin extraction from black liquor*

Kraft lignin was separated from black liquor (BL) by diluting samples of BL in distilled water to 5% solids content. EDTA-2Na$^+$ was included at 5.00g/l concentration to chelate with metal ions and then the pH was reduced to 6 using 2 M H$_2$SO$_4$. Afterwards, the solution was stirred for 1 h and then acidified to pH 3. The solution was frozen over night, thawed, and then filtered through a medium-grade sintered glass funnel. The retentate was then dissolved in pH 3 aqueous H$_2$SO$_4$ solution to 5% solids and this freeze-thaw to filtration process was repeated thrice to ensure effective salt removal. Retentates were then air dried overnight and Soxhlet extracted with pentane to remove sulfur and extractive content for 48 h. Moreover, samples were dissolved (1 g/l) in a 9:1 dioxane:water solution. Residual impurities were then removed via filtration through a medium-grade sintered glass funnel. The removal of dioxane was performed under reduced pressure and verified via NMR analysis. Samples were freeze dried and a stored below 0°C until further use. The resulting highly purified kraft lignin sample was implemented in polymerization strategies detailed in Chapter 5. Lignoboost lignin (LBL) was obtained from black liquor via the LignoBoost process described in literature [207]. This sample of Lignoboost lignin was used in ultrasonication study described in Chapter 6.

3.2.6 Ultrasonication of lignin

For Chapter 5 and 6, all ultrasonic irradiation treatments were performed with a Model CU33 tapered ultrasonic cell disruptor horn (PGC Scientific, Frederick, MD) utilizing a 12.7 mm dia. tip and controlled with a GEX 500 ultrasonic processor (Sonics & Materials, Newton, CT, USA).For the Chapter 5 study, highly-purified Kraft lignin was dissolved in a pH 12 aqueous solution (adjusted with 5% NaOH, 2.66% w/v, 100.00 mL) and sonicated with an output amplitude of 35% for a total duration of 60 min at 15°C. Reaction samples (8.00 mL) were pipetted during continuous sonication treatment at specified intervals and immediately precipitated at pH 3 with H_2SO_4 (2.00 M), collected on a medium sintered glass funnel, washed with DI water, and lyophilized before further analysis.

For the Chapter 6 study, LBL was dissolved in an aqueous alkaline solution (3.50% w/v). The alkalinity of the solution was adjusted to pH 10 with 2M NaOH, which is approximate to the pK_a of several prominent guaiacyl-type moieties found in softwood lignin[142]. Volumes of 4 mL were sonicated for 30 min at 15°C at amplitude settings of 25% (~30 µm) and 50% (~60 µm), which were used to measure the effects of low and high intensity sonication, respectively. After sonaration, LBL samples were precipitated by acidification to pH 3 with 2M H_2SO_4, washed with a porosity grade 4 (10-16 µm) sintered glass funnel, lyophilized, and stored at 0°C before further analysis.

3.3 Analytical procedures

3.3.1 Carbohydrate analysis of fermentation broth

Carbohydrate profiles were measured with HPAEC-PAD on a Dionex ICS-3000 ion chromatography with CarboPactm PA-1 column set at 23°C. Eluent A was 100% DI water (18 MΩ-cm) and eluent B was 200 mM NaOH. The flow rate was 0.3 mL/min[187].

3.3.2 Molecular mass determination of aromatic lignocellulosic constituents

For Chapters 4 and 5, lignin was first acetylated by dissolving samples (20 mg) in 1:1 solution of acetic-anhydride:pyridine and stirring at room temperature for 72 h. The solvent mixture was then removed under reduced pressure at 50°C. The acetylated lignin was then dissolved in 50 mL of chloroform and washed with 20 mL of DI water. The organic fraction was then dried over anhydrous $MgSO_4$ and filtered through a medium sintered glass funnel. The chloroform was removed under reduced pressure at 50°C. Lignin samples were then solvated with tetrahydrofuran (1 mg/mL) and filtered through a 0.45 µm PTFE membrane before GPC analysis. Samples were injected into a Agilent GPC Security 1200 system equipped with four WatersStyragel ® 7.8 × 300 mm columns: HR6, HR4, HR2, and HR0.5(Milford, MA, USA) and an Agilent UV detector set to a wavelength of 270 nm. THF was utilized as the mobile phase(1.00 mL/min) with an injection volume of 20 µL. A calibration curve was constructed based on ten narrow polystyrene standards ranging in molecular mass from 9.4×10^1 to 3.64×10^6 g/mol. Data collection and processing was performed using Polymer Standards Service WinGPC Unity software (Build 6807).

For Chapter 6, lyophilized lignin samples were dissolved in DMSO with 10 mM LiBr, which was also utilized as an eluent. Samples passed through a 0.2 µm filter and were then injected into a PL-GPC 50 Plus integrated GPC System equipped with two PolarGel-M columns (300 x 7.5 mm), a guard column (50 x 7.5 mm), an inline RI and UV detector (270 nm), and a PL-AS RT auto-sampler (Polymer Laboratories, Varian Inc.). Molecular weight determinations were based on the elution time of a ten-point Pullulan calibration curve ranging from 1.80 x 10^2 to 7.08 x 10^5 g/mol (PL2090-0100, Varian). All reported values are a mean of triplicate measurements. Data was analyzed with Cirrus GPC version 3.2.

3.3.3 FT-IR spectroscopy of lignin

FT-IR spectra were obtained using a Perkin-Elmer Spectrum 100spectrophotometer equipped with a DATR 1 bounce diamond/ZnSe universal attenuated-total-reflection (ATR) sampling accessory (PerkinElmer, Waltham, MA).Spectra were obtained in the 650–4000 cm^{-1} range and for each sample 16 scans were taken at a resolution of 4 cm^{-1}.

3.3.4 NMR spectroscopy of lignin

NMR experiments were performed at room temperature using a400 MHz Bruker AMX-400 spectrometer (Billerica, MA, USA).^{13}C-NMR spectra were acquired using deuterated dimethylsulfoxide (DMSO)-d6 (600 µL) as the solvent for the kraft lignin samples (100 mg), with an inverse-gated decoupling sequence, 90° pulse angle, 12 s pulse delay, 220 ppm sweep width, 3200 scans, and 0.63 acquisition time. Quantitative

^{31}P NMR were acquired after in situ derivatization of the samples using 21.0 mg of lignin with 2-chloro-4,4,5,5-tetramethyl-1,3,2-dioxaphospholane(TMDP) in a solution of (1.6:1 v/v) pyridine/$CDCl_3$, chromium acetylacetonate (relaxation agent), and endo-N-hydroxy-5-norbornene-2,3-dicarboximide (NHND, internal standard). The spectrum was acquired using an inverse-gated decoupling sequence, 90° pulse angle, 25 s pulse delay, 128 scans, and 0.77 s acquisition time. NMR data were processed using TopSpin 2.1 software (Bruker BioSpin).

3.3.5   TGA analysis of lignin

TGA was performed using a Perkin Elmer TGA 7 analyzer. Experiments were conducted with a nitrogen gas flow of 20.0 ml/min and a temperature range of 23-500°C. Data was analyzed with Pyris version 7.

3.3.6   Error Analysis

The margin of error associated with HPAED-PAD were below ±1%. Multiple measurements of the same sample for NMR resulted in ±4.0% semi-quantitative ^{13}C-NMR, ±2.0% quantitative ^{1}H-NMR, and ±1.8% quantitative ^{31}P- NMR. Estimated total lipid contents via GC-MS are within ±2.88% error margin. Dry mass of samples were calculated to the nearest milligram. GPC was assessed with a calibration curve fit with a 2nd order polynomial fit function with an error margin no greater than ±2%. TGA analysis was performed in triplicate with an error margin below ±1%.

CHAPTER 4: BIOCONVERSIONOF LIGNOCELLULOSIC PRETREATMENT EFFLUENT VIA OLEAGINEOUS RHODOCOCCUS OPACUS DSM 1069

4.1   Introduction

Metabolic conversion of plant biomass into biofuel can broaden the application of lignocellulose and thereby optimize integrated biorefinery strategy while reducing the carbon footprint incurred with fossil fuel usage [22, 57, 70, 102, 195, 205]. Cellulose is a predominant component of lignocellulosic biomass that has broad utilization in both biomaterial and bioenergy production [135]. Yet, in wood, direct chemical access to cellulose is impeded due to a recalcitrant lignin-hemicellulose matrix that surrounds cellulosic polymers [134]. To overcome this challenge, pretreatment strategies are implemented in order to degrade, solubilize and reduce the overall recalcitrance of this matrix and provide greater access to cellulose fibrils for subsequent chemical processes [139]. Common industrial pretreatment strategies that are being optimized for biorefinery include steam explosion, dilute acid and organosolv pretreatment [18, 98, 101, 124, 128, 134, 139, 179].Notably, these methods generate a secondary aqueous effluent that is predominantly enriched with degraded hemicellulose and lignin oligomers among other components such as deteriorated units of amorphous cellulose and furan-based compounds [45, 150]. Currently, these effluent fractions are often discarded as industrial wastewater with limited utilization [42, 107, 122, 149, 150]. Alternatively, a more optimal usage of pretreatment effluents may be to use this complex mixture of solubilized compounds as a feedstock for the development of microbial lipids that are composed of energy-rich triacylglycerols that can be implemented as a fungible fuel for

diesel engines after transesterification or hydrotreatment [47, 89, 122, 184]. Such a system can improve biorefinery carbon efficiency while reducing collateral pollution generated during the pretreatment of lignocellulosic biomass. Additionally, the bioconversion of an industrial waste stream to biodiesel as a commercial product presents an intriguing potential means of enhancing cost effectiveness for integrated biorefineries.

The production of microbial biodiesel has been extensively studied among microorganisms that have the quality of being oleaginous, which is defined as being capable of accumulating over 20% of cellular dry weight in intracellular lipids (>20% CDW) [89, 102]. For example, Alvarez *et al.* demonstrated high rates of oleaginicity (>80% CDW) by *R. opacus* using glucose, an essential carbohydrate of prokaryotic fatty acid synthesis and a major component of lignocellulose [4, 5]. *R. opacus* also employs the β-ketoadipate pathway (β-KAP), which is an enzyme mediated aryl-ring degradation sequence that converts certain substituted cyclic aromatic moieties common to lignin into acetyl-CoA, a major precursor for fatty acid biosynthesis [184]. The β-KAP was explored by Kosa *et. al* who reported on the concept of lignin-to-lipid conversion with *R. opacus* PD 630 and DSM 1069 using aromatic compounds based on monolignol units as sole sources of carbon [86]. In a subsequent study, Kosa *et al.* demonstrated native pine lignin-to-lipid bioconversion with *R. opacus* DSM 1069 that resulted in limited accumulation of lipids (4.08% CDW) [87]. Overall, *R. opacus* has established potential for the conversion of certain lignocellulosic sugars or aromatics into microbial single cell oils[87, 92]. Interestingly, the simultaneous conversion of these two components may provide improved oleaginicity, a unique and efficient approach to biodiesel production, and a novel route for biorefinery waste stream optimization.

Therefore we assess the use of pretreatment effluent as a sole resource of carbon and energy for cellular growth and development of lipids by oleaginous *R. opacus* DSM1069 as detailed in Figure 4.1. Cellular dry weight (CDW), total cell concentration as measured by optical density (OD), living cell concentration (colony forming units/mL, CFU/mL), and the percentage of accumulated lipids (% CDW) were measured throughout fermentation. The compositions and total content of the accumulated lipids at different periods during fermentation were characterized with gas chromatography-mass spectrometry (GC-MS). The effluent substrate was characterized with respect to the remaining proportion of monosaccharides via high-performance anion exchange chromatography with pulsed amperometric detection (HPAEC-PAD) and the determination of the molecular weight of solubilized aromatic components via gel permeation chromatography with UV detection (GPC).
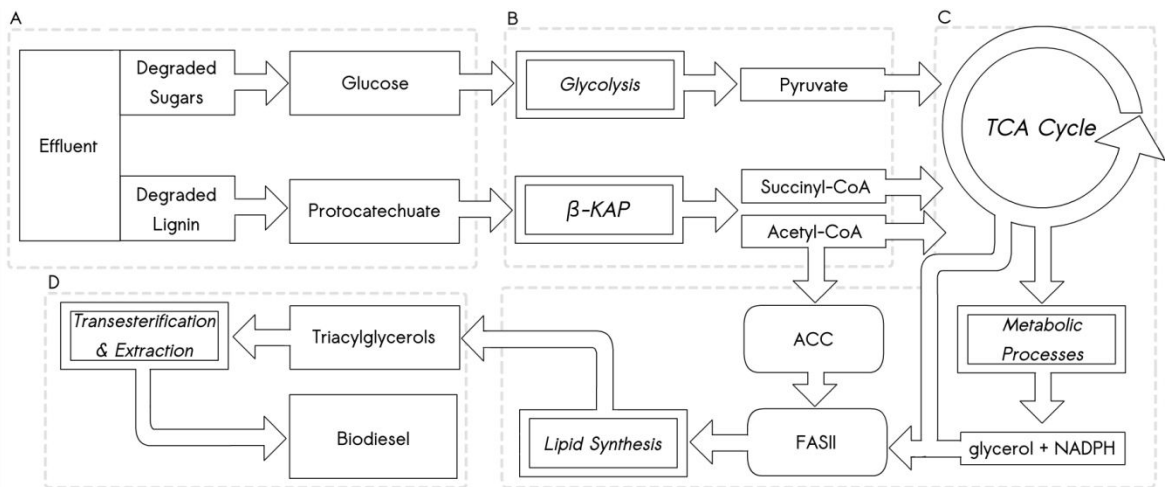
Figure 4.1. Overview of the bioconversion of pretreatment effluent into biodiesel via oleaginous *R. opacus* DSM 1069.(A) Effluent enriched with degraded oligosaccharides and lignin is processed by bacteria. (B)Through glycolysis, glucose is converted into pyruvate while protocatechuate is converted into succinyl-CoA and acetyl-CoA via the β-ketoadipate pathway (β-KAP). (C) These products may enter the TCA cycle or acetyl-

CoA may ultimately be implemented as a co-product by acetyl-CoA carboxylase (ACC) and fatty acid synthase II (FASII) towards lipid synthesis[184]. (D) Intracellular lipids are accumulated in the form of triacylglycerols, which may be transesterified into fatty acid methyl esters (FAMEs) well suited as biodiesel[89].

4.2 Materials and Methods

EOP effluent was obtained from the organosolv pretreatment of softwood loblolly pine (*Pinus taeda*) [124]. In brief, loblolly pine chips with an initial chemical composition of 64.3% sugars, 31.3% lignin, 3.4% extractives, and 1.0% ash on a dry weight basis were Soxhlet extracted (toluene:ethanol 2:1 solvent mixture, 48 h) and then organosolv pretreated (170ºC, 1 h, biomass:solvent 1:8, 65% EtOH, 0.76 dry wt.% H_2SO_4). The aqueous fraction was separated from solids based on published methods [68, 124]. The pH of the sample was then increased to 10.3 with 2 M NaOH, sterilized by passing through a 0.2 µm filter, and then neutralized with 2 M H_2SO_4 [87]. The resulting solution was 1.5% w/v solids, from which 1.0 and 0.5% w/v dilutions were prepared using sterile minimal media.

Fermentation procedure, including medium contents and growth conditions were performed based on established literature [87]. Cell growth monitoring, methanolysis and GC-MS procedures were followed according to established literature [86, 87]. Estimated total lipid contents are within ±2.88% error margin. Fermentation broth was centrifuged to generate a bacterial pellet for cell growth monitoring. The supernatant was stored at 0ºC for HPAEC-PAD and GPC analysis, as described previously [69, 87].

4.2 Results and discussion

4.2.1 Fermentation

The fermentation experiment detailed in Chapter 4 can be aptly understood as a three-part process composed of sequential stages: a *cell harvesting stage*, an *adaptation stage*, and a *lipid accumulation stage*, Figure 3.2. The purpose of the *cell harvesting stage* is to amass enough bacteria to initiate the experiment; and this was done by inoculating bacterium into 50 mL aerobic shaker tubes containing 10.00 mL of full media. The components of full media are listed in Appendix B. The duration of the cell growth was 10 h, at which point the cellular density of the solution, as determined by OD, increased from undetectable limits to 0.6. The amassed population of cells were converted into a pellet by centrifugation and washed with 20.00 mL thrice to remove traces of full media. These washed cells were then resuspended in 20.00 mL of minimal media and a 1.50 mL aliquot of this solution was used for the initial adaptation step.

Cell Harvesting Stage

Cell Conc. (OD): 0.0 to 0.6 in 10 h

Substrate: Full Media

Adaptation Stage

Cell Conc. (OD): 0.0 to 1.0 in 72 h

Substrate: Effluent

Lipid Accumulation Stage

Cell Conc. (OD): 0.0 to 0.6 in 60 h

Substrate: Effluent w/reduced N
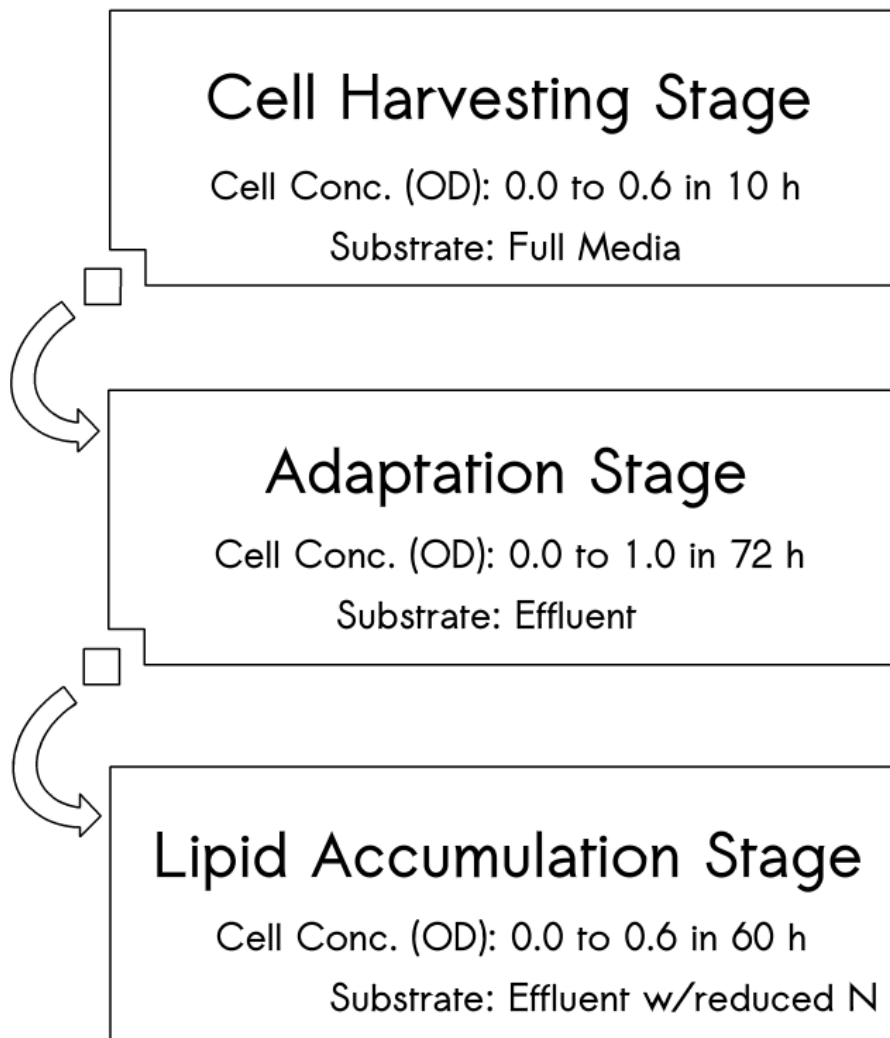
Figure4.2. Timeline of fermentation stages with *R. opacus* DSM 1069. Cells were harvested with full media for 10 h where the cell concentration based on optical density (OD) increased from 0.0 to 0.6. A small inoculum was then transferred to the adaptation stage where the cellular concentration increased from 0.0 to 1.0 in 72 h. Finally, an inoculum of these cells was transferred to the lipid accumulation stage where the cell concentration increased from 0.0 to 0.6 h in 60 h. The duration of the final stage was extended for an additional 60 h, for a total of 120 h. Overall, microbes were exposed to effluent as a substrate for 192 h. "N" during the lipid accumulation stage refers to nitrogen source.

The purpose of the *adaptation stage* was to provide a period for the cells to

acclimate to different concentrations of pretreatment effluent in an effort to determine a

feasible parameter set for the final lipid accumulation step. The adaptation stage was performed with 150.00 mL of 1.5, 1.0, and 0.5 w/v% concentrations of pretreatment effluentwith 0.10 w/v% nitrogen source provided by DSMZ minimal salt media solution. Salt media solution ingredients are provided in Appendix B. Observably, after the cell harvest stage inoculums were added to each of the adaptation stage solutions, the cell densities of three samples were initially undetectable with OD analysis. This was expected and also implicated that, in order for a low concentration of cells to proliferate to a significant cell density, the microbes would be forced to use the available materials in the effluent as a source of carbon in very much the same manner as how DSM 1069 utilized full media as a substrate during the cell harvesting stage. Alternatively, cells that were unable to adapt to the effluent or were exposed to an inadequate supply of resources for a considerable duration would ultimately perish despite any energy accumulated during the cell cultivation step.

The results of the adaptation step were collected after 72 h, only cells exposed to the highest effluent concentration of 1.5 w/v% survived; this concentration amassed a cellular density that corresponded to an OD of 1.0 and a CFU/mL magnitude of 10^7. Consequently, these surviving cells were pelleted and washed thrice with minimal media and then resuspended in 20.00 mL of minimal media solution. From this solution, a 1.50 mL aliquot was removed for the lipid accumulation stage. The remaining volume of cells provided a yield sufficient for oleaginicity calculation, which was determined to be 22.09% CDW (± 2.88%).

The lipid accumulation stage was performed with 150.00 mL of 1.5w/v% concentrations of pretreatment effluent with minimal salt media for duration of 120 h.

Notably, this stage was unique compared to the adaptation step in light of two significant distinctions. Firstly, the nitrogen content of the salt media was reduced from 0.10 to 0.05 w/v%, thereby limiting available nitrogen needed for cellular replication so that more energy could theoretically be devoted towards the production of oils. Secondly, the inoculums utilized in this step contained cellular matter that was predominantly derived from solubilized pretreatment effluent material. Hence, the performance of cells during the lipid accumulation step largely reflected microbes with cellular mass fully derived from pretreatment effluent.

4.2.2 Cell growth characterization

When the pretreatment effluent containing degraded aromatic and carbohydrate plant polymers and minimal media solution (Appendix A) was utilized as a sole source of carbon and energy with a concentration of 1.5 w/v% with 0.05 w/v% nitrogen content, cells exhibited viable growth patterns. As illustrated in Figure 4.2, CFU/mL increased over 15,000-fold to a magnitude of 10^5 during the 0-48 h interval of incubation, which indicated a rapid proliferation during this timeframe. Likewise, OD and CDW also improved during this period. At 48 h, an oleaginous amount of accumulated lipid content was determined at 26.88% CDW. During the 48-96 h timeframe, the accumulated lipids percentage depleted resulting in leaner, considerably lighter cells as reflected by a decrease in CDW and level OD. The utilization of SCOs as an intracellular energy reserve prolonged cell viability while also limiting further proliferation as indicated by the reduced rate of propagation by CFU and stagnating OD during the 48-96 h interval, respectively. At 96 h, lipid reserves were nearly expended at 1.68% CDW. Afterwards,

the CDW continued to decrease and CFU sharply declined, indicating the apparent

starvation of cells. To review, cells were capable of rapid proliferation during 0-48 h,

then likely consumed remaining exploitable resources resulting in the depletion of

intracellular lipids during 48-96 h, and finally experienced acute starvation from 96-120

h.

No contaminations were detected based on the results of SPD throughout

fermentation. Moreover, living cells collected at 120 h were returned to full media and

later identified as *R. opacus* with an optical microscope. Fermentation trials utilizing 1.0

and 0.5 w/v% concentrations of effluent resulted in complete cell death within 48 h.
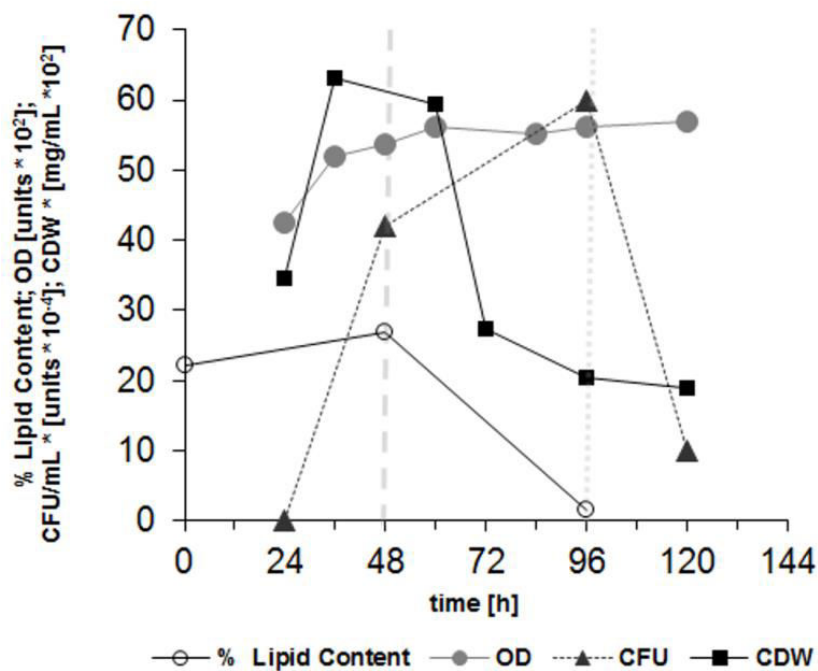
Figure4.3.   Growth of *R. opacus* DSM 1069 during incubation with pretreatment
effluent as a sole carbon source. Periods are separated at 48 h (dashed
line) and 96 h (dotted line). The initial percentage of lipid content
corresponds to the final lipid content measurement during previous
fermentation when cells were utilizing effluent as a sole substrate but with
0.10 w/v% nitrogen content based on fermentation methodology described

elsewhere [87]. Optical density (OD) and cell dry weight (CDW) were multiplied by 10^2 while colony forming units (CFU) were divided by 10^4 to enable a more optimal visual comparison within the same chart. CFU value at 24 h is 0.0025 CFU/mL.

4.2.3   HPAEC-PAD analysis of sugar monomer fractions during fermentation

The results of HPAEC-PAD are illustrated in Figure 4.3. The monosaccharide composition and initial order of abundance were typical of softwood hemicellulose: mannose, xylose, glucose, galactose, and arabinose, respectively[113]. During 0-48 h, the concentration of glucose monomers was preferentially depleted, which occurred alongside the rapid proliferation timeline established with CDW, CFU/mL, and OD measurements. This indicates that glucose was a key substrate for cell growth during the 0-48 h interval. During 48-96 h, concentrations of glucose fell below detectable levels. This period coincided with the interval of decreased proliferation and distinct lipid catabolysis that was indicated during cellular growth characterization. Fluctuations of glucose concentrations during this interval may be attributed to the bacterial degradation of low molecular weight cellulose and subsequent freeing of glycosyl units. The minor depletion of mannose and xylose during this timeframe may possibly be due to an unsuccessful attempt by cells to degrade and metabolize alternative sugars since the inability of wild type DSM 1069 to metabolize alternative plant sugars such as xylose is well documented [192].
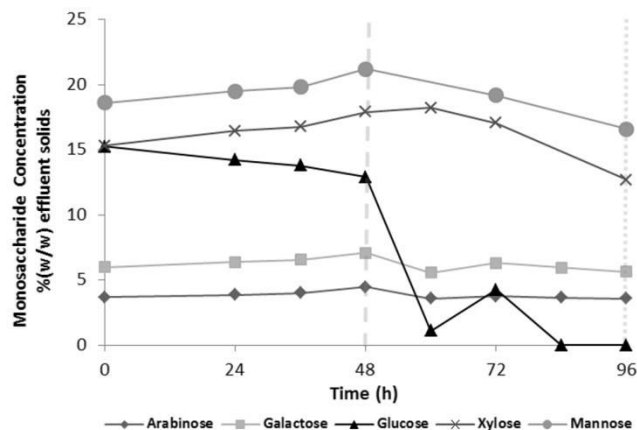
Figure4.4. Concentrations of monosaccharide during fermentation with *R. opacus* DSM1069 determined via HPAEC-PAD. Intervals are separated at 48 h (dashed line) and 96 h (dotted line).

4.2.4 *GPC analysis of aromatic constituents in substrate*

The molecular mass distribution profiles of aromatic compounds based on GPC analysis with UV detection were recorded during the 0 h, 48 h, and 96 h interval of incubation with results illustrated in Figure4.4. Each of the retention curve profiles were trimodal and asymmetric. The single major peak and two minor peaks corresponded to molecular masses of 5.0×10^2 g/mol and $1.5\text{-}2.5 \times 10^2$ g/mol, respectively. The significant change from 0-48 h was the depletion of minor peaks, which support that low molecular weight aromatics were degraded simultaneously with sugars during this interval. The rate of aromatic degradation increased during 48-96 h when cell density had reached an apex and glucose concentrations had been depleted.

66
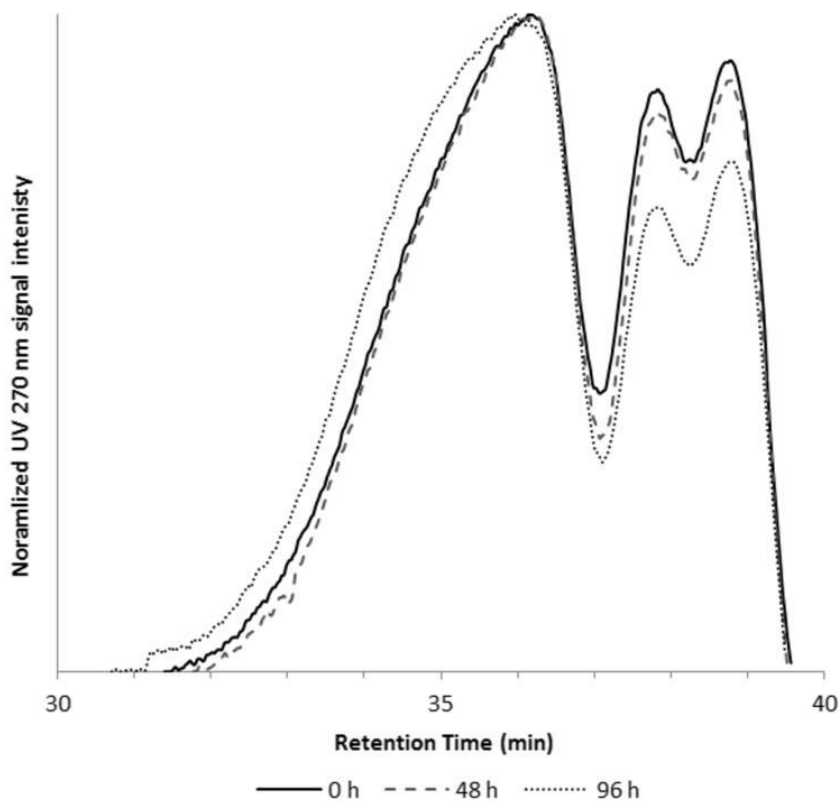
Figure 4.5. Retention curve profiles of pretreatment effluent at the 0 h (solid line), 48 h (dashed line), and 96 h (dotted line) interval after exposure to DSM 1069 during lipid accumulation stage. The single major peak and two minor peaks refer to molecular masses of 5.0 x 10^2 g/mol and 1.5-2.5 x 10^2 g/mol, respectively.

4.2.5 Lipid characterization of FAMEs via GC-MS

The transesterification of cellular lipids was performed at the 0 h, 48 h, and 96 h interval of incubation. The compositions of the resulting FAMEs were characterized via GC/MS with results summarized in Figure 4.5. Overall, the FAME compositions at 0 h and 48 h were consistent and chiefly composed of even number carbon fatty acids. In detail, the proportions were ~30% 9-octadecenoic (oleic, C18:1), ~20% of hexadecanoic (palmitic, C16:0), and ~17% octadecanoic (stearic, C18:0) acid, followed by smaller fractions of FAMEs composed of ~9% heptadecanoic (margaric, C17:0), ~7.5% 9-

hexadecenoic (palmitoleic, C16:1), ~7% cis-10-heptadecenoic (C17:1), ~5%

pentadecanoic (C15:0), and ~4.5% tetradecanoic (myristic, C14:0) acid. The highest

proportion of oleic acid was recorded at 0 h and the lowest at 96 h. These results

coincide with previous reports regarding the development of microbial lipids from DSM

1069 using lignocellulosic material as a feedstock [89]. Accordingly, yields at 48 h, the

highest recorded point of oleaginicity were calculated such that the mass of lipids

produced per mass consumed (Y_{lipid}) was 0.06 (g/g) and mass of cells produced per mass

consumed (Y_{cell}) was 0.25 (g/g).
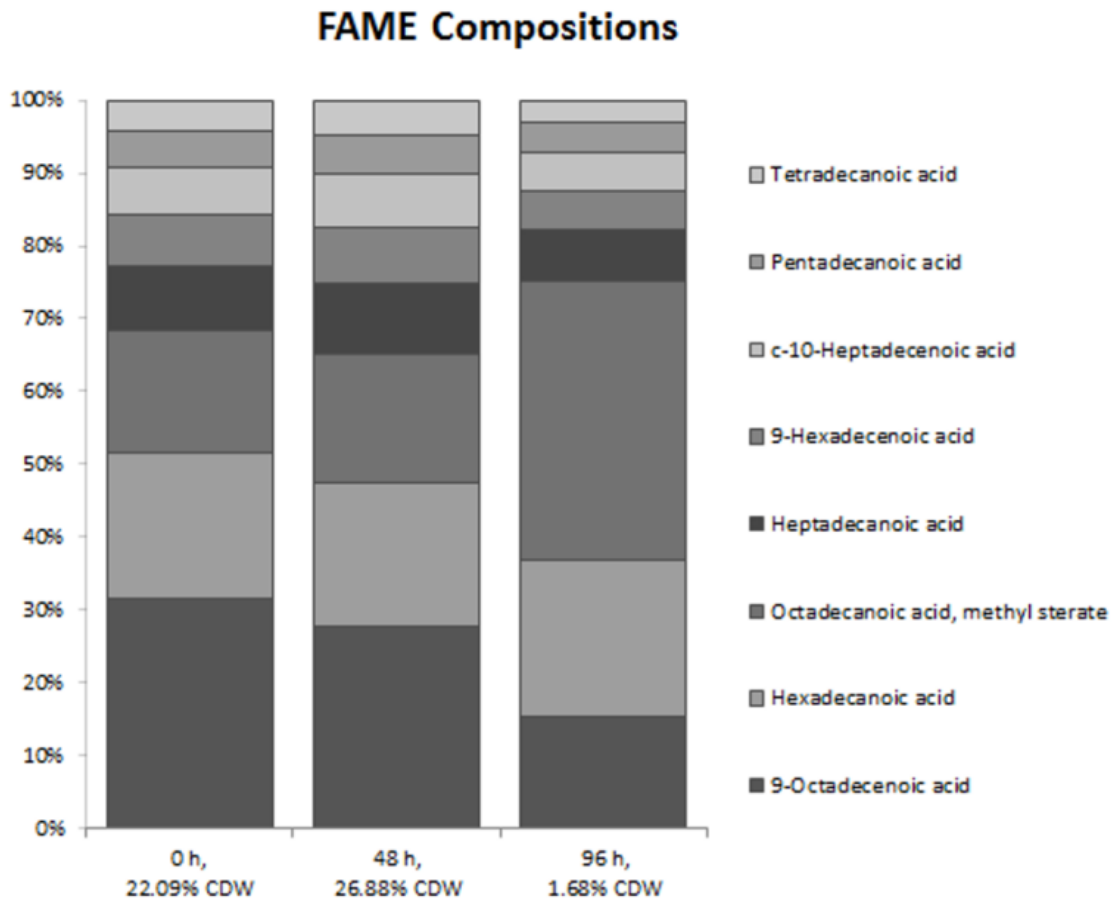
Figure4.6. Composition of FAMEs at the 0 h, 48 h, and 96 h interval of the lipid accumulation phase.

4.2.6   Conclusions

Unmodified *R. opacus* DSM 1069 can simultaneously utilize sugars and aromatics derived from lignocellulosic effluents as a sole carbon and energy resource towards the development and accumulation of single cell oils at oleaginous yields, here determined at 26.88% CDW. Currently, yields were on the order of 0.06 grams of lipids produced per 1.00 gram of carbon consumed. Upon transesterification, the composition of FAMEs were determined to be largely composed of even numbered monounsaturated and saturated fatty acids that included oleic, palmitic, and stearic acid. Overall, these results establish that certain agricultural and forestry waste effluents enriched with lignin-derived aromatics and wood sugars can be utilized as a feedstock by oleaginous DSM 1069 towards the production of biofuel, thereby providing a comprehensive and sustainable route towards biorefinery optimization. These results establish a promising foundation for further studies involving the search for alternative or genetic engineering of oleaginous soil bacteria for the purpose of optimizing single cell oil yields and improving carbon efficiency.

In contrast to current literature, this is the first oleaginous (>20% CDW) fermentation using bacteria and substrate derived from woody biomass. The closest parallel studies were conducted by Alvarez *et al.* who demonstrated 80% CDW in *R. opacus* using commercial glucose and Kosa *et al.* who recorded non-oleaginous (<5% CDW) development of lipids using highly purified kraft lignin derived from black liquor as a sole source of carbon and energy [5, 88]. Furthermore, this is also the first case of utilizing industrial waste contaminated with aromatics as a substrate for lipid and biofuel

development. This presents an intriguing and novel route for industrial waste stream optimization.

CHAPTER 5: POLYMERIZATION OF KRAFT LIGNIN VIA ULTRASONICATION WITH SUSTAINED CAVITATION

5.1   Introduction

Lignin is one of the major components of the secondary cellular wall of plants and has a remarkably complex structure. The biomacromolecule exists as a three-dimensional aromatic polymer composed of monolignol monomers: sinapyl, *p*-coumaryl, and coniferyl alcohol. These monolignols are consolidated into the macromolecular structure of lignin units including syringyl (S), *p*-hydroxyphenyl (H), and guaiacyl (G), respectively. After cellulose, lignin is the second-most common biopolymer on earth, and it is industrially accumulated at a rate of millions of tons per year by the global chemical pulping industry [118]. Delignification on an industrial scale encompasses an extensive variety of methodologies (e.g., ethanol organosolv pulping, sulfite and sulfate process) that result in an isolated lignin polymer with unique properties and potentials for biomaterial applications[11, 99, 153]. Kraft lignin is a fragmented and alkaline-soluble version of lignin produced during the Kraft (sulfate) pulping process. During this procedure, woodchips are cooked with NaSH and NaOH in order to cleave lignin alpha- and beta-aryl ether linkages thereby solubilizing lignin fragments. Currently, an estimated 98% of Kraft lignin is burned as a non-optimized energy resource within the pulp mill recovery boiler in order to recover energy and pulping chemicals[182]. This low-value use of Kraft lignin and the capital costs associated with a recovery furnace has spurred research to repurpose the polymer for higher-utility functions; and while Kraft

lignin can be upgraded as a biofuel [21], alternative enhancements may significantly broaden the range of new and value-added chemical applications.

Previous studies have demonstrated that Kraft lignin can be repurposed for the generation of value-added low-molecular weight (LMW) and HMW compounds. The degradative conversion of Kraft lignin towards LMW compounds has yielded practical chemicals such as dimethyl sulfoxide, phenols and aromatics (e.g., vanillin) . HMW applications of Kraft lignin include the generation of adhesives, carbon fibers, and thermally-stable copolyester but necessitate an upgrading process that increases the DP. These potential uses have increased the demand for HMW lignins, which has initiated research based on suitable lignin polymerization strategies [51, 82, 175, 182].

Ultrasonic polymerization has steadily gained interest since 1950 where it was first introduced as a means to cross-couple acrylonitrile in aqueous systems. Since that time, ultrasound has been incorporated into a wide variety of polymer-based applications including the synthesis of homo- and copolymers, preparation of hydrogels, and the activation of free radical initiators. Ultrasonic polymerization relies on the generation of highly reactive free radicals in solution, which can be caused by cavitation. Cavitation occurs during the rarefaction sequence of an applied sonication wave, which causes the formation of solvent cavities when the solution pressure drops below ambient. These expanding gas pockets rigorously collapse due to escalating stresses in their walls, releasing large amounts of energy in the form of high local pressure and temperatures. The onset and intensity of cavitation is influenced by various factors including the viscosity of the solution and duration of ultrasonic treatment [173, 182].

In this study, Kraft lignin derived from pine was subjected to sustained cavitation with the goal to increase DP and to analyze the stereochemical effects of the ultrasonic polymerization process. Changes in DP and structure were determined before, during and after the onset of cavitation while ultrasonication occurred. The weight-average molar mass (Mw), number-average molar mass (Mn), and polydispersity index (PDI, calculated as Mw /Mn) of the lignin samples were characterized via gel permeation chromatography (GPC), while FT-IR, ^{13}C and ^{31}P-NMR spectroscopy were used to discern structural changes caused by ultrasonic irradiation.

5.2 Materials and Methods

5.2.1. Materials and ultrasonication of Kraft lignin

Softwood Kraft black liquor was received from a commercial Kraft pulp mill located in Southeastern USA and the lignin was isolated from the cooking liquor following published methods [182]. All ultrasonic irradiation treatments were performed with a ModelCU33 tapered ultrasonic cell disruptor horn (PGC Scientific, Frederick, MD) utilizing a 12.7 mm dia. tip and controlled with a GEX 500 ultrasonic processor with an output amplitude of 35% (Sonics & Materials, Newton, CT, USA). The isolated Kraft lignin was dissolved in a pH 12 aqueous solution (adjusted with 5% NaOH, 2.66% w/v, 100.00 mL) and sonicated for a total duration of 60 min at 15°C. Reaction samples (8.00 mL) were pipetted during continuous sonication treatment at specified intervals and immediately precipitated at pH 3 with H_2SO_4 (2.00 M), collected on a medium sintered glass funnel, washed with DI water, and lyophilized before further analysis.

73

5.2.2. Molecular weight determination and spectroscopic characterization of Kraft lignin

Molecular weight determinations were performed using an Agilent GPC Security 1200 system equipped with four Waters Styragel ® 7.8 × 300 mm columns: HR6, HR4, HR2, and HR0.5 (Milford, MA, USA) and an Agilent UV detector set to a wavelength of 270 nm. THF was utilized as the mobile phase(1.00 mL/min) with an injection volume of 20 µL. A calibration curve was constructed based on ten narrow polystyrene standards ranging in molecular mass from 9.4×10^1 to 3.64×10^6 g/mol. Data collection and processing was performed using Polymer Standards Service WinGPC Unity software (Build 6807). Lignin was acetylated prior to measuring and whole curve integration was performed referring to published methods [182]. All reported values for M w , M n and DP were the mean of triplicate samples. FT-IR spectra were obtained using a Perkin-Elmer Spectrum 100spectrophotometer equipped with a DATR 1 bounce diamond/ZnSe universal attenuated-total-reflection (ATR) sampling accessory. Spectra were obtained in the 650–4000 cm^{-1}range and for each sample 16 scans were taken at a resolution of 4 cm^{-1}. NMR experiments were performed at room temperature using a Bruker AMX-400 spectrometer.^{13}C-NMR spectra were acquired using deuterated dimethylsulfoxide (DMSO)-$_{d6}$ (600 µL) as the solvent for the Kraft lignin samples (100 mg), with an inverse-gated decoupling sequence, 90° pulse angle, 12 s pulse delay, 3200 scans, and 0.63 acquisition time. Quantitative ^{31}P NMR were acquired after in situ derivatization of the samples using 21.0 mg of lignin with 2-chloro-4,4,5,5-tetramethyl-1,3,2-dioxaphospholane(TMDP) in a solution of (1.6:1 v/v) pyridine/CDCl3, chromium acetylacetonate (relaxation agent), and endo-N-hydroxy-5-norbornene-2,3-dicarboximide (NHND, internal standard). The spectrum was acquired using an inverse-gated

decoupling sequence, 90° pulse angle, 25 s pulse delay, 128 scans, and 0.77 s acquisition time. NMR data were processed using TopSpin 2.1 software (Bruker BioSpin).

5.3   Results and discussion

5.3.1   Timeline of sonication experiments

During ultrasonic irradiation, cavitation initiated after 30 min of sonoration and was evidenced by rigorous frothing of the solution. This cavitation event lasted for 15 min. Afterward, ultrasonication without cavitation occurred for an additional 15 min. This resulted in a total treatment time of 60 min.

5.3.2   Molecular weight determination

The molecular mass distributions of the Kraft lignin samples were characterized via GPC and the resulting retention profiles are illustrated in Figure5.1. The retention profile of Kraft lignin irradiated for 0 min (Kraft-00) represents the initial mass distribution of the sample before treatment. The retention profile illustrating Kraft lignin after 30 min of ultrasonication (Kraft-30) is low-mass shifted and has an asymmetrical and multimodal distribution. This strongly suggests that non-uniform degradation is a significant consequence of prolonged ultrasonic treatment (lacking cavitation) with Kraft lignin. The resulting retention profile of Kraft lignin ultrasonicated for 40 min (Kraft-40CAV) and 45 min (Kraft-45CAV) illustrate the gradual formation of a HMW fraction generated during the first 10 and total 15 min of cavitation, respectively. During the immediate cessation of cavitation (Kraft-45CAV), the retention profile had separated into two distinct peaks signifying the formation of a HMW and LMW fraction representing,

approximately 35% and 65% of the total sample, respectively. Based on retention times, the HMW fraction of Kraft-45CAV represents sample with a significantly greater DP compared to the initial non-irradiated sample, Kraft-00.
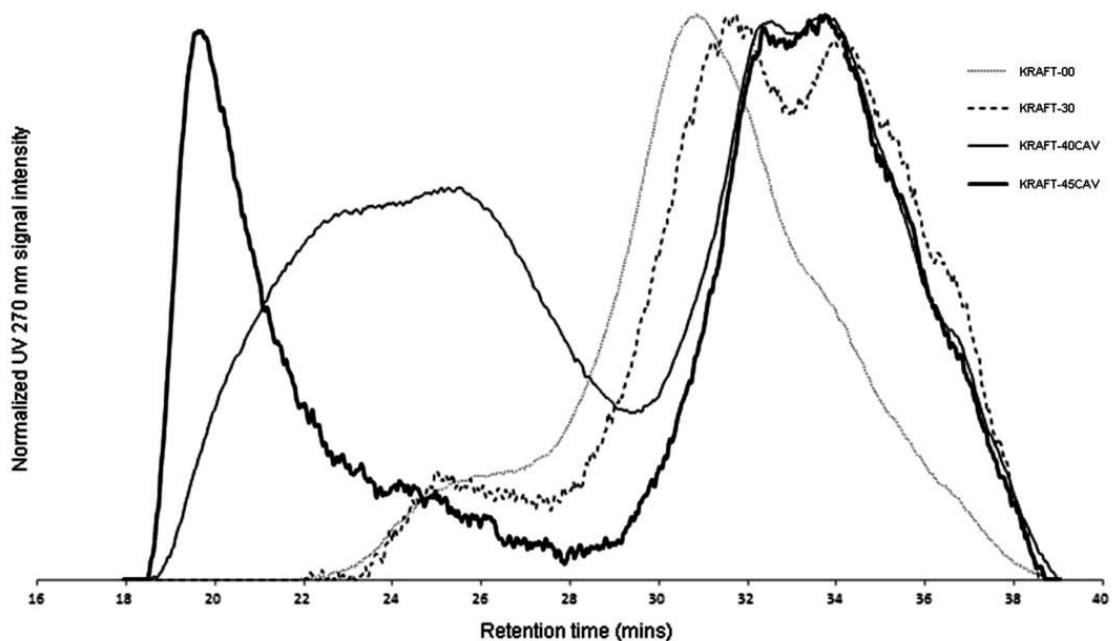
Figure 5.1. Retention curve profiles of Kraft lignin ultrasonicated for 0 min (Kraft-00), 30 min (Kraft-30), 40 min (Kraft-40CAV) and 45 min (Kraft-45CAV)

The M_w of the Kraft-45CAV HMW fraction (3.70×10^6 g/mol) was over 450-fold greater than the molar mass of Kraft-00 (7.64×10^3 g/mol). This also represented a molecular mass increase of approximately 600-fold after a span of 15 min relative to the initiation of cavitation, Kraft-30 (6.11×10^3 g/mol). After the cavitation event, the HMW fraction fully degraded after an additional period of 15 min of applied ultrasonic irradiation (Kraft-60). These results are summarized in Table 5.1.

Table 5.1. Molecular mass determination of ultrasonic irradiated Kraft lignin samples.

Lignin sample	Sonication time (min)	Mn(g/mol)	Mw(g/mol)	PDI (Mw/Mn)
Kraft-00	0	7.46×10^2	7.64×10^3	10.2
Kraft-30	30	1.00×10^3	6.11×10^3	6.1
Kraft-40CAV (LMW)	40	8.19×10^2	1.86×10^3	2.3
Kraft-40CAV (HMW)	40	2.55×10^5	1.35×10^6	5.4
Kraft-45CAV (LMW)	45	8.83×10^2	2.17×10^3	2.5
Kraft-45CAV (HMW)	45	1.21×10^6	3.70×10^6	3.1
Kraft-60	60	4.38×10^2	1.07×10^3	2.4

5.2.3 *Spectroscopic characterization via FT-IR*

FT-IR was used to characterize Kraft-00, Kraft-30, and Kraft 45CAV with the resulting spectra illustrated in Figure5.2. The observable signals of softwood lignin analyzed with FT-IR were assigned based on previous literature [182]. All spectral figures were characteristic of lignin derived from gymnosperms (G, H-type):stretches in unconjugated carbonyls and ketones (1702 cm^{-1}), aromatic skeletal vibrations (1598, 1509, and 1451 cm^{-1}), asymmetrical C–H deformations (1423 cm^{-1}), guaiacyl ring distortion(1263 cm^{-1}), deformations in C–O bonds of secondary alcohols and aliphatic ethers ($^{-1}$089 cm^{-1}), in-plane (1028 cm^{-1}) and out-of-plane C-H deformations (854 cm^{-1}). FT-IR showed increase in hydroxyls, carbonyls, and carboxyls, while further investigation with NMR techniques has been conducted to detail these changes.
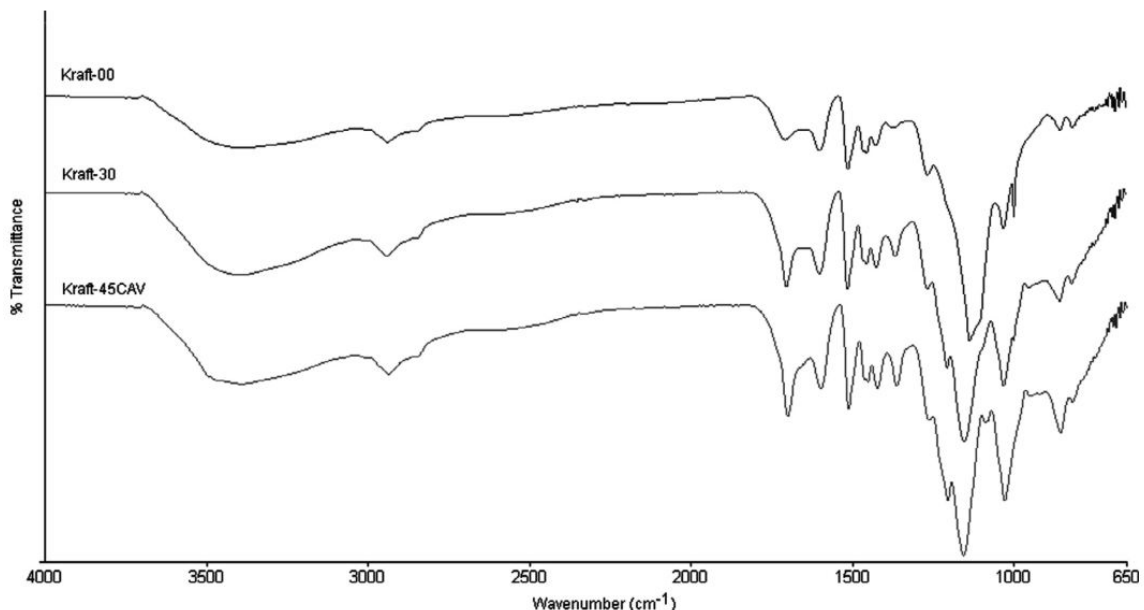
Figure 5.2. FT-IR of Kraft-00, Kraft-30, and Kraft-45CAV

5.3.4 Spectroscopic characterization via ^{13}C-NMR

Quantitative 13 C-NMR experiments were performed with Kraft-00, Kraft-30, and Kraft-45CAV with spectra of the latter shown inFigure5.3. The chemical shift assignments were based on literature [43, 50, 75]. Signals within the ^{13}C-NMR aromatic region (154–106 ppm) were characteristic of lignin derived from gymnosperms (H, G) in accordance with the FT-IR data. Guaiacyl units were identified with major peaks appearing at 149.2 (C-3 etherified guaiacyl units), 147.4 (C-4 in etherified guaiacyl units), 135.2 (C-1 in etherified guaiacyl β-O-4 units), 133.7 (C-1 in nonetherified guaiacyl β-O-4), 119.4 (C-6 in guaiacyl etherified and nonetherified units), 115.4 (C-5 in guaiacyl etherified and nonetherified units), and 111.2 ppm(C-2 guaiacyl units). Regarding linkages, all spectra had peaks distinctively assignable to C-5/C-5 0 in 5–5 linkages (132.3 ppm), C-5/C-5 0 in nonetherified units (125.9 ppm), C-C in guaiacyl β-β linkages (71.1 ppm), C-C in β-O-4 with an α-carbonyl and β-5 (63.1 ppm), and C-C in β-

78

O-4 units (60.2 ppm). The absence of peaks between 102–90 ppm indicate a lack or trace amounts of carbohydrate content. These assignments are summarized in Table 5.2 along with the results of the integrated regions forKraft-00, Kraft-30, and Kraft-45CAV. These integrations were performed by calculating the integral of the aromatic region (154–106 ppm) and calibrating that value to 6.00, which represents six aromatic carbons. Hence, the integrated regions of all functional groups were recorded as equivalences per aromatic ring (equiv/Ar) [182].
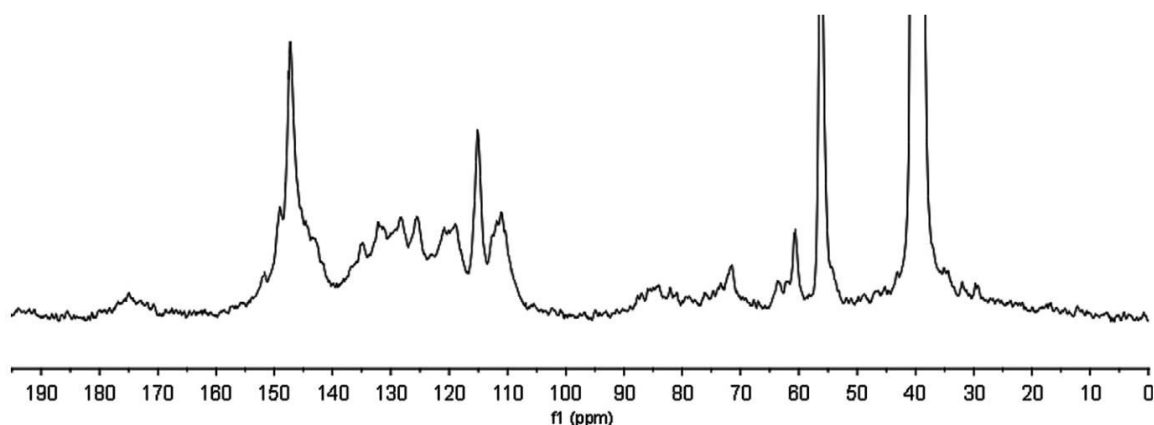
Figure 5.3. ^{13}C-NMR of Kraft-45 with DMSO-d$_6$ solvent peat at 39.51 ppm.

Table 5.2.   Quantitative comparison among ultrasonicated Kraft samples based on ^{13}C-NMR spectra.

^{13}C-NMR Chemical Shift Range (ppm)	Assignment	Number of Carbons/ Aromatic Ring		
		Kraft-00	Kraft-30	Kraft-45CAV
178.0-167.5	Unconjugated -COOH	0.41	0.49	0.23
167.5-162.5	Conjugated -COOH	0.09	0.16	0.11
154.0-140.0	C3, C4 aromatic ether, or hydroxyl	2.18	2.18	1.94
140.0-127.0	C1, aromatic C-C bond	1.51	1.41	1.41
127.0-123.0	C5 in nonetherified, aromatic C-C bond	0.51	0.54	0.58
123.0-117.0	C6, aromatic C-H bond	0.73	0.74	0.75

Table 5.2.   Continued

117.0-114.0	C5, aromatic C-H bond	0.50	0.45	0.45
114.0-106.0	C2 , aromatic C-H bond	0.62	0.69	0.79
90.0-78.0	Aliphatic C-O bond, Cα in β-O-4, Cα in β-5 and β-β	0.50	0.39	0.32
79.0-67.0	Aliphatic C-O bond, Cα in β-O-4	0.69	0.60	0.36
65.0-61.5	Aliphatic COR	0.21	0.17	0.11
61.5-57.5	Aliphatic C-O, Cγ in β-O-4	0.41	0.30	0.17
57.5-54.0	Methoxyl -OCH$_3$	1.12	1.07	0.86
54.0-52.0	Cβ in β-β and Cβ in β-5	0.13	0.14	0.15

During the first 30 min of ultrasonic irradiation (Kraft-00 toKraft-30), Kraft lignin samples were cleaved at sites of aliphatic ether linkages (90.0–57.5 ppm) and demethoxylated (57.5–54.0 ppm). This result is in agreement with previous studies concerning ultrasonicated lignin with proposed pathways detailing the homolytic sonolysis of alkyl-phenyl ethers shown in Figure5.4[87, 90, 100, 120, 151]. The aryl units of lignin were increasingly cleaved of aliphatic moieties as evidenced by the loss of C–C linkages atC1 (140.0–127.0 ppm). In contrast, C5 aromatic C–C substitutions increased (127.0-123.0 ppm), which is in accordance with diminishing C–H bonds at C5 (117.0–114.0 ppm). This data supports the condensing of phenols as a result of ultrasonic irradiation. Moreover, the presence of carboxyl moieties increased (178.0–162.5 ppm), which is in accordance with data obtained via FTIR.
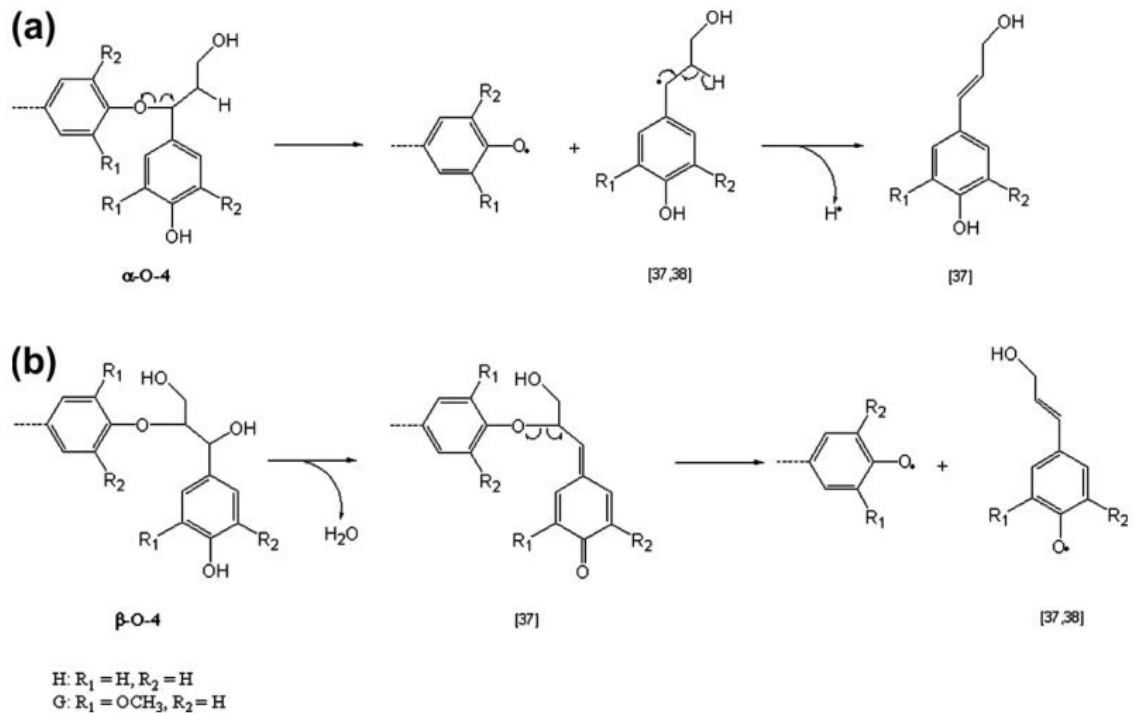
Figure 5.4. Proposed homolytic sonolysis mechanisms of (a) α-O-4 ether linkage and (b) β-O-aryl ether linkages[182].

In comparison, ultrasonic irradiation with cavitation (Kraft-30 to Kraft-45CAV) caused decarboxylation, a continued degradation of aliphatic ethers, and a greater extent of both demethoxylation and condensing of phenols.

5.3.5 Spectroscopic characterization via ^{31}P-NMR

The basis of ^{31}P-NMR experimentation involves the derivatization of lignin phenolic structures via TMDP, as exemplified in Figure 5.5 [133]. This process allows for the phenolic hydroxyl contents to be calculated based on the integrated region of the internal standard, NHND (150.8–151.5 ppm). Quantitative ^{31}P-NMR experiments were performed with phosphitylated Kraft-00, Kraft-30, and Kraft-45CAV with spectra of the

latter shown in Figure5.6. The results of the quantitative analysis are summarized in Table 3. The chemical shift assignments were based on literature [43, 50, 75].
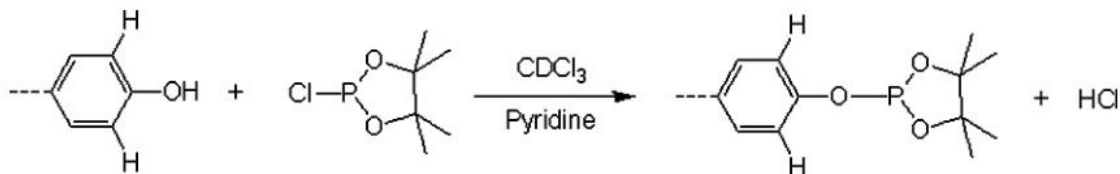
Figure 5.5. Phosphitylation of hydroxyl group in *para*-hydroxyphenyl lignin units with 2-chrlor-4,4,5,5-tetramethyl-1,3,2-dioxaphospholane (TMDP) [182].
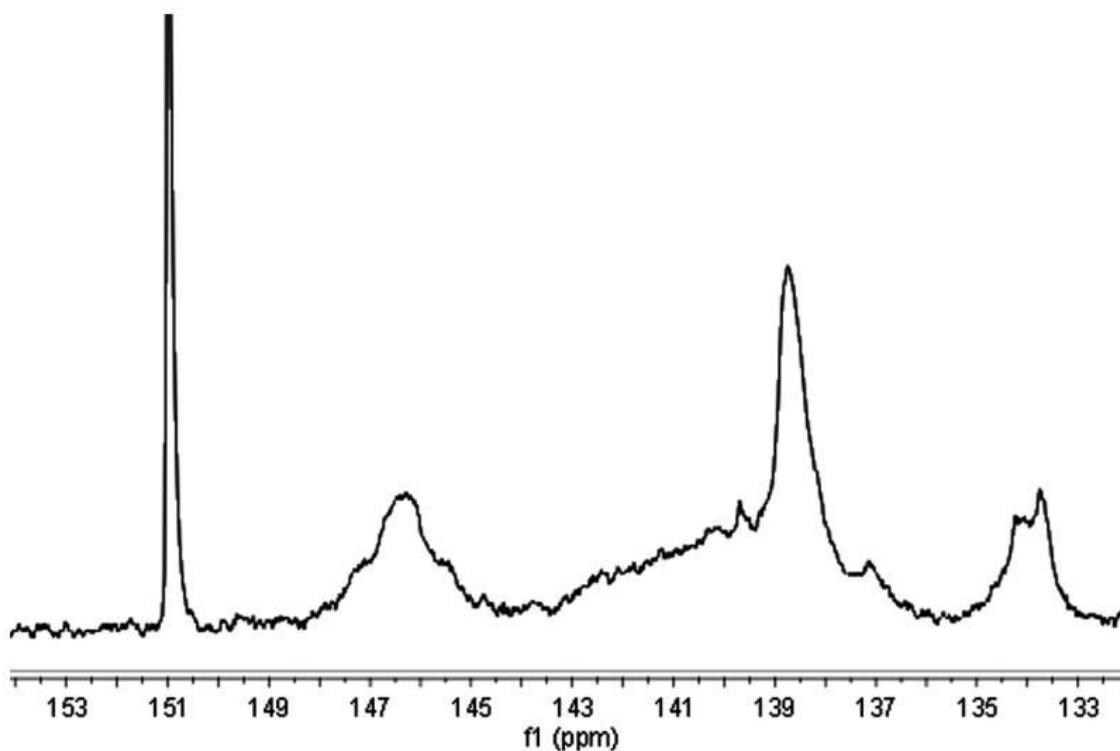
Figure 5.6. ^{31}P-NMR of phosphitylated Kraft-45CAV

During the first 30 min of ultrasonication (Kraft-00 to Kraft-30), aliphatic moieties decreased (148.5–145 ppm) while the concentration of carboxylic acids increased (135.133.5 ppm). The presence of condensed phenols also increased (144.5–

140.2 ppm) despite an overall degradation of phenols (144–137.6 ppm). During

cavitation (Kraft-30 to Kraft-45CAV), lignin underwent significant decarboxylation and

decrease in guaiacols due, in part, to demethoxylation. However, condensed phenols were

generated at a significantly greater rate during this period with proposed pathways shown

in Figure 5.6. In summary, these trends are in agreement with data obtained via ^{13}C-NMR

and support previous spectroscopic data concerning ultrasonic irradiated lignin [100, 120,

151, 185]. The overall loss of phenols (144–137.6 ppm) is in accordance with the loss of

guaiacyl-type units, which make up the major proportion of monolignol units derived

from gymnosperms. The concentration of *p*-hydroxyphenyl units (137.5–136.5 ppm)

increased during ultrasonic irradiation. This may be attributed to the liberation of a minor

proportion of H-type lignin during the cleavage of alkyl-phenyl ether linkages, as

Figure5.4 illustrates. Polymerization of condensed phenol linkages are formed in Figure

5.7 [43, 50, 75].
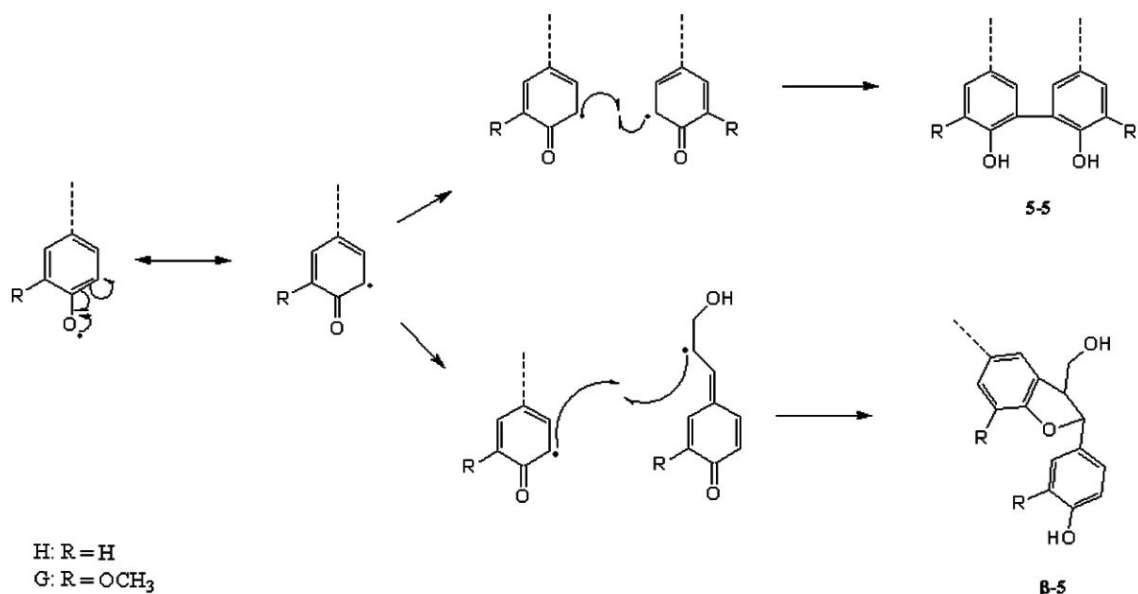
Figure 5.7.   Proposed homolytic sonolysis mechanisms of (a) α-O-4 ether linkage and (b) β-O-aryl ether linkages [182].

5.4   Conclusions

5.4.1   *Comparison to recent lignin polymerization methods*

The results of the ultrasonic polymerization of Kraft lignin can be compared to previous polymerization studies of commercial lignins using enzymatic and non-enzymatic methods. Enzymatic routes involve the formation of highly reactive phenoxy radicals. This event allows for the cross-coupling of radical species at different lignin macromolecules and the subsequent increase in the molecular mass of the biopolymer. Notable polymerization studies have been performed using peroxidase and laccase enzymes. These enzymes offer high coupling selectivity, mild reaction conditions, and utilize benign oxidants such as hydrogen peroxide (peroxidase) and molecular oxygen (laccase). Exemplary polymerization work with laccase enzyme (*Trametes villosa*) and hardwood sulfite lignin led to a 23-fold increase in molecular mass after a treatment period of 4 h [28, 63, 94, 103, 182, 206].

Alternatively, non-enzymatic methods may involve oxidative polymerization with consequential radical cross-coupling. Other methods include the use of cross-linking agents such as epichlorohydrin, acrylamide, maleic anhydride, polystyrene, and sebacoyl chloride that operate by bridging different lignin monomer units together at specific functional groups. Recent polymerization work using sebacoyl chloride to produce ester links between Kraft lignin molecules led to an overall 6-fold average molecular weight increase after treatment duration of 10 h [28, 63, 94, 103, 182, 206]. Additionally, ultrasonication has been documented to cause slight polymerization of lignin as seen with samples extracted from bamboo and wheat straw [105]. These literature results are summarized in Table 5.4.

Table 5.3. Quantitative comparison among ultrasonicated Kraft samples based on ^{31}P-NMR spectra

Chemical Shift Range (ppm)	Assignment	Phenolic Hydroxyl (mmol/g lignin)		
		Kraft-00	Kraft-30	Kraft-45CAV
148.5-145	Aliphatic -OH	2.33	2.04	0.92
144.5-140.2	Condensed phenolic	0.85	0.87	0.97
144-137.6	Phenols	2.84	2.70	2.58
139.5-138.0	Guaiacyl	1.49	1.34	1.11
137.5-136.5	*para*-hyroxyphenol	0.08	0.15	0.17
135-133.5	Carboxylic acid -OH	0.59	0.62	0.48

Table 5.4. Comparison of recent polymerization methods of various isolated lignin [182]

Polymerization Agent/Method	Lignin Type	Temp.	Duration	Initial M_w (g/mol)	Final M_w (g/mol)	Final PDI	M_w Fold Increase
Laccase enzyme (*T. villosa*)	Sulfite	50°C	4 hr	~6 × 10^3	~1.38 ×10^5	~3.2	~23
Cross-linking with sebacoyl chloride	Kraft	120°C	10 hr	6.50 × 10^3	3.97 × 10^4	3	6.1
Sonication	Bamboo	20°C	50 min	1.47 × 10^3	~1.65 × 10^3	~1.0	1.1
Sonication	Wheat Straw	35°C	15 min	2.89 × 10^3	3.47 × 10^3	~2.1	1.2
Sonication w/ sustained cavitation	Kraft	15°C	45 min	7.64 × 10^3	**3.70 × 10^6**	3.1	**484**

Kraft lignin in aqueous alkaline solution was subjected to ultrasonic irradiation with sustained cavitation, which resulted in the formation of a high molecular mass fraction (~35% of lignin content) with a weight average molecular weight over 450-fold greater than the original sample after less than 1 h of treatment. Based on spectroscopic analysis, condensed phenols were generated during ultrasonic irradiation; and this event occurred at an emphasized rate during cavitation. This polymerization method is suitable for comparison to recent enzymatic and non-enzymatic processes, while demonstrating a

simpler experimental design and faster polymerization rate. These results may unlock

new potential avenues in which Kraft lignin can be further developed as a bioresource for

higher DP applications.

CHAPTER 6: TGA STUDY OF ULTRASONIC TREATED LIGNOBOOST LIGNIN

6.1   Introduction

Lignin is an abundant and recalcitrant biorenewable polymer derived from woody biomass composed of varying proportions of cross-linked phenylpropane units of syringal, coniferyl, and paracoumaryl alcohol [24, 82]. Lignin is industrially extracted from biomass on the order of 50 millions of tons per year by the global pulp and paper industry via various delignification methodologies, of which the most prominent is the sulfate (kraft) pulping process [90]. During kraft pulping, wood is impregnated with cooking liquor containing bisulfide and hydroxide anions in order to principally cleave lignin-based aryl-ether linkages, which result in the solubilization and separation of lignin fragments away from higher-valued wood components and the generation of black liquor as a byproduct. Nearly 98% of kraft lignin contained in black liquor is subsequently burned as a non-optimized energy resource within pulp mill recovery boilers in order to recover chemical and energy costs. Alternatively, the capital costs associated with a recovery furnace and the desire by the pulping industry to obtain higher material yields have spurred increasing interest towards repurposing greater fractions of kraft lignin as a bioresource for sustainable and higher-utility commercial applications [135].

Currently, kraft lignin has been investigated as a precursor for commercial polymeric biomaterials including thermoplastics, copolyesters, and carbon fibers [25, 185]. However, these investigations typically incorporate a preliminary lignin modification procedure in order to reduce recalcitrance, enhance thermal stability, and/or augment the degree of polymerization (DP) among other alterations that directly and

demonstrably improve the chemical, thermal and mechanical properties of the final product, respectively [25, 82, 112, 157]. Specifically, the development of effective lignin thermostabilization and polymerization methods have gained significance interest towards enhancing lignin-based biomaterials [9, 59].

Previously, we described the ultrasonic polymerization of extensively purified kraft lignin that resulted in a 400-fold increase of the DP after approximately 1 h at 15°C [185]. This procedure was dependent on cavitation, which is a phenomenon that occurs during the rarefaction sequence of an applied sonication wave in the form of microscopic ruptures, or microbubbles, that rapidly collapse in solution and release significant amounts energy into the system as illustrated in Figure 1 [120]. This energy can cause homolytic cleavage of covalent bonds and increase the concentration of free radicals in solution, thereby generating a more optimal environment for cross-coupling reactions to occur among neighboring lignin oligomers. Spectroscopic analysis indicated that as a result of sonication aliphatic functional groups and ether linkages were degraded while comparatively stronger C5-C5' aryl-aryl bonds were formed.

Interestingly, these changes suggested that sonic polymerization can both polymerize as well as considerably alter the thermogravimetric properties of lignin [120, 185]. However, these effects were not thoroughly investigated with via thermogravimetric analysis (TGA). Hence, this study will detail the thermogravimetric attributes that result from the sonically-treated kraft lignin. For this study, lignin samples were extracted from black liquor via the LignoBoost process (LignoBoost lignin, LBL). Molecular weight was determined via gel permeation chromatography (GPC), structural analysis was elucidated via quantitative carbon nuclear magnetic resonance spectroscopy

(^{13}C-NMR), and thermogravimetric analysis (TGA) was implemented to determine rates of weight loss upon heating.
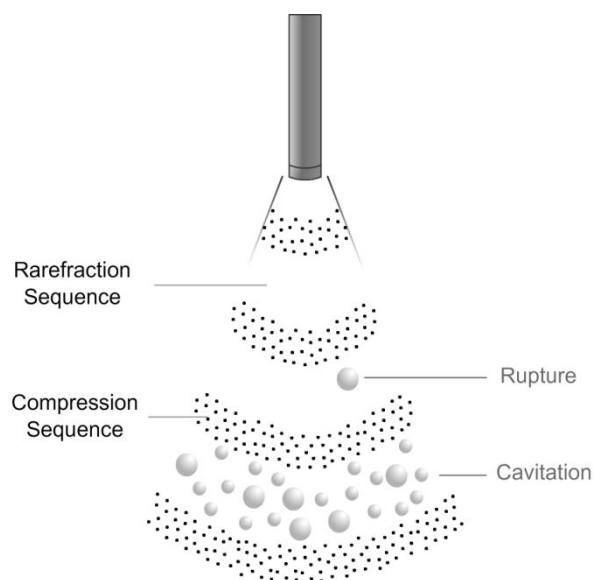
Figure 6.1.   Ultrasonication by means of a disruptor horn.

6.2   Results and discussion

6.3.1   GPC analysis

The average molecular mass of the LBL before ultrasonication was 1.73 x 10^4 g/mol, as determined by GPC analysis. Interestingly, low amplitude (intensity) sonication of LBL at pH 10 resulted in the degradation of the sample (1.58 x 10^4 g/mol, 8.75% loss), whereas prolonged high intensity sonication with immediate and turbulent cavitation caused the DP to increase (5.44 × 10^4 g/mol, 314.5% increase).   The extent of polymerization observed here is on par with previous reports detailing the ultrasonication of various lignin types that were not extensively purified [185]. These results are summarized in Table 1.

Table 6.1. GPC Results of ultrasonically unmodified, degraded and polymerized LignoBoost lignin (LBL) at pH 10 and sonication treatment duration of 30 min.

Sample	M_n (g/mol)	M_w (g/mol)	PDI (M_w/M_n)
Unmodified LBL	5.41 x 10^3	1.73 x 10^4	3.2
Degraded LBL	5.67 x 10^3	1.58 x 10^4	3.0
Polymerized LBL	7.52 x 10^3	5.44 x 10^4	7.2

6.3.2 ^{13}C-NMR analysis

Quantitative ^{13}C-NMR experiments were performed with Unmodified, Degraded, and Polymerized LBL samples. The chemical shift assignments were referenced from literature regarding structural characterization of gymnosperm lignin and summarized in Table 2 [43]. Overall, signals were in accordance with softwood lignin with major guaiacyl peaks appearing at 147.9 (C4 in etherified guaiacyl units), 120.8 (C6 in guaiacyl etherified and nonetherified units), 115.7 (C5 in guaiacyl etherified and nonetherified units), and 111.7 ppm (C2 guaiacyl units). No peaks were evident from 102-90 ppm, which is indicative of a lack of carbohydrate content.

For Degraded LBL and Polymerized LBL samples, integrals pertaining to aliphatic functional groups (90.0-57.5 ppm) and methoxyl moieties (57.5-54.0 ppm) were significantly diminished compared to Unmodified LBL. This supports that sonication caused the degradation of aliphatics (e.g. aliphatic-aryl ethers and aliphatic side chains) and demethoxylation, respectively. Additionally, the integral for C5 aryl C-C bonds (127.0-123.0 ppm) increased alongside a loss of the integral corresponding to C5 C-H bonds (117.0-114.0), which support the condensation of lignin during sonaration. Comparing just the sonicated samples, Polymerized LBL exhibited more extensive decarboxylation, aliphatic degradation, demethoxylation, and condensation compared to

Degraded LBL. These results comport with previous investigations regarding the

ultrasonic treatment of lignin [182].

Table 6.2. ^{13}C-NMR chemical shifts, assignments and quantitative integral comparison among LignoBoost lignin samples.

^{13}C-NMR Chemical Shift Range (ppm)	Assignment	Number of Carbons/ Aromatic Ring		
		Unmodified LBL	Degraded LBL	Polymerized LBL
178.0-167.5	Unconjugated -COOH	0.23	0.25	0.18
167.5-162.5	Conjugated -COOH	0.28	0.29	0.28
154.0-140.0	C3, C4 aromatic ether, or hydroxyl	2.43	2.31	2.28
140.0-127.0	C1, aromatic C-C bond	1.53	1.49	1.47
127.0-123.0	C5 in nonetherified, aromatic C-C bond	0.45	0.56	0.57
123.0-117.0	C6, aromatic C-H bond	0.64	0.65	0.71
117.0-114.0	C5, aromatic C-H bond	0.54	0.53	0.51
114.0-106.0	C2 , aromatic C-H bond	0.41	0.46	0.46
90.0-78.0	Aliphatic C-O bond, Cα in β-O-4, Cα in β-5 and β-β	0.31	0.27	0.26
79.0-67.0	Aliphatic C-O bond, Cα in β-O-4	0.16	0.15	0.10
65.0-61.5	Aliphatic COR	0.10	0.09	0.08
61.5-57.5	Aliphatic C-O, Cγ in β-O-4	0.26	0.22	0.10
57.5-54.0	Methoxyl -OCH$_3$	1.69	1.61	1.41
54.0-52.0	Cβ in β-β and Cβ in β-5	0.07	0.08	0.09

6.3.3 TGA results

The resulting thermogravimetric (TG) and derivative thermogravimetric (DTG)

thermograms of Unmodified, Degraded, and Polymerized LBL are shown in Figure 2 and

summarized in Table 3. TG curves reference the percent of residual material as a

function of temperature; DTG curves represent the degradation rate as a function of

temperature. The temperature at the onset of the maximum degradation rate (T_{DTGmax})

was determined by referencing the lowest point of the DTG curve. TG and DTG data

support that the lignin samples degraded over an extended temperature range and the resulting T_{DTGmax} values were within 355-385°C, which is in agreement with previous observations of wood-derived lignin [30, 112, 175].

Unmodified LBL exhibited the highest T_{DTGmax} but also displayed several prominent DTG fluctuations at temperatures below 300°C. These fluctuations are attributed to overlapping degradation steps involving the volatilization of aliphatic alcohols, acids, and esters. Despite exhibiting lower T_{DTGmax} values, these fluctuations were not apparent for sonicated LBL samples, in part due to the degradation of aliphatic functional groups during ultrasonication, as supported with ^{13}C-NMR. Rates of degradation were also higher for Unmodified LBL from 325-500°C compared to sonicated samples that were characterized as enriched with C5 condensed phenolic structures. Consequently, the percentage of residual material was consistently in favor of Polymerized LBL and Degraded LBL. As a result, sonicated LBL samples demonstrated considerably enhanced thermal stability over Unmodified LBL.

Table 6.3. Thermogravimetric analysis of LignoBoost lignin samples.

Sample	Point(s) of Max. Degradation	DTG at 175°C (%/°C)	DTG at 250°C (%/°C)	DTG at 350°C (%/°C)
Unmodified LBL	175.0°C (local) 251.2°C (local) 385.5°C (T_{DTGmax}) 3 points	-0.34	-0.59	-0.79
Degraded LBL	351.3°C (T_{DTGmax}) 1 point	-0.09	-0.28	-0.65
Polymerized LBL	377.6°C (T_{DTGmax}) 1 point	-0.16	-0.30	-0.72
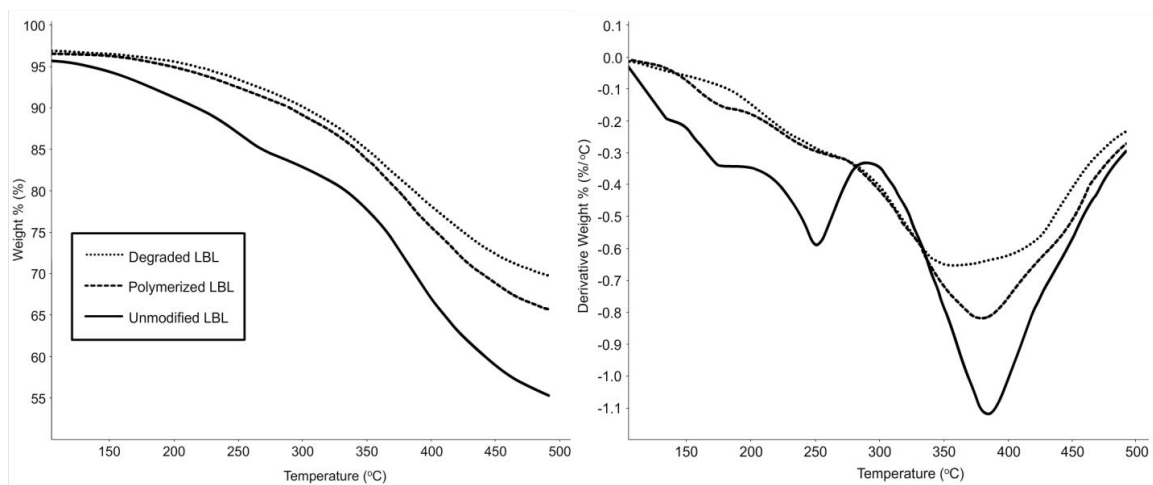
Figure 6.2. Thermogravimetric analysis (TGA) plots of modified and unmodified LignoBoost lignin (LBL) samples. (Left) The weight percent vs. temperature. Changes in weight percent from 23-100°C were attributed to the loss of residual moisture. (Right) Derivative weight percent vs. temperature.

6.3.4 Critique, practicality towards carbon fiber production

While sonication can provide controlled polymerization and degradation of lignin in conjunction with enhanced thermogravimetric attributes, this process remains at a fundamental stage. For the specific interests of carbon fiber production, the process in its current form would not be applicable. This is due to thermostabilization, which is a step during carbon fiber production to prevent the softening of lignin fibers. This process is conducted in an inhomogeneous phase (involving solid-gas, solid-liquid reactions). Necessarily, the sonic procedure disclosed in this study are performed in homogenous solution phases. In addition, the thermogravimetric qualities above 500°C would need to be considered as carbon fiber production involves more temperate treatments. Furthermore, until fibers developed from sonicated lignin are drawn, detailed benefits will remain ambiguous. However, it would be intriguing to compare the effect of sonic

treatment on the ability to form a fiber from LBL by common fiber production methods such as melt or solution spinning, and thereby study the effect of ultrasonication on thermal softening and stability or solubility in a suitable spinning solvent. In these aspects, this process could be further researched towards carbon fiber development.

6.3   Conclusion

The thermostabilization effects rendered during ultrasonic irradiation of LBL are demonstrably two-fold. Firstly, ultrasonication causes the degradation of aliphatic and ether linkages, thereby reducing the proportion of more volatile compounds during exposure to escalating temperatures. Secondly, sonaration reinforces the polymer via the condensing of phenolic units. These consequences enhance the thermal stability of sonicated lignin compared to untreated sample. These findings are in agreement with analogous research regarding the thermogravimetric study of ultrasonicated hydrolysis lignin [30, 112, 175]. Interestingly, these benefits were rendered to both ultrasonically polymerized and degraded lignin samples, which may unlock new avenues such that kraft lignin can be developed as a sustainable precursor for products of with broad degrees of polymerization.

CHAPTER 7: OVERALL CONCLUSIONS

New optimization routes for biorefinery will benefit industry, consumers, and the environment. The first project details the generation of bioenergy from lignin sourced from biorefinery waste streams. This dissertation provides the groundwork strategy for such a practice that, with future work, can additional revenue for industry, secure a domestic supply of biodiesel for the general public, and reduce pollution through effective and green waste management. Alternatively, the second research initiative details the impact of green technology capable of converting lignin sourced as a byproduct of the pulp and paper industry into precursors for heat-stable polymeric biomaterials, such as carbon fibers. This dissertation marks the first steps where this future technology can enable higher material yields for the pulp and paper industry and broaden the availability of low-to-medium quality carbon fibers for the general public.

7.1   Lignin for bioenergy

The industrial pretreatment of lignocellulosic biomass (ex. organosolv, steam explosion, dilute acid, etc.) generates an aqueous effluent fraction that is often discarded as industrial wastewater with limited utilization. Here, an experimental outline for a more optimal usage of pretreatment effluents was discussed. In detail, this effluent solution that was characterized as aqueous and contaminated with a complex mixture of solubilized carbonaceous compounds was implemented as a feedstock for the

development of microbial lipids. These oils were transesterified form triacylglycerides to fatty acid methyl esters suitable as a supplemental biodiesel.

Rhodococcus opacus DSM 1069 demonstrated an ability to utilized pine organosolv pretreatment effluent as a sole carbon and energy resource for 120 h at 1.5 w/v% solids concentration and accumulated a maximum of 26.99±2.88% of its cellular dry weight in numbered monounsaturated and saturated fatty acids such as oleic, palmitic, and stearic fatty acids. Currently, yields were on the order of 0.06 grams of lipids produced per 1.00 gram of carbon consumed. The future of this work is discussed in Chapter 8. Overall, this procedure presents a incredible potential to dramatically improve biorefinery carbon efficiency while reducing collateral pollution generated during the pretreatment of lignocellulosic biomass while promoting the principles of green chemistry.

7.2   Lignin for biomaterials

Kraft lignin is an inexpensive and abundant byproduct of pulp mills that can be used as a precursor for polymeric materials such as adhesives and carbon fibers along with energy production. Some of these material applications favor the utilization of high molecular weight (HMW) lignin. This dissertation investigated the use of ultrasonics as a means to increase the degree of polymerization (DP) of highly purified Kraft lignin. The results showed that ultrasonication with sustained high intensity cavitation generated a high molecular-weight fraction (~35%) that had a molecular weight over 450-fold greater than the initial Kraft lignin sample. A comprehensive NMR analysis indicated that the highly-polymerized fraction was enriched with C5 condensed phenolic structures and that

aliphatic moieties along with aryl-methoxyl groups were significantly degraded. In other words, as a result of sonic treatment, the proportion of lignin inter-unit linkages shifted from weaker aliphatic bonds to stronger aryl-aryl linkages.

In order to assess the benefits of this effect, a subsequent study was performed using Lignoboost lignin derived from Kraft black liquor. Ultrasonicated Lignoboost samples exhibited improved thermal stability for temperatures as high as 500°C due to sonic-enabled enrichment of C5 condensed phenolic groups and the breakdown of aliphatic functional groups. High intensity ultrasonication was also shown to simultaneously polymerize lignin, implying the potential for an expeditious one-step homogenization, thermostabilization and polymerization methodology toward green material applications. Interestingly, these enhancements were rendered to both polymerized as well as degraded lignin samples. The implications of this discovery are outlined in Chapter 8.

Conclusively, the potential of sourcing biomaterial precursors from industrial aromatic-contaminated waste streams can enable higher material yields by biorefineries with limited recovery boiler capacity and optimize the use of a commonly underutilized biopolymer along the tenets of green chemistry.

CHAPTER 8: RECOMMENDATIONS FOR FUTURE WORK

8.1 Future bioenergy studies

The bioconversion of pretreatment effluents into microbial oils is in a basic stage. At this point, these would be intriguing methods that can be considered for future developments within this field:

- *Continuous fermentation*: Currently, fermentation work was performed in batch reactors based on commercial Biostat fermenters. The term "batch reactor" refers to the functionally closed system where microbes exists with a limited amount of available nutrients. A bioreactor based on a continuous flow reactor with an inflow of sterile nutrient solution and outflow of primed cells at oleaginous capacity would be a more ideal system for industrial upscaling. Fortunately, such reactors exist at pilot and commercial scale (and even the current used Biostat reactor can be modified to provide similar functions at smaller volumes). Currently, there are two different types of commercial continuous flow reactors: Firstly, is a plug flow reactor, which is a continuous fermentation system where fermentation broth flows through a tubular reactor without back mixing. This system would not necessarily be ideal as the number of cells, mass transfer of the nutrient, and productivity will vary at different locations within the system. In addition to this, new cells must be continuously added along with the nutrient solution at the entrance of the reactor. The second type of continuous flow reactor is a homogeneously mixed bioreactor that operates as either a chemostat or turbidostat. For reference, in a chemostat, cell growth is maintained by

adjusting the concentration of available substrate (typically one specific nutrient required for proliferation such as nitrogen salts). Alternatively, a turbidostat controls cell growth via constantly measuring turbidity to monitor the concentration of biomass in the reactor and automatically adjusting the rate of nutrient solution feeding accordingly. In this sense, the turbidostat-based continuous fermentation system would, in theory, provide the highest quality of automated cell maintenance.

- *Recombinant strains*: Genetic modification is currently an untapped potential for this study. Current research is currently investigating recombinant *Rhodococci* capable of digesting woody carbohydrates other than glucose [192]. This caliber of work can greatly influence the capabilities and overall efficiency of lignocellulosic waste stream bioconversion.

- *Optimization of the substrate*: Pine-derived ethanol organosolv pretreatment effluent was utilized in this dissertation. This experiment proved the concept that microbes can utilize biorefinery effluents as a means to produce biodiesel, but there is still a wide variety of alternative pretreatment effluents that can be implemented as a substrate. Steam Explosion (STEX) effluent is a strong candidate for future work. STEX pretreatment waste is near pH neutral, contains no organic solvent component, and is gaining popularity as a means of treating corn stover (for subsequent enzymatic hydrolysis). STEX effluent from corn is likely to be enriched with sugar fractions and minimal aromatic constituents compared to pine, which may be ideal for biodiesel production. A foreseeable

issue is that unlike EOP used in this study, STEX effluent will have hydrocarbon contaminants that will effect characterization as well as yield determination.

- *Labeled substrate*: If possible, radio-labeled biomass should be implemented as a substrate so that the generated fats can be characterized with NMR to determine where the atoms result due to bacterial bioconversion. Foreseeable complications are the need of radio-labeled model compounds for reproducible measurements, the lack of sensitivity of ^{13}C experiments, and the inherent difficulty of characterizing long chain fatty acids with NMR.

8.2   Future biomaterial studies

Cavitational treatment of lignin is a wholly novel subject with many exciting future developments. Improvements should be primarily focused on demonstrating utility via comparing final products produced with and without cavitational pretreatment methods. Producing cavitation without the need for sonication will also be preferred path in order to reduce energy needs and improve efficient distribution of cavitational energy.

- *Cavitator:* In studies discussed in this dissertation, cavitation was generated via ultrasonic horns. Although this may prove the concept, this method is also energy-intensive, difficult to upscale, limited to low solvent (50 mL) batch reactions. A commercial cavitator, such as the APV Cavitator, provides controlled cavitation via a spinning rotor instead of sound, a continuous flow reactor set up, flow rate control, scale-free heating, and uniform cavitation exposure.   In terms of processing, the use of a cavitator for future cavitation-based experiments is the most apparent step forward.

- *Other varieties of lignin*: In this study, only softwood lignin kraft lignin was investigated. Hardwood kraft lignin will likely provided impaired results due to the need to demethoxylate S-type lignin to generate condensed phenol linkages (in simple terms: Aryl-OMe's at the C5 position of lignin get in the way of 5-5 and β-5 linkages, so G-type lignin isn't ideal and S-type lignin would thereby be, hypothetically, worse). An experiment comparing softwood and hardwood kraft lignin may demonstrate this.

- *Development towards biomaterials*: To better understand the utility of this method, polymerized lignin should be implemented as an aspect in the design of a physical biomaterial. As a suggestion, laboratory films of polyvinyl acetate (PVA) can be made with increasing proportions of cavitationally polymerized and untreated lignin. These samples can then be treated on aspects such as tensile strength, heating, sheer strength, etc. Ultrasonic or cavitationally degraded lignin would also be an interesting aspect to study during this copolymer assessment. Hypothetically, polymerized lignin should provide improved tensile strength due to matrix-on-filler interactions, as well as improved thermostability of the material compared to neat PVA films and untreated lignin copolymer films at parallel concentration.

APPENDIX A

A.1   Varieties of Ethanol Organosolv Pretreatment Parameters

Heating	Time (min)	Biomass:Solvent	%EtOH	%H_2SO_4	Reference
160-170°C	30-60	1:8	65%	0.70-0.80%	[187]
160	50	1:7	75%	0.90%	[124]
180	50	1:7	75%	0.90%	[124]
160	70	1:7	55%	0.90%	[124]
180	70	1:7	55%	0.90%	[124]
185	80	1:7	60%	1.50%	[124]
185	80	1:7	60%	2.34%	[124]
170	80	1:7	60%	1.50%	[124]
170	80	1:7	60%	1.20%	[124]
170	40	1:7	60%	1.20%	[124]
170	80	1:7	70%	1.20%	[124]
170	60	1:7	70%	1.00%	[124]
160	60	1:7	70%	1.00%	[124]
160	100	1:7	70%	1.00%	[124]
190	120	1:7	60%	2.50%	[124]

A.2   Varieties of Kraft Cooking Parameters

Active Alkaili	Sulfidity	Temperature	Liquor:Wood	Reference
17	28%	160	4:1	[125]
14	28%	160	4:1	[125]
21	28%	160	4:1	[125]
24	28%	160	4:1	[125]
17	15%	160	4:1	[125]
17	21%	160	4:1	[125]
17	37%	160	4:1	[125]
15	22.5%	170	4:1	[155]
13	22.5%	170	4:1	[155]
17	22.5%	165	4:1	[155]

A.3   Referenced enzymes from Chapter 2.3

Enzyme abbr.	Functional description	EC no.	Gene designation (model organism) [186]
β-Ketoadipate pathway			
P3,4O	Protocatechuate 3,4-dioxygenase (ring cleavage dioxygenase)	1.13.11.3	pcaGH (P. putida)
CMLE	b-Carboxy-*cis,cis*-muconate lactonizingenzyme (cycloisomerase)	5.5.1.2	pcaB (P. putida)
CMD	γ-Carboxy-muconolactone decarboxylase	4.1.1.44	pcaC (P. putida)
ELH	β-ketoadipate enol-lactone hydrolase	3.1.1.24	pcaD (P. putida), catD (A. calcoaceticus)
TR	β-ketoadipate succinyl-CoA transferase	2.8.3.6	pcaIJ (P. putida), catIJ (A. calcoaceticus)
TH	b-Ketoadipyl-CoA thiolase	2.3.1.-	pcaF (P. putida), catF (A. calcoaceticus)
C1,2O	Catechol 1,2-dioxygenase	1.13.11.1	catA (A. calcoaceticus)
MLE	*cis,cis*-Muconate lactonizing enzyme (cycloisomerase)	5.5.1.1	catB (P. putida)
MI	Muconolactone isomerase	5.3.3.4	catC (P. putida)
***ortho*-Nitrophenol degradation pathway**			
ONP2O	*ortho*-Nitrophenol 2-monooxygenase	1.14.13.31	onpA (P. putida B2, Alcaligenes sp. NyZ215)
OBQR	*ortho*-Benzoquinone reductase	1.6.99.-	onpB (Alcaligenes sp. NyZ215)
MAR	Maleylacetate reductase	1.3.1.32	mnpE, tcpD (C. necator JMP134), pnpE (Pseudomonas sp. WBC-3), npdC (R. opacus SAO101), pcpE (S. chlorophenolicum ATCC 39723), linF (S. japonicium strain UT26, S. indicum B90A, and Sphingobium sp. BHC-A)

A.3. Continued

***meta*-Nitrophenol degradation pathway**			
NR	*meta*-Nitrophenol nitroreductase	1.6.6.-	mnpA (P. putida B2, C. necator JMP134)
HAPM	3-Hydroxylaminophenol mutase (glutamine synthetase)	6.3.1.2	glnA (C. necator JMP134)
AHQO	Aminohydroquinone dioxygenase	1.13.11.-	mnpC (C. necator JMP134)
ESA	Enantiomer selective amidase	3.5.1.4	mnpD (C. necator JMP134)
HAPL	*meta*-Hydroxylaminophenol lyase	4.3.1.- –	(P. putida B2)
1,2,4BTO	1,2,4-Benzenetriol dioxygenase	1.13.11.37	npdB, npcC (R. opacus SAO101)
***para*-Nitrophenol degradation pathway**			
PNP4O	*para*-Nitrophenol 4-monooxygenase	1.14.13.-	pnpA (Pseudomonas sp. WBC-3), npdA1A2
BQR	*para*-Benzoquinone reductase	1.6.5.-	pnpB (Pseudomonas sp. WBC-3), npdA2
H1,2O	Hydroquinone 1,2-dioxygenase (chlorohydroquinone 1,2-dioxygenase)	1.13.11.-	pnpC (Pseudomonas sp. WBC-3), linE/linEb
4HSD	cis,trans-4-Hydroxymuconic semialdehyde dehydrogenase	1.2.1.61	pnpD (Pseudomonas sp. WBC-3)
PNP2O	*para*-Nitrophenol 2-monooxygenase	1.14.13.29	nphA1A2, npcAB (Rhodococcus sp. PN1,R. opacus SAO101)
N4O	4-Nitrocatechol 4-monooxygenase	1.14.-	npdA1A2, npcAB (Rhodococcus sp. PN1,R. opacus SAO101)
QR	2-Hydroxy-1,4-benzoquinone reductase	1.6.5.7	npcAB (R. opacus SAO101)
Organophosphate degradation pathway			
OPH	Organophosphate hydrolase (methyl parathion	3.1.8.1	opd (Flavobacterium sp. ATCC 27551)

A.3. Continued

	hydrolase, Paraoxon hydrolase)		
Pentachlorophenol degradation pathway			
PCPO	PCP 4-monooxygenase	1.14.13.50	pcpB (S. chlorophenolicum L-1)
TCBQR	Tetrachlorobenzoquinone reductase	1.14.13.50	pcpD (S. chlorophenolicum L-1)
HQD	Tetrachlorohydroquinone dehalogenase, (2,3,6-trichlorohydroquinone dehalogenase)	1.8.99.-	pcpC (S. chlorophenolicum L-1)
2,6H1,2O	2,6-Dichlorohydroquinone 1,2-dioxygenase	1.13.11.-	pcpA (S. chlorophenolicum ATCC 39723)
2,4,6-Trichlorophenol degradation pathway			
TCPO	2,4,6-TCP monooxygenase	1.14.13.-	tcpA (C. necator JMP134)
6H1,2O	6-Chlorohydroxyquinol 1,2-dioxygenase	1.13.11.-	tcpC (C. necator JMP134)
Hexachlorohexane degradation pathway			
DHC	Dehydrochlorinase	4.5.1.-	linA (S. japonicium strain UT26, S. indicum B90A, and Sphingobium sp. BHC-A)
HAD	Haloalkane dehalogenase	3.8.1.5	linB (S. japonicium strain UT26, S. indicum B90A, and Sphingobium sp. BHC-A)
DCD	2,5-Dichloro-2,5-cyclohexadiene-1,4-diol dehydrogenase	1.1.1-	linC (S. japonicium strain UT26, S. indicum B90A,

			and Sphingobium sp. BHC-A)
RD	Reductive dehalogenase (2,5-dichlorohydroquinone reductive dehalogenase)	1.97.1.-	linD (S. japonicium strain UT26, S. indicum B90A, and Sphingobium sp. BHC-A)
b-O-Aryl ether degradation pathway			
CAD	Ca-Dehydrogenase	1.1.1.-	ligD (S. paucimobilis SYK-6)
BE	b-Etherase	2.5.1.18	ligEFG (S. paucimobilis SYK-6)
LP	Lignin peroxidase	1.11.1.14	lipA/lipB, O282, GLG5, V4, GLG4 (P. chrysosporium)dypA/dypB (R. jostii RHA1)
VDH	Vanillate dehydrogenase	1.2.1.67	ligV ((S. paucimobilis SYK-6),vdh (Pseudomonas sp. HR 199)
VO	Vanillate monooxygenase(Vanillate demethylase)	1.14.13.82	ligM (S. paucimobilis SYK-6)
Fatty acid biosynthesis pathway			
MAT	Malonyl-CoA:ACP transacylase	2.3.1.-	fabD (E. coli)
KS	b-Ketoacyl-ACP synthase	2.3.1.41	fabBFH (E. coli), fas2 (S. cerevisiae)
KR	b-Ketoacyl-ACP reductase	1.1.1.100	fabG (E. coli), fas2 (S. cerevisiae)
DH	b-Hydroxyacyl-ACP dehydratase	4.2.1.17	fabZ, fabA (E. coli), fas1 (S. cerevisiae)
ER	Enoyl-ACP reductase	1.3.1.9	fabI (E. coli), fas1 (S. cerevisiae)
MPT	Malonyl-palmitoyl transacylase (ACP S-malonyltransferase)	2.3.1.39	fas1 (S. cerevisiae)

ACC	Acetyl-CoA carboxylase, (carboxyl-transferase, AccA), biotin carboxyl carrier protein (AccB), biotin carboxylase (AccC), carboxyl-transferase (AccD)	6.4.1.2	accA, accB, accC, accD (E. coli)
AAG3P	Acyl-ACP:G3P acyltransferase	2.3.1.15	plsB (E. coli)
Triacylglycerol biosynthesis pathway			
GK	Glycerol kinase	2.7.1.30	gut1 (S. cerevisiae)
G3PAT	Glycerol-3-phosphate O-acyltransferase	2.3.1.15	gat1/gpt2, gat2, sct1 (S. cerevisiae)
AG3PAT	Acyl-CoA-1-acyl-glycerol-3-phosphate acyltransferase	2.3.1.51	slc1/slc4/ict1 (S. cerevisiae)
PAP	Phosphatidate phosphatase	3.1.3.4	pgpB (E. coli), pah1, dpp1, lpp1 (S. cerevisiae)
DGAT	Acyl-CoA: diacylglycerol acyltransferase	2.3.1.20	atf1/atf2 (E. coli), dga1, are1/are2 (S. cerevisiae)

A.4 Liquid Minimal and Full Media Components

Minimal media: Mass per liter of distilled water.

0.40 g	KH_2PO_4
1.60 g	K_2HPO_4
0.20 g	$MgSO_4 \times 7\ H_2O$
0.015 g	$FeCl_3$
0.5 mg	$MnSO_4 \times H_2O$
1.0 mg	$CuSO_4 \times 5H_2O$
1.0 mg	$ZnSO_4 \times 7\ H_2O$
0.5 mg	$CaCl_2$
0.1 mg	KCl
0.5 mg	H_3BO_3

Adjusted pH to 7 with NaOH and H_2SO_4 and sterile filtered before use[46].

Full media: Mass per liter of distilled water

4.0 g	Glucose
4.0 g	Yeast extract
10.0 g	Malt extract

Adjusted pH to 7.2 and sterile filtered before use [46].

A.5   Varieties of Lignin Discussed Throughout Dissertation

Chapter	Lignin Discussed	Process
1	N/A	N/A
2	N/A	N/A
3	N/A	N/A
4	Degraded **organosolv lignin** (and carbohydrates) solvated in the aqueous effluent stream of ethanol organosolv pretreatment	**Soxhlet Extracted Biomass: (toluene:ethanol 2:1 solvent mixture, reflux for 48 h) Organosolv Pretreatment(170˚C, 1 h, biomass:solvent 1:8, 65% EtOH, 0.76 dry wt.% H2SO4)**
5	**Highly purified kraft lignin** isolated from kraft black liquor, purification removed salt and extractive contaminants.	*As described in 3.2.5*
6	**Lignoboost lignin** isolated from kraft black liquor via the Lignoboost process.	[207]

APPENDIX B

B.1   Copyright Permission from Trends in Biotechnology

ELSEVIER LICENSE
TERMS AND CONDITIONS
Nov 07, 201

This is a License Agreement between Tyrone Wells ("You") and Elsevier ("Elsevier") provided by Copyright Clearance Center ("CCC"). The license consists of your order details, the terms and conditions provided by Elsevier, and the payment terms and conditions.

All payments must be made in full to CCC. For payment instructions, please see information listed at the bottom of this form.

Supplier	Elsevier Limited The Boulevard, Langford Lane Kidlington,Oxford,OX5 1GB,UK
Registered Company Number	1982084
Customer name	Tyrone Wells
Customer address	Renewable Bioproducts Institute ATLANTA, GA 30311
License number	3475640656379
License date	Sep 24, 2014
Licensed content publisher	Elsevier
Licensed content publication	Trends in Biotechnology
Licensed content title	Biotechnological opportunities with the β-ketoadipate pathway
Licensed content author	Tyrone Wells, Arthur J. Ragauskas
Licensed content date	December 2012
Licensed content volume number	30
Licensed content issue number	12
Number of pages	11
Start Page	627
End Page	637
Type of Use	reuse in a thesis/dissertation
Portion	full article
Format	both print and electronic
Are you the author of this Elsevier article?	Yes
Will you be translating?	No
Order reference number	24601

111

Title of your thesis/dissertation	Lignin for Bioenergy & Biomaterials
Expected completion date	Oct 2014
Estimated size (number of pages)	250
Elsevier VAT number	GB 494 6272 12
Permissions price	0.00 USD
VAT/Local Sales Tax	0.00 USD / 0.00 GBP
Total	0.00 USD

Terms and Conditions

INTRODUCTION
1. The publisher for this copyrighted material is Elsevier. By clicking "accept" in connection with completing this licensing transaction, you agree that the following terms and conditions apply to this transaction (along with the Billing and Payment terms and conditions established by Copyright Clearance Center, Inc. ("CCC"), at the time that you opened your Rightslink account and that are available at any time at http://myaccount.copyright.com).

GENERAL TERMS
2. Elsevier hereby grants you permission to reproduce the aforementioned material subject to the terms and conditions indicated.

3. Acknowledgement: If any part of the material to be used (for example, figures) has appeared in our publication with credit or acknowledgement to another source, permission must also be sought from that source. If such permission is not obtained then that material may not be included in your publication/copies. Suitable acknowledgement to the source must be made, either as a footnote or in a reference list at the end of your publication, as follows:

"Reprinted from Publication title, Vol /edition number, Author(s), Title of article / title of chapter, Pages No., Copyright (Year), with permission from Elsevier [OR APPLICABLE SOCIETY COPYRIGHT OWNER]." Also Lancet special credit - "Reprinted from The Lancet, Vol. number, Author(s), Title of article, Pages No., Copyright (Year), with permission from Elsevier."

4. Reproduction of this material is confined to the purpose and/or media for which permission is hereby given.

5. Altering/Modifying Material: Not Permitted. However figures and illustrations may be altered/adapted minimally to serve your work. Any other abbreviations, additions, deletions and/or any other alterations shall be made only with prior written authorization of Elsevier Ltd. (Please contact Elsevier at permissions@elsevier.com)

6. If the permission fee for the requested use of our material is waived in this instance, please be advised that your future requests for Elsevier materials may attract a fee.

7. Reservation of Rights: Publisher reserves all rights not specifically granted in the combination of (i) the license details provided by you and accepted in the course of this licensing transaction, (ii) these terms and conditions and (iii) CCC's Billing and Payment terms and conditions.

8. License Contingent Upon Payment: While you may exercise the rights licensed immediately upon issuance of the license at the end of the licensing process for the transaction, provided that you have disclosed complete and accurate details of your proposed use, no license is finally effective unless and until full payment is received from you (either by publisher or by CCC) as provided in CCC's Billing and Payment terms and conditions. If full payment is not received on a timely basis, then any license preliminarily granted shall be deemed automatically revoked and shall be void as if never granted. Further, in the event that you breach any of these terms and conditions or any of CCC's Billing and Payment terms and conditions, the license is automatically revoked and shall be void as if never granted. Use of materials as described in a revoked license, as well as any use of the materials beyond the scope of an unrevoked license, may constitute copyright infringement and publisher reserves the right to take any and all action to protect its copyright in the materials.

9. Warranties: Publisher makes no representations or warranties with respect to the licensed material.

10. Indemnity: You hereby indemnify and agree to hold harmless publisher and CCC, and their respective officers, directors, employees and agents, from and against any and all claims arising out of your use of the licensed material other than as specifically authorized pursuant to this license.

11. No Transfer of License: This license is personal to you and may not be sublicensed, assigned, or transferred by you to any other person without publisher's written permission.

12. No Amendment Except in Writing: This license may not be amended except in a writing signed by both parties (or, in the case of publisher, by CCC on publisher's behalf).

13. Objection to Contrary Terms: Publisher hereby objects to any terms contained in any purchase order, acknowledgment, check endorsement or other writing prepared by you, which terms are inconsistent with these terms and conditions or CCC's Billing and Payment terms and conditions. These terms and conditions, together with CCC's Billing and Payment terms and conditions (which are incorporated herein), comprise the entire agreement between you and publisher (and CCC) concerning this licensing transaction. In the event of any conflict between your obligations established by these terms and conditions and those established by CCC's Billing and Payment terms and conditions, these terms and conditions shall control.

14. Revocation: Elsevier or Copyright Clearance Center may deny the permissions described in this License at their sole discretion, for any reason or no reason, with a full refund payable to you. Notice of such denial will be made using the contact information provided by you. Failure to receive such notice will not alter or invalidate the denial. In no event will Elsevier or Copyright Clearance Center be responsible or liable for any costs, expenses or damage incurred by you as a result of a denial of your permission request, other than a refund of the amount(s) paid by you to Elsevier and/or Copyright Clearance Center for denied permissions.

LIMITED LICENSE

The following terms and conditions apply only to specific license types:

15. **Translation**: This permission is granted for non-exclusive world **English** rights only unless your license was granted for translation rights. If you licensed translation rights you may only translate this content into the languages you requested. A professional translator must perform all translations and reproduce the content word for word preserving the integrity of the article. If this license is to re-use 1 or 2 figures then permission is granted for non-exclusive world rights in all languages.

16. **Posting licensed content on any Website**: The following terms and conditions apply as follows: Licensing material from an Elsevier journal: All content posted to the web site must maintain the copyright information line on the bottom of each image; A hyper-text must be included to the Homepage of the journal from which you are licensing at http://www.sciencedirect.com/science/journal/xxxxx or the Elsevier homepage for books at http://www.elsevier.com; Central Storage: This license does not include permission for a scanned version of the material to be stored in a central repository such as that provided by Heron/XanEdu. Licensing material from an Elsevier book: A hyper-text link must be included to the Elsevier homepage at http://www.elsevier.com . All content posted to the web site must maintain the copyright information line on the bottom of each image.

Posting licensed content on Electronic reserve: In addition to the above the following clauses are applicable: The web site must be password-protected and made available only to bona fide students registered on a relevant course. This permission is granted for 1 year only. You may obtain a new license for future website posting.

For journal authors: the following clauses are applicable in addition to the above: Permission granted is limited to the author accepted manuscript version* of your paper.

*Accepted Author Manuscript(AAM)Definition: An accepted author manuscript (AAM) is the

author's version of the manuscript of an article that has been accepted for publication and which may include any author-incorporated changes suggested through the processes of submission processing, peer review, and editor-author communications. AAMs do not include other publisher value-added contributions such as copy-editing, formatting, technical enhancements and (if relevant) pagination.

You are not allowed to download and post the published journal article (whether PDF or HTML, proof or final version), nor may you scan the printed edition to create an electronic version. A hyper-text must be included to the Homepage of the journal from which you are licensing at http://www.sciencedirect.com/science/journal/xxxxx. As part of our normal production process, you will receive an e-mail notice when your article appears on Elsevier's online service ScienceDirect (www.sciencedirect.com). That e-mail will include the article's Digital Object Identifier (DOI). This number provides the electronic link to the published article and should be included in the posting of your personal version. We ask that you wait until you receive this e-mail and have the DOI to do any posting.

Posting to a repository: Authors may post their AAM immediately to their employer's institutional repository for internal use only and may make their manuscript publically available after the journal-specific embargo period has ended.

Please also refer to Elsevier's Article Posting Policy for further information.

18. **For book authors** the following clauses are applicable in addition to the above: Authors are permitted to place a brief summary of their work online only.. You are not allowed to download and post the published electronic version of your chapter, nor may you scan the printed edition to create an electronic version. **Posting to a repository:** Authors are permitted to post a summary of their chapter only in their institution's repository.

20. **Thesis/Dissertation**: If your license is for use in a thesis/dissertation your thesis may be submitted to your institution in either print or electronic form. Should your thesis be published commercially, please reapply for permission. These requirements include permission for the Library and Archives of Canada to supply single copies, on demand, of the complete thesis and include permission for Proquest/UMI to supply single copies, on demand, of the complete thesis. Should your thesis be published commercially, please reapply for permission.

Elsevier Open Access Terms and Conditions

Elsevier publishes Open Access articles in both its Open Access journals and via its Open Access articles option in subscription journals.

Authors publishing in an Open Access journal or who choose to make their article Open Access in an Elsevier subscription journal select one of the following Creative Commons user licenses, which define how a reader may reuse their work: Creative Commons Attribution License (CC BY), Creative Commons Attribution – Non Commercial - ShareAlike (CC BY NC SA) and Creative Commons Attribution – Non Commercial – No Derivatives (CC BY NC ND)

Terms & Conditions applicable to all Elsevier Open Access articles:

Any reuse of the article must not represent the author as endorsing the adaptation of the article nor should the article be modified in such a way as to damage the author's honour or reputation.

The author(s) must be appropriately credited.

If any part of the material to be used (for example, figures) has appeared in our publication with credit or acknowledgement to another source it is the responsibility of the user to ensure their reuse complies with the terms and conditions determined by the rights holder.

Additional Terms & Conditions applicable to each Creative Commons user license:

CC BY: You may distribute and copy the article, create extracts, abstracts, and other revised versions, adaptations or derivative works of or from an article (such as a translation), to include in a collective work (such as an anthology), to text or data mine the article, including for commercial purposes without permission from Elsevier

114

B.2   Permission from Ultrasonics Sonochemistry

Will you be translating?	No
Order reference number	24602
Title of your thesis/dissertation	Lignin for Bioenergy & Biomaterials
Expected completion date	Oct 2014
Estimated size (number of pages)	250
Elsevier VAT number	GB 494 6272 12
Permissions price	0.00 USD
VAT/Local Sales Tax	0.00 USD / 0.00 GBP
Total	0.00 USD
Terms and Conditions	

INTRODUCTION

1. The publisher for this copyrighted material is Elsevier. By clicking "accept" in connection with completing this licensing transaction, you agree that the following terms and conditions apply to this transaction (along with the Billing and Payment terms and conditions established by Copyright Clearance Center, Inc. ("CCC"), at the time that you opened your Rightslink account and that are available at any time at http://myaccount.copyright.com).

GENERAL TERMS

2. Elsevier hereby grants you permission to reproduce the aforementioned material subject to the terms and conditions indicated.

3. Acknowledgement: If any part of the material to be used (for example, figures) has appeared in our publication with credit or acknowledgement to another source, permission must also be sought from that source. If such permission is not obtained then that material may not be included in your publication/copies. Suitable acknowledgement to the source must be made, either as a footnote or in a reference list at the end of your publication, as follows:

"Reprinted from Publication title, Vol /edition number, Author(s), Title of article / title of chapter, Pages No., Copyright (Year), with permission from Elsevier [OR APPLICABLE SOCIETY COPYRIGHT OWNER]." Also Lancet special credit - "Reprinted from The Lancet, Vol. number, Author(s), Title of article, Pages No., Copyright (Year), with permission from Elsevier."

4. Reproduction of this material is confined to the purpose and/or media for which permission is hereby given.

5. Altering/Modifying Material: Not Permitted. However figures and illustrations may be altered/adapted minimally to serve your work. Any other abbreviations, additions, deletions and/or any other alterations shall be made only with prior written authorization of Elsevier Ltd. (Please contact Elsevier at permissions@elsevier.com)

6. If the permission fee for the requested use of our material is waived in this instance, please be advised that your future requests for Elsevier materials may attract a fee.

7. Reservation of Rights: Publisher reserves all rights not specifically granted in the combination of (i) the license details provided by you and accepted in the course of this licensing transaction, (ii) these terms and conditions and (iii) CCC's Billing and Payment terms and conditions.

8. License Contingent Upon Payment: While you may exercise the rights licensed immediately upon issuance of the license at the end of the licensing process for the transaction, provided that you have disclosed complete and accurate details of your proposed use, no license is finally effective unless and until full payment is received from you (either by publisher or by CCC) as provided in CCC's Billing and Payment terms and conditions. If full payment is not received on a timely basis, then any

license preliminarily granted shall be deemed automatically revoked and shall be void as if never granted. Further, in the event that you breach any of these terms and conditions or any of CCC's Billing and Payment terms and conditions, the license is automatically revoked and shall be void as if never granted. Use of materials as described in a revoked license, as well as any use of the materials beyond the scope of an unrevoked license, may constitute copyright infringement and publisher reserves the right to take any and all action to protect its copyright in the materials.

9. Warranties: Publisher makes no representations or warranties with respect to the licensed material.

10. Indemnity: You hereby indemnify and agree to hold harmless publisher and CCC, and their respective officers, directors, employees and agents, from and against any and all claims arising out of your use of the licensed material other than as specifically authorized pursuant to this license.

11. No Transfer of License: This license is personal to you and may not be sublicensed, assigned, or transferred by you to any other person without publisher's written permission.

12. No Amendment Except in Writing: This license may not be amended except in a writing signed by both parties (or, in the case of publisher, by CCC on publisher's behalf).

13. Objection to Contrary Terms: Publisher hereby objects to any terms contained in any purchase order, acknowledgment, check endorsement or other writing prepared by you, which terms are inconsistent with these terms and conditions or CCC's Billing and Payment terms and conditions. These terms and conditions, together with CCC's Billing and Payment terms and conditions (which are incorporated herein), comprise the entire agreement between you and publisher (and CCC) concerning this licensing transaction. In the event of any conflict between your obligations established by these terms and conditions and those established by CCC's Billing and Payment terms and conditions, these terms and conditions shall control.

14. Revocation: Elsevier or Copyright Clearance Center may deny the permissions described in this License at their sole discretion, for any reason or no reason, with a full refund payable to you. Notice of such denial will be made using the contact information provided by you. Failure to receive such notice will not alter or invalidate the denial. In no event will Elsevier or Copyright Clearance Center be responsible or liable for any costs, expenses or damage incurred by you as a result of a denial of your permission request, other than a refund of the amount(s) paid by you to Elsevier and/or Copyright Clearance Center for denied permissions.

LIMITED LICENSE

The following terms and conditions apply only to specific license types:

15. **Translation**: This permission is granted for non-exclusive world **English** rights only unless your license was granted for translation rights. If you licensed translation rights you may only translate this content into the languages you requested. A professional translator must perform all translations and reproduce the content word for word preserving the integrity of the article. If this license is to re-use 1 or 2 figures then permission is granted for non-exclusive world rights in all languages.

16. **Posting licensed content on any Website**: The following terms and conditions apply as follows: Licensing material from an Elsevier journal: All content posted to the web site must maintain the copyright information line on the bottom of each image; A hyper-text must be included to the Homepage of the journal from which you are licensing at http://www.sciencedirect.com/science/journal/xxxxx or the Elsevier homepage for books at http://www.elsevier.com; Central Storage: This license does not include permission for a scanned version of the material to be stored in a central repository such as that provided by Heron/XanEdu. Licensing material from an Elsevier book: A hyper-text link must be included to the Elsevier homepage at http://www.elsevier.com . All content posted to the web site must maintain the copyright information line on the bottom of each image.

Posting licensed content on Electronic reserve: In addition to the above the following clauses are applicable: The web site must be password-protected and made available only to bona fide students registered on a relevant course. This permission is granted for 1 year only. You may obtain a new

license for future website posting.

For journal authors: the following clauses are applicable in addition to the above: Permission granted is limited to the author accepted manuscript version* of your paper.

***Accepted Author Manuscript(AAM)Definition:** An accepted author manuscript (AAM) is the author's version of the manuscript of an article that has been accepted for publication and which may include any author-incorporated changes suggested through the processes of submission processing, peer review, and editor-author communications. AAMs do not include other publisher value-added contributions such as copy-editing, formatting, technical enhancements and (if relevant) pagination. You are not allowed to download and post the published journal article (whether PDF or HTML, proof or final version), nor may you scan the printed edition to create an electronic version. A hyper-text must be included to the Homepage of the journal from which you are licensing at http://www.sciencedirect.com/science/journal/xxxxx. As part of our normal production process, you will receive an e-mail notice when your article appears on Elsevier's online service ScienceDirect (www.sciencedirect.com). That e-mail will include the article's Digital Object Identifier (DOI). This number provides the electronic link to the published article and should be included in the posting of your personal version. We ask that you wait until you receive this e-mail and have the DOI to do any posting.

Posting to a repository: Authors may post their AAM immediately to their employer's institutional repository for internal use only and may make their manuscript publically available after the journal-specific embargo period has ended.

Please also refer to Elsevier's Article Posting Policy for further information.

18. **For book authors** the following clauses are applicable in addition to the above: Authors are permitted to place a brief summary of their work online only.. You are not allowed to download and post the published electronic version of your chapter, nor may you scan the printed edition to create an electronic version. **Posting to a repository:** Authors are permitted to post a summary of their chapter only in their institution's repository.

20. **Thesis/Dissertation**: If your license is for use in a thesis/dissertation your thesis may be submitted to your institution in either print or electronic form. Should your thesis be published commercially, please reapply for permission. These requirements include permission for the Library and Archives of Canada to supply single copies, on demand, of the complete thesis and include permission for Proquest/UMI to supply single copies, on demand, of the complete thesis. Should your thesis be published commercially, please reapply for permission.

Elsevier Open Access Terms and Conditions

Elsevier publishes Open Access articles in both its Open Access journals and via its Open Access articles option in subscription journals.

Authors publishing in an Open Access journal or who choose to make their article Open Access in an Elsevier subscription journal select one of the following Creative Commons user licenses, which define how a reader may reuse their work: Creative Commons Attribution License (CC BY), Creative Commons Attribution – Non Commercial - ShareAlike (CC BY NC SA) and Creative Commons Attribution – Non Commercial – No Derivatives (CC BY NC ND)

Terms & Conditions applicable to all Elsevier Open Access articles:

Any reuse of the article must not represent the author as endorsing the adaptation of the article nor should the article be modified in such a way as to damage the author's honour or reputation.

The author(s) must be appropriately credited.

If any part of the material to be used (for example, figures) has appeared in our publication with credit or acknowledgement to another source it is the responsibility of the user to ensure their reuse complies with the terms and conditions determined by the rights holder.

Additional Terms & Conditions applicable to each Creative Commons user license:

CC BY: You may distribute and copy the article, create extracts, abstracts, and other revised

versions, adaptations or derivative works of or from an article (such as a translation), to include in a collective work (such as an anthology), to text or data mine the article, including for commercial purposes without permission from Elsevier

CC BY NC SA: For non-commercial purposes you may distribute and copy the article, create extracts, abstracts and other revised versions, adaptations or derivative works of or from an article (such as a translation), to include in a collective work (such as an anthology), to text and data mine the article and license new adaptations or creations under identical terms without permission from Elsevier

CC BY NC ND: For non-commercial purposes you may distribute and copy the article and include it in a collective work (such as an anthology), provided you do not alter or modify the article, without permission from Elsevier

Any commercial reuse of Open Access articles published with a CC BY NC SA or CC BY NC ND license requires permission from Elsevier and will be subject to a fee.

Commercial reuse includes:

- Promotional purposes (advertising or marketing)
- Commercial exploitation (e.g. a product for sale or loan)
- Systematic distribution (for a fee or free of charge)

Please refer to Elsevier's Open Access Policy for further information.

ELSEVIER LICENSE
TERMS AND CONDITIONS
Feb 12, 2015

This is a License Agreement between Tyrone Wells ("You") and Elsevier ("Elsevier") provided by Copyright Clearance Center ("CCC"). The license consists of your order details, the terms and conditions provided by Elsevier, and the payment terms and conditions.

All payments must be made in full to CCC. For payment instructions, please see information listed at the bottom of this form.

Supplier	Elsevier Limited
	The Boulevard, Langford Lane
	Kidlington,Oxford,OX5 1GB,UK
Registered Company Number	1982084
Customer name	Tyrone Wells
Customer address	Renewable Bioproducts Institute
	ATLANTA, GA 30311
License number	3566620055001
License date	Feb 12, 2015
Licensed content publisher	Elsevier
Licensed content publication	Biomass and Bioenergy
Licensed content title	Bioconversion of lignocellulosic pretreatment effluent via oleaginous Rhodococcus opacus DSM 1069
Licensed content author	None
Licensed content date	January 2015
Licensed content volume number	72
Licensed content issue number	n/a
Number of pages	6
Start Page	200
End Page	205
Type of Use	reuse in a thesis/dissertation
Portion	full article

Format	both print and electronic
Are you the author of this Elsevier article?	Yes
Will you be translating?	No
Title of your thesis/dissertation	Lignin for Bioenergy & Biomaterials
Expected completion date	May 2015
Estimated size (number of pages)	160
Elsevier VAT number	GB 494 6272 12
Permissions price	0.00 USD
VAT/Local Sales Tax	0.00 USD / 0.00 GBP
Total	0.00 USD

Terms and Conditions

INTRODUCTION
1. The publisher for this copyrighted material is Elsevier. By clicking "accept" in connection with completing this licensing transaction, you agree that the following terms and conditions apply to this transaction (along with the Billing and Payment terms and conditions established by Copyright Clearance Center, Inc. ("CCC"), at the time that you opened your Rightslink account and that are available at any time at http://myaccount.copyright.com).

GENERAL TERMS
2. Elsevier hereby grants you permission to reproduce the aforementioned material subject to the terms and conditions indicated.
3. Acknowledgement: If any part of the material to be used (for example, figures) has appeared in our publication with credit or acknowledgement to another source, permission must also be sought from that source. If such permission is not obtained then that material may not be included in your publication/copies. Suitable acknowledgement to the source must be made, either as a footnote or in a reference list at the end of your publication, as follows:
"Reprinted from Publication title, Vol /edition number, Author(s), Title of article / title of chapter, Pages No., Copyright (Year), with permission from Elsevier [OR APPLICABLE SOCIETY COPYRIGHT OWNER]." Also Lancet special credit - "Reprinted from The Lancet, Vol. number, Author(s), Title of article, Pages No., Copyright (Year), with permission from Elsevier."
4. Reproduction of this material is confined to the purpose and/or media for which permission is hereby given.
5. Altering/Modifying Material: Not Permitted. However figures and illustrations may be altered/adapted minimally to serve your work. Any other abbreviations, additions, deletions and/or any other alterations shall be made only with prior written authorization of Elsevier Ltd. (Please contact Elsevier at permissions@elsevier.com)
6. If the permission fee for the requested use of our material is waived in this instance, please be advised that your future requests for Elsevier materials may attract a fee.
7. Reservation of Rights: Publisher reserves all rights not specifically granted in the combination of (i) the license details provided by you and accepted in the course of this

licensing transaction, (ii) these terms and conditions and (iii) CCC's Billing and Payment terms and conditions.

8. License Contingent Upon Payment: While you may exercise the rights licensed immediately upon issuance of the license at the end of the licensing process for the transaction, provided that you have disclosed complete and accurate details of your proposed use, no license is finally effective unless and until full payment is received from you (either by publisher or by CCC) as provided in CCC's Billing and Payment terms and conditions. If full payment is not received on a timely basis, then any license preliminarily granted shall be deemed automatically revoked and shall be void as if never granted. Further, in the event that you breach any of these terms and conditions or any of CCC's Billing and Payment terms and conditions, the license is automatically revoked and shall be void as if never granted. Use of materials as described in a revoked license, as well as any use of the materials beyond the scope of an unrevoked license, may constitute copyright infringement and publisher reserves the right to take any and all action to protect its copyright in the materials.

9. Warranties: Publisher makes no representations or warranties with respect to the licensed material.

10. Indemnity: You hereby indemnify and agree to hold harmless publisher and CCC, and their respective officers, directors, employees and agents, from and against any and all claims arising out of your use of the licensed material other than as specifically authorized pursuant to this license.

11. No Transfer of License: This license is personal to you and may not be sublicensed, assigned, or transferred by you to any other person without publisher's written permission.

12. No Amendment Except in Writing: This license may not be amended except in a writing signed by both parties (or, in the case of publisher, by CCC on publisher's behalf).

13. Objection to Contrary Terms: Publisher hereby objects to any terms contained in any purchase order, acknowledgment, check endorsement or other writing prepared by you, which terms are inconsistent with these terms and conditions or CCC's Billing and Payment terms and conditions. These terms and conditions, together with CCC's Billing and Payment terms and conditions (which are incorporated herein), comprise the entire agreement between you and publisher (and CCC) concerning this licensing transaction. In the event of any conflict between your obligations established by these terms and conditions and those established by CCC's Billing and Payment terms and conditions, these terms and conditions shall control.

14. Revocation: Elsevier or Copyright Clearance Center may deny the permissions described in this License at their sole discretion, for any reason or no reason, with a full refund payable to you. Notice of such denial will be made using the contact information provided by you. Failure to receive such notice will not alter or invalidate the denial. In no event will Elsevier or Copyright Clearance Center be responsible or liable for any costs, expenses or damage incurred by you as a result of a denial of your permission request, other than a refund of the amount(s) paid by you to Elsevier and/or Copyright Clearance Center for denied permissions.

LIMITED LICENSE

The following terms and conditions apply only to specific license types:

15. **Translation**: This permission is granted for non-exclusive world **English** rights only unless your license was granted for translation rights. If you licensed translation rights you

may only translate this content into the languages you requested. A professional translator must perform all translations and reproduce the content word for word preserving the integrity of the article. If this license is to re-use 1 or 2 figures then permission is granted for non-exclusive world rights in all languages.

16. **Posting licensed content on any Website**: The following terms and conditions apply as follows: Licensing material from an Elsevier journal: All content posted to the web site must maintain the copyright information line on the bottom of each image; A hyper-text must be included to the Homepage of the journal from which you are licensing at http://www.sciencedirect.com/science/journal/xxxxx or the Elsevier homepage for books at http://www.elsevier.com; Central Storage: This license does not include permission for a scanned version of the material to be stored in a central repository such as that provided by Heron/XanEdu.

Licensing material from an Elsevier book: A hyper-text link must be included to the Elsevier homepage at http://www.elsevier.com . All content posted to the web site must maintain the copyright information line on the bottom of each image.

Posting licensed content on Electronic reserve: In addition to the above the following clauses are applicable: The web site must be password-protected and made available only to bona fide students registered on a relevant course. This permission is granted for 1 year only. You may obtain a new license for future website posting.

17. **For journal authors:** the following clauses are applicable in addition to the above: Permission granted is limited to the author accepted manuscript version* of your paper.

*Accepted Author Manuscript (AAM) Definition: An accepted author manuscript (AAM) is the author's version of the manuscript of an article that has been accepted for publication and which may include any author-incorporated changes suggested through the processes of submission processing, peer review, and editor-author communications. AAMs do not include other publisher value-added contributions such as copy-editing, formatting, technical enhancements and (if relevant) pagination.

You are not allowed to download and post the published journal article (whether PDF or HTML, proof or final version), nor may you scan the printed edition to create an electronic version. A hyper-text must be included to the Homepage of the journal from which you are licensing at http://www.sciencedirect.com/science/journal/xxxxx. As part of our normal production process, you will receive an e-mail notice when your article appears on Elsevier's online service ScienceDirect (www.sciencedirect.com). That e-mail will include the article's Digital Object Identifier (DOI). This number provides the electronic link to the published article and should be included in the posting of your personal version. We ask that you wait until you receive this e-mail and have the DOI to do any posting.

18. **Posting to a repository:** Authors may post their AAM immediately to their employer's institutional repository for internal use only and may make their manuscript publically available after the journal-specific embargo period has ended.

Please also refer to Elsevier's Article Posting Policy for further information.

19. **For book authors** the following clauses are applicable in addition to the above: Authors are permitted to place a brief summary of their work online only.. You are not allowed to download and post the published electronic version of your chapter, nor may you scan the printed edition to create an electronic version. **Posting to a repository:** Authors are permitted to post a summary of their chapter only in their institution's

repository.

20. **Thesis/Dissertation**: If your license is for use in a thesis/dissertation your thesis may be submitted to your institution in either print or electronic form. Should your thesis be published commercially, please reapply for permission. These requirements include permission for the Library and Archives of Canada to supply single copies, on demand, of the complete thesis and include permission for Proquest/UMI to supply single copies, on demand, of the complete thesis. Should your thesis be published commercially, please reapply for permission.

Elsevier Open Access Terms and Conditions

Elsevier publishes Open Access articles in both its Open Access journals and via its Open Access articles option in subscription journals.

Authors publishing in an Open Access journal or who choose to make their article Open Access in an Elsevier subscription journal select one of the following Creative Commons user licenses, which define how a reader may reuse their work: Creative Commons Attribution License (CC BY), Creative Commons Attribution – Non Commercial - ShareAlike (CC BY NC SA) and Creative Commons Attribution – Non Commercial – No Derivatives (CC BY NC ND)

Terms & Conditions applicable to all Elsevier Open Access articles:

Any reuse of the article must not represent the author as endorsing the adaptation of the article nor should the article be modified in such a way as to damage the author's honour or reputation.

The author(s) must be appropriately credited.

If any part of the material to be used (for example, figures) has appeared in our publication with credit or acknowledgement to another source it is the responsibility of the user to ensure their reuse complies with the terms and conditions determined by the rights holder.

Additional Terms & Conditions applicable to each Creative Commons user license:

CC BY: You may distribute and copy the article, create extracts, abstracts, and other revised versions, adaptations or derivative works of or from an article (such as a translation), to include in a collective work (such as an anthology), to text or data mine the article, including for commercial purposes without permission from Elsevier

CC BY NC SA: For non-commercial purposes you may distribute and copy the article, create extracts, abstracts and other revised versions, adaptations or derivative works of or from an article (such as a translation), to include in a collective work (such as an anthology), to text and data mine the article and license new adaptations or creations under identical terms without permission from Elsevier

CC BY NC ND: For non-commercial purposes you may distribute and copy the article and include it in a collective work (such as an anthology), provided you do not alter or modify the article, without permission from Elsevier

Any commercial reuse of Open Access articles published with a CC BY NC SA or CC BY NC ND license requires permission from Elsevier and will be subject to a fee.

Commercial reuse includes:

- Promotional purposes (advertising or marketing)
- Commercial exploitation (e.g. a product for sale or loan)
- Systematic distribution (for a fee or free of charge)

Please refer to Elsevier's Open Access Policy for further information.

21. **Other Conditions**:

v1.7

Questions? customercare@copyright.com or +1-855-239-3415 (toll free in the US) or +1-978-646-2777.

Gratis licenses (referencing $0 in the Total field) are free. Please retain this printable license for your reference. No payment is required.

REFERENCES

1   Aardema, H., Meertens, J., Ligtenberg, J., et al., *Organophosphorus Pesticide Poisoning: Cases and Developments.* Neth J Med, 2008. **66**: p. 149-153.

2   Ahmad, M., Roberts, J.N., Hardiman, E.M., et al., *Identification of Dypb from Rhodococcus Jostii Rha1 as a Lignin Peroxidase.* Biochemistry, 2011. **50**: p. 5096-5107.

3   Albersheim, P., Darvill, A., Roberts, K., et al., *Plant Cell Walls: From Chemistry to Biology*Garland Science, Taylor and Francis Group, LLC, 2010).

4   Alvarez, H.M., Kalscheuer, R., and Steinbuchel, A., *Accumulation and Mobilization of Storage Lipids by Rhodococcus Opacus Pd630 and Rhodococcus Ruber Ncimb 40126.* Appl. Microbiol. Biotechnol., 2000. **54**: p. 218-223.

5   Alvarez, H.M., and Steinbuechel, A., *Triacylglycerols in Prokaryotic Microorganisms.* Appl. Microbiol. Biotechnol., 2002. **60**: p. 367-376.

6   Anastas, P.T., and Kirchhoff, M.M., *Origins, Current Status, and Future Challenges of Green Chemistry.* Accounts of chemical research, 2002. **35**: p. 686-694.

7   Anastas, P.T., and Warner, J.C., *Green Chemistry: Theory and Practice*Oxford University Press, 2000).

8   Anastas, P.T., and Zimmerman, J.B., *Peer Reviewed: Design through the 12 Principles of Green Engineering.* Environmental science & technology, 2003. **37**: p. 94A-101A.

9   Areskogh, D., Li, J., Gellerstedt, G., et al., *Investigation of the Molecular Weight Increase of Commercial Lignosulfonates by Laccase Catalysis.* Biomacromolecules, 2010. **11**: p. 904-910.

10   Arkell, A., Olsson, J., Stigsson, L., et al., 'Extraction of Lignin from Kraft Black Liquor by Membrane Filtration', in *Nordic Wood Biorefinery Conference*Innventia, 2014), p. 219-220.

11   Assi, J.A., King, A.J., and Vander, G.J., *Co2 Evolution Rate During Solid-State Fermentation for Preparation of Tomato Pomace as Poultry Feed Ingredient.* Int. J. Agric. Biol. Eng., 2009. **2**: p. 28-32.

12   Bacic, A., Harris, P.J., and Stone, B.A., *Structure and Function of Plant Cell Walls.* The biochemistry of plants, 1988. **14**: p. 297-371.

13   Baker, D.A., and Rials, T.G., *Recent Advances in Low-Cost Carbon Fiber Manufacture from Lignin.* J. Appl. Polym. Sci., 2013. **130**: p. 713-728.

14   Barr, L.M., *Cercla Made Simple: An Analysis of the Cases under the Comprehensive Environmental Response, Compensation and Liability Act of 1980.* The Business Lawyer, 1990. p. 923-1001.

15   Basheer, F., Isa, M.H., and Farooqi, I.H., *Biodegradation of O-Nitrophenol by Aerobic Granules with Glucose as Co-Substrate.* Water Sci Technol, 2012. **65**: p. 2132-2139.

16   Basheer, S., Kunhi, A., Varadaraj, M., et al., *Nuclear Magnetic Resonance Spectroscopic Studies on the Microbial Degradation of Mononitrophenol Isomers.* World Journal of Microbiology and Biotechnology, 2007. **23**: p. 49-63.

17   Basheer, S., Kunhi, A.A.M., Varadaraj, M.C., et al., *Nuclear Magnetic Resonance Spectroscopic Studies on the Microbial Degradation of Mononitrophenol Isomers.* World J. Microbiol. Biotechnol., 2007. **23**: p. 49-63.

18   Ben, H., Mu, W., Deng, Y., et al., *Production of Renewable Gasoline from Aqueous Phase Hydrogenation of Lignin Pyrolysis Oil.* Fuel, 2013. **103**: p. 1148-1153.

19   Ben, H., and Ragauskas, A.J., *Heteronuclear Single-Quantum Correlation-Nuclear Magnetic Resonance (Hsqc-Nmr) Fingerprint Analysis of Pyrolysis Oils.* Energy Fuels, 2011. **25**: p. 5791-5801.

20   *In Situ Nmr Characterization of Pyrolysis Oil During Accelerated Aging.* ChemSusChem, 2012. **5**: p. 1687-1693.

21   *Pyrolysis of Biomass to Biofuels.* Prepr. Symp. - Am. Chem. Soc., Div. Fuel Chem., 2012. **57**: p. 140-141.

22   Bianchi, D., Franzosi, G., and Romano, A.M., 'Process for the Production of Lipids from Biomass', Eni S.p.A., Italy . 2012), p. 41pp.

23   Bleichrodt, F.S., Fischer, R., and Gerischer, U.C., *The Beta-Ketoadipate Pathway of Acinetobacter Baylyi Undergoes Carbon Catabolite Repression, Cross-Regulation and Vertical Regulation, and Is Affected by Crc.* Microbiology, 2010. **156**: p. 1313-1322.

24   Braun, J.L., Holtman, K.M., and Kadla, J.F., *Lignin-Based Carbon Fibers: Oxidative Thermostabilization of Kraft Lignin.* Carbon, 2005. **43**: p. 385-394.

25   Brodin, I., Ernstsson, M., Gellerstedt, G., et al., *Oxidative Stabilisation of Kraft Lignin for Carbon Fiber Production.* Holzforschung, 2012. **66**: p. 141-147.

26   Carpita, N.C., *Progress in the Biological Synthesis of the Plant Cell Wall: New Ideas for Improving Biomass for Bioenergy.* Curr. Opin. Biotechnol., 2012. **23**: p. 330-337.

27   Carson, R., *Silent Spring*Houghton Mifflin Harcourt, 2002).

28   Cateto, C., Hu, G., and Ragauskas, A., *Enzymatic Hydrolysis of Organosolv Kanlow Switchgrass and Its Impact on Cellulose Crystallinity and Degree of Polymerization.* Energy Environ. Sci., 2011. **4**: p. 1516-1521.

29   Chakar, F.S., and Ragauskas, A.J., *Review of Current and Future Softwood Kraft Lignin Process Chemistry.* Industrial Crops and Products, 2004. **20**: p. 131-141.

30   Chatterjee, S., Clingenpeel, A., McKenna, A., et al., *Synthesis and Characterization of Lignin-Based Carbon Materials with Tunable Microstructure.* RSC Advances, 2014. **4**: p. 4743-4753.

31   Chatterjee, S., and Dutta, T.K., *Complete Degradation of Butyl Benzyl Phthalate by a Defined Bacterial Consortium: Role of Individual Isolates in the Assimilation Pathway.* Chemosphere, 2008. **70**: p. 933-941.

32   Chatterjee, S., Rios, O., and Johs, A., 'Preparation and Characterization of Modified Lignin for Energy Storage Applications', American Chemical Society, 2013), p. ENVR-113.

33   Chaudhry, M.T., Huang, Y., Shen, X.-H., et al., *Genome-Wide Investigation of Aromatic Acid Transporters in Corynebacterium Glutamicum.* Microbiology (Reading, U. K.), 2007. **153**: p. 857-865.

34   Chauhan, A., and Jain, R.K., *Biodegradation: Gaining Insight through Proteomics.* Biodegradation, 2010. **21**: p. 861-879.

35   Chauhan, A., Pandey, G., Sharma, N.K., et al., *P-Nitrophenol Degradation Via 4-Nitrocatechol in Burkholderia Sp. Sj98 and Cloning of Some of the Lower Pathway Genes.* Environ. Sci. Technol.*,* 2010. **44**: p. 3435-3441.

36   Choi, J.-W., Faix, O., and Meier, D., *Characterization of Residual Lignins from Chemical Pulps of Spruce (Picea Abies L.) and Beech (Fagus Sylvatica L.) by Analytical Pyrolysis–Gas Chromatography/Mass Spectrometry.* Holzforschung*,* 2001. **55**: p. 185-192.

37   Chung, I., Kim, T., and Mays, J., 'Lignin Based Carbon Fiber Precursors', American Chemical Society, 2013), p. POLY-489.

38   Ciolacu, D., Ciolacu, F., and Popa, V.I., *Amorphous Cellulose—Structure and Characterization.* Cellulose chemistry and technology*,* 2011. **45**: p. 13.

39   Clinton, P.B., *Chemical Weapons Convention.* US Department nf State Dispatch*,* 1993. **4**: p. 849-851.

40   Cui, C., Sadeghifar, H., Sen, S., et al., *Toward Thermoplastic Lignin Polymers; Part Ii: Thermal & Polymer Characteristics of Kraft Lignin & Derivatives.* BioResources*,* 2013. **8**: p. 864-886.

41   de, l.T.M.J., Moral, A., Hernandez, M.D., et al., *Organosolv Lignin for Biofuel.* Ind. Crops Prod.*,* 2013. **45**: p. 58-63.

42   Dhillon, G.S., Brar, S.K., Kaur, S., et al., *Screening of Agro-Industrial Wastes for Citric Acid Bioproduction by Aspergillus Niger Nrrl 2001 through Solid State Fermentation.* J. Sci. Food Agric.*,* 2013. **93**: p. 1560-1567.

43   Dimitris, S.A., 'Heteronuclear Nmr Spectroscopy of Lignins', in *Lignin and Lignans*, CRC Press, 2010), p. 245-265.

44   Donald, D., and Göran, G., 'Chemistry of Alkaline Pulping', in *Lignin and Lignans*, CRC Press, 2010), p. 349-391.

45   Duan, Y., Wan, J., Wang, Y., et al., *Study on Saccharification of Eucalyptus Lignocelluloses Hydrolysis and Reaction Kinetics in Supercritical Water.* Taiyangneng Xuebao*,* 2013. **34**: p. 689-695.

46   Eggeling, L., and Sahm, H., *Degradation of Coniferyl Alcohol and Other Lignin-Related Aromatic Compounds by Nocardia Sp. Dsm 1069.* Archives of Microbiology*,* 1980. **126**: p. 141-148.

47   Feng, C., Kang, J., Jian, Z., et al., *Research Advance of Renewable Energy Micro-Biodiesel.* Zhongguo Youzhi*,* 2012. **37**: p. 76-80.

48   Ferreira, M.I.M., Iida, T., Hasan, S.A., et al., *Analysis of Two Gene Clusters Involved in the Degradation of 4-Fluorophenol by Arthrobacter Sp. Strain If1.* Appl. Environ. Microbiol.*,* 2009. **75**: p. 7767-7773.

49   Foston, M., Hubbell, C.A., Samuel, R., et al., *Chemical, Ultrastructural and Supramolecular Analysis of Tension Wood in Populus Tremula X Alba as a Model Substrate for Reduced Recalcitrance.* Energy Environ. Sci.*,* 2011. **4**: p. 4962-4971.

50   Foston, M., Nunnery, G.A., Meng, X., et al., *Nmr a Critical Tool to Study the Production of Carbon Fiber from Lignin.* Carbon*,* 2013. **52**: p. 65-73.

51   Frank, E., Steudle, L.M., Ingildeev, D., et al., *Carbon Fibers: Precursor Systems, Processing, Structure, and Properties.* Angew. Chem., Int. Ed.*,* 2014. **53**: p. 5262-5298.

52   Friedlingstein, P., Andrew, R., Rogelj, J., et al., *Persistent Growth of Co2 Emissions and Implications for Reaching Climate Targets.* Nature Geoscience, 2014. **7**: p. 709-715.

53   Gan, H.M., Ibrahim, Z., Shahir, S., et al., *Identification of Genes Involved in the 4-Aminobenzenesulfonate Degradation Pathway of Hydrogenophaga Sp. Pbc Via Transposon Mutagenesis.* FEMS Microbiol. Lett., 2011. **318**: p. 108-114.

54   Giedraityte, G., and Kalediene, L., *Catechol 1,2-Dioxygenase from A-Naphthol Degrading Thermophilic Geobacillus Sp. Strain: Purification and Properties.* Cent. Eur. J. Biol., 2009. **4**: p. 68-73.

55   Glasser, W.G., and Glasser, H.R., *Evaluation of Lignin's Chemical Structure by Experimental and Computer Simulation Techniques.* Paperi ja puu, 1981. p.

56   Glazebrook, J., 'Role of the Plant Cell Wall in Resistance to Pathogen Attack', in *Research Meeting*, 2012), p. 16.

57   Gong, Z., Shen, H., Wang, Q., et al., *Efficient Conversion of Biomass into Lipids by Using the Simultaneous Saccharification and Enhanced Lipid Production Process.* Biotechnol. Biofuels, 2013. **6**: p. 36.

58   Gouveia, S., Fernández-Costas, C., Sanromán, M., et al., *Polymerisation of Kraft Lignin from Black Liquors by Laccase from Myceliophthora Thermophila: Effect of Operational Conditions and Black Liquor Origin.* Bioresource technology, 2013. p.

59   Gouveia, S., Fernandez-Costas, C., Sanroman, M.A., et al., *Polymerisation of Kraft Lignin from Black Liquors by Laccase from Myceliophthora Thermophila: Effect of Operational Conditions and Black Liquor Origin.* Bioresour. Technol., 2013. **131**: p. 288-294.

60   Guerra, A., Filpponen, I., Lucia, L.A., et al., *Comparative Evaluation of Three Lignin Isolation Protocols for Various Wood Species.* Journal of agricultural and food chemistry, 2006. **54**: p. 9696-9705.

61   Haghighi Mood, S., Hossein Golfeshan, A., Tabatabaei, M., et al., *Lignocellulosic Biomass to Bioethanol, a Comprehensive Review with a Focus on Pretreatment.* Renewable and Sustainable Energy Reviews, 2013. **27**: p. 77-93.

62   Hallac, B.B., *Fundamental Understanding of the Biochemical Conversion of Buddleja Davidii to Fermentable Sugars.* 2011. p.

63   Hallac, B.B., and Ragauskas, A.J., *Analyzing Cellulose Degree of Polymerization and Its Relevancy to Cellulosic Ethanol.* Biofuels, Bioprod. Biorefin., 2011. **5**: p. 215-225.

64   Hamaguchi, M., Kautto, J., and Vakkilainen, E., *Effects of Hemicellulose Extraction on the Kraft Pulp Mill Operation and Energy Use: Review and Case Study with Lignin Removal.* Chemical Engineering Research and Design, 2013. **91**: p. 1284-1291.

65   Harwood, C.S., and Parales, R.E., *The B-Ketoadipate Pathway and the Biology of Self-Identity.* Annu. Rev. Microbiol., 1996. **50**: p. 553-590.

66   Haussmann, U., and Poetsch, A., *Global Proteome Survey of Protocatechuate- and Glucose-Grown Corynebacterium Glutamicum Reveals Multiple Physiological Differences.* J. Proteomics, 2012. **75**: p. 2649-2659.

67   Hodge, G., and Woodbridge, W., *Use of near Infrared Spectroscopy to Predict Lignin Content in Tropical and Sub-Tropical Pines.* Journal of near infrared spectroscopy*,* 2005. **12**: p. 381-390.

68   Hu, G., Cateto, C., Pu, Y., et al., *Structural Characterization of Switchgrass Lignin after Ethanol Organosolv Pretreatment.* Energy Fuels*,* 2012. **26**: p. 740-745.

69   Hu, Z., Foston, M.B., and Ragauskas, A.J., *Biomass Characterization of Morphological Portions of Alamo Switchgrass.* J. Agric. Food Chem.*,* 2011. **59**: p. 7765-7772.

70   Huang, D., and Qian, J., 'Method for Producing High-Purity Mannooligosaccharide Via Enzymic Hydrolysis of Manna-Containing Hemicellulose', Peop. Rep. China . 2013), p. 11pp.; Chemical Indexing Equivalent to 156:388287 (CN).

71   Ioelovich, M., *Cellulose as a Nanostructured Polymer: A Short Review.* BioResources*,* 2008. **3**: p. 1403-1418.

72   Ishida, H., *Quantitative Surface Ft-Ir Spectroscopic Analysis of Polymers.* Rubber chemistry and technology*,* 1987. **60**: p. 497-554.

73   Jeffries, T.W., 'Biodegradation of Lignin and Hemicelluloses', in *Biochemistry of Microbial Degradation*, Springer, 1994), p. 233-277.

74   Jia, Z., Qin, Q., Darvill, A.G., et al., *Structure of the Xyloglucan Produced by Suspension-Cultured Tomato Cells.* Carbohydr. Res.*,* 2003. **338**: p. 1197-1208.

75   John, R., and Larry, L.L., 'Nmr of Lignins', in *Lignin and Lignans*, CRC Press, 2010), p. 137-243.

76   Johnson, S.M., *From Reaction to Proaction: The 1990 Pollution Prevention Act.* Colum. J. Envtl. L.*,* 1992. **17**: p. 153.

77   Jones, E.J., *The Infrared Spectrum of Spruce Native Lignin.* Journal of the American Chemical Society*,* 1948. **70**: p. 1984-1985.

78   Ju, K.-S., and Parales, R.E., *Nitroaromatic Compounds, from Synthesis to Biodegradation.* Microbiology and molecular biology reviews, 2010. **74**: p. 250-272.

79   Kim, S.-J., Kweon, O., Jones, R.C., et al., *Genomic Analysis of Polycyclic Aromatic Hydrocarbon Degradation in Mycobacterium Vanbaalenii Pyr-1.* Biodegradation*,* 2008. **19**: p. 859-881.

80   *Genomic Analysis of Polycyclic Aromatic Hydrocarbon Degradation in Mycobacterium Vanbaalenii Pyr-1.* Biodegradation*,* 2008. **19**: p. 859-881.

81   Kim, S.-J., Kweon, O., Jones, R.C., et al., *Complete and Integrated Pyrene Degradation Pathway in Mycobacterium Vanbaalenii Pyr-1 Based on Systems Biology.* J. Bacteriol.*,* 2007. **189**: p. 464-472.

82   Ko, F., *Lignin Based Carbon Nanofibers by Electrospinning.* Bulletin of the American Physical Society*,* 2014. p.

83   Komatsu, T., and Kikuchi, J., *Comprehensive Signal Assignment of 13c-Labeled Lignocellulose Using Multidimensional Solution Nmr and 13c Chemical Shift Comparison with Solid-State Nmr.* Anal. Chem. (Washington, DC, U. S.)*,* 2013. **85**: p. 8857-8865.

84   Kopf, P.G., and Walker, M.K., *Overview of Developmental Heart Defects by Dioxins, Pcbs, and Pesticides.* Journal of Environmental Science and Health, Part C*, 2009. **27**: p. 276-285.

85   Kosa, M., and Ragauskas, A., *Lignin to Lipid Bioconversion.* Prepr. Symp. - Am. Chem. Soc., Div. Fuel Chem.*, 2011. **56**: p. 130.

86   Kosa, M., and Ragauskas, A.J., *Bioconversion of Lignin Model Compounds with Oleaginous Rhodococci.* Appl. Microbiol. Biotechnol.*, 2012. **93**: p. 891-900.

87   *Lignin to Lipid Bioconversion by Oleaginous Rhodococci.* Green Chem.*, 2013. **15**: p. 2070-2074.

88   'Lignin to Lipid Bioconversion by Rhodococci Bacteria', American Chemical Society, 2011), p. FUEL-411.

89   *Lipids from Heterotrophic Microbes: Advances in Metabolism Research.* Trends Biotechnol*, 2011. **29**: p. 53-61.

90   Kozlowski, R., Batog, J., Kubica, S., et al., *Nanolignin as an Effective Uv Blocker for Fabrics, Nonwoven and Polymers Foils.* Sci. Isr.--Technol. Advantages*, 2012. **14**: p. 69-73.

91   Kulkarni, M., and Chaudhari, A., *Microbial Remediation of Nitro-Aromatic Compounds: An Overview.* Journal of Environmental Management*, 2007. **85**: p. 496-512.

92   Kurosawa, K., Boccazzi, P., de, A.N.M., et al., *High-Cell-Density Batch Fermentation of Rhodococcus Opacus Pd630 Using a High Glucose Concentration for Triacylglycerol Production.* J. Biotechnol.*, 2010. **147**: p. 212-218.

93   Lee, H.Y., and Yang, J.K., *Crystallization and Preliminary X-Ray Crystallographic Analysis of Γ-Carboxymuconolactone Decarboxylase from Sulfolobus Solfataricus.* Acta Crystallogr., Sect. F: Struct. Biol. Cryst. Commun.*, 2009. **F65**: p. 1197-1199.

94   Lee, Y., and Chen, J., *Study on Graft Copolymerization of Bagasse Kraft Lignin with Acrylamide.* Cellul. Chem. Technol.*, 1990. **24**: p. 611-616.

95   Leigh, M.B., Pellizari, V.H., Uhlik, O., et al., *Biphenyl-Utilizing Bacteria and Their Functional Genes in a Pine Root Zone Contaminated with Polychlorinated Biphenyls (Pcbs).* ISME J.*, 2007. **1**: p. 134-148.

96   Leveau, J.H.J., and Gerards, S., *Discovery of a Bacterial Gene Cluster for Catabolism of the Plant Hormone Indole 3-Acetic Acid.* FEMS Microbiol. Ecol.*, 2008. **65**: p. 238-250.

97   Li, D., Yan, Y., Ping, S., et al., *Genome-Wide Investigation and Functional Characterization of the B-Ketoadipate Pathway in the Nitrogen-Fixing and Root-Associated Bacterium Pseudomonas Stutzeri A1501.* BMC Microbiol.*, 2010. **10**: p. No pp. given.

98   Li, H., and Chen, H., *Detoxification of Steam-Exploded Corn Straw Produced by an Industrial-Scale Reactor.* Process Biochem. (Amsterdam, Neth.)*, 2008. **43**: p. 1447-1451.

99   Li, M., Foster, C., Kelkar, S., et al., *Structural Characterization of Alkaline Hydrogen Peroxide Pretreated Grasses Exhibiting Diverse Lignin Phenotypes.* Biotechnol. Biofuels*, 2012. **5**: p. 38.

100   Li, M.F., Sun, S.N., Xu, F., et al., *Ultrasound-Enhanced Extraction of Lignin from Bamboo (Neosinocalamus Affinis): Characterization of the Ethanol-Soluble Fractions.* Ultrasonics sonochemistry*, 2012. **19**: p. 243-249.

101   Li, S., Mazloumpour, M., Willoughby, J., et al., 'Phase Behavior and Properties of the Oil-in-Water Emulsions Stabilized by Carboxymethylated and Acetylated Lignins', American Chemical Society, 2013), p. COLL-602.

102   Liang, M.-H., and Jiang, J.-G., *Advancing Oleaginous Microorganisms to Produce Lipid Via Metabolic Engineering Technology.* Prog Lipid Res*, 2013. **52**: p. 395-408.

103   Liu, H., and Chen, J., *Study on Graft Copolymerization of Bagasse Kraft Lignin with Maleic Anhydride.* Cellul. Chem. Technol.*, 1991. **25**: p. 79-84.

104   Lu, Y., Wei, X., Zong, Z., et al., *Structural Investigation and Application of Lignins.* Huaxue Jinzhan*, 2013. **25**: p. 838-858.

105   Luo, J., Fang, Z., and Smith Jr, R.L., *Ultrasound-Enhanced Conversion of Biomass to Biofuels.* Progress in Energy and Combustion Science*, 2013. p.

106   Martin-Sampedro, R., Eugenio, M.E., Moreno, J.A., et al., *Integration of a Kraft Pulping Mill into a Forest Biorefinery: Pre-Extraction of Hemicellulose by Steam Explosion Versus Steam Treatment.* Bioresource technology*, 2014. **153**: p. 236-244.

107   Martinez, C., Cotes, T., and Corpas, F.A., *Recovering Wastes from the Paper Industry: Development of Ceramic Materials.* Fuel Process. Technol.*, 2012. **103**: p. 117-124.

108   Mazzoli, R., Pessione, E., Giuffrida, M.G., et al., *Degradation of Aromatic Compounds by Acinetobacter Radioresistens S13: Growth Characteristics on Single Substrates and Mixtures.* Arch. Microbiol.*, 2007. **188**: p. 55-68.

109   Miao, C., and Hamad, W.Y., *Cellulose Reinforced Polymer Composites and Nanocomposites: A Critical Review.* Cellulose*, 2013. **20**: p. 2221-2262.

110   Michniewicz, M., and Janiga, M., *Possibilities of Using Lignocellulosic Biomass - Production of Renewable Fuels and Chemicals.* Przegl. Papier.*, 2011. **67**: p. 727-732.

111   Mohanty, A., Misra, M., and Drzal, L., *Sustainable Bio-Composites from Renewable Resources: Opportunities and Challenges in the Green Materials World.* Journal of Polymers and the Environment*, 2002. **10**: p. 19-26.

112   Monteil-Rivera, F., Phuong, M., Ye, M., et al., *Isolation and Characterization of Herbaceous Lignins for Applications in Biomaterials.* Industrial Crops and Products*, 2013. **41**: p. 356-364.

113   Mudhoo, A., *Biogas Production: Pretreatment Methods in Anaerobic Digestion*John Wiley & Sons, 2012).

114   Nabholz, J., Clements, R., and Zeeman, M., *Information Needs for Risk Assessment in Epa's Office of Pollution Prevention and Toxics.* Ecological Applications*, 1997. **7**: p. 1094-1098.

115   Nagata, Y., Natsui, S., Endo, R., et al., *Genomic Organization and Genomic Structural Rearrangements of Sphingobium Japonicum Ut26, an Archetypal Γ-Hexachlorocyclohexane-Degrading Bacterium.* Enzyme Microb. Technol.*, 2011. **49**: p. 499-508.

116   Nagy, M., *Biofuels from Lignin and Novel Biodiesel Analysis.* 2009. p.

117   Nagy, M., Kosa, M., Ragauskas, A.J., et al., 'New Energy: Fuel Resources from Kraft Pulping', American Chemical Society, 2009), p. CELL-191.

118   Nagy, M., Kosa, M., Theliander, H., et al., *Characterization of Co2 Precipitated Kraft Lignin to Promote Its Utilization.* Green Chem.*,* 2010. **12**: p. 31-34.

119   Najavand, S., Lotfi, A.S., Noghabi, K.A., et al., *A High Potential Organophosphorus Pesticide-Degrading Enzyme from a Newly Characterized, Pseudomonas Aeruginosa Nl01.* Afr. J. Microbiol. Res*,* 2012. **6**: p. 4261-4269.

120   Niemczewski, B., *Cavitation Intensity of Water under Practical Ultrasonic Cleaning Conditions.* Ultrasonics sonochemistry*,* 2014. **21**: p. 354-359.

121   Olaniran, A.O., and Igbinosa, E.O., *Chlorophenols and Other Related Derivatives of Environmental Concern: Properties, Distribution and Microbial Degradation Processes.* Chemosphere*,* 2011. **83**: p. 1297-1306.

122   Olguin, E.J., *Dual Purpose Microalgae-Bacteria-Based Systems That Treat Wastewater and Produce Biodiesel and Chemical Products within a Biorefinery.* Biotechnol. Adv.*,* 2012. **30**: p. 1031-1046.

123   Ornston, L., and Stanier, R., *The Conversion of Catechol and Protocatechuate to B-Ketoadipate by Pseudomonas Putida I. Biochemistry.* Journal of biological chemistry*,* 1966. **241**: p. 3776-3786.

124   Pan, X., Xie, D., Yu, R.W., et al., *The Bioconversion of Mountain Pine Beetle-Killed Lodgepole Pine to Fuel Ethanol Using the Organosolv Process.* Biotechnol. Bioeng.*,* 2008. **101**: p. 39-48.

125   Pascoal Neto, C., Evtuguin, D.V., Furtado, F.P., et al., *Effect of Pulping Conditions on the Ecf Bleachability of Eucalyptus Globulus Kraft Pulps.* Industrial & engineering chemistry research*,* 2002. **41**: p. 6200-6206.

126   Patrauchan, M.A., Florizone, C., Eapen, S., et al., *Roles of Ring-Hydroxylating Dioxygenases in Styrene and Benzene Catabolism in Rhodococcus Jostii Rha1.* J. Bacteriol.*,* 2008. **190**: p. 37-47.

127   *Roles of Ring-Hydroxylating Dioxygenases in Styrene and Benzene Catabolism in Rhodococcus Jostii Rha1.* J. Bacteriol.*,* 2008. **190**: p. 37-47.

128   Peng, X., and Chen, H., *Hemicellulose Sugar Recovery from Steam-Exploded Wheat Straw for Microbial Oil Production.* Process Biochem. (Oxford, U. K.)*,* 2012. **47**: p. 209-215.

129   Peressutti, S.R., Alvarez, H.M., and Pucci, O.H., *Dynamics of Hydrocarbon-Degrading Bacteriocenosis of an Experimental Oil Pollution in Patagonian Soil.* Int. Biodeterior. Biodegrad.*,* 2003. **52**: p. 21-30.

130   Perez-Pantoja, D., De, l.I.R., Pieper, D.H., et al., *Metabolic Reconstruction of Aromatic Compounds Degradation from the Genome of the Amazing Pollutant-Degrading Bacterium Cupriavidus Necator Jmp134.* FEMS Microbiol. Rev.*,* 2008. **32**: p. 736-794.

131   Pinto, P.C., Evtuguin, D.V., and Pascoal Neto, C., *Chemical Composition and Structural Features of the Macromolecular Components of Plantation Acacia Mangium Wood.* Journal of agricultural and food chemistry*,* 2005. **53**: p. 7856-7862.

132   Poke, F.S., and Raymond, C.A., *Predicting Extractives, Lignin, and Cellulose Contents Using near Infrared Spectroscopy on Solid Wood in Eucalyptus Globulus.* Journal of Wood Chemistry and Technology*,* 2006. **26**: p. 187-199.

133   Pu, Y., Cao, S., and Ragauskas, A.J., *Application of Quantitative 31p Nmr in Biomass Lignin and Biofuel Precursors Characterization.* Energy Environ. Sci.*,* 2011. **4**: p. 3154-3166.

134   Pu, Y., Hu, F., Huang, F., et al., *Assessing the Molecular Structure Basis for Biomass Recalcitrance During Dilute Acid and Hydrothermal Pretreatments.* Biotechnol. Biofuels*,* 2013. **6**: p. 15.

135   Pu, Y., Kosa, M., Kalluri, U.C., et al., *Challenges of the Utilization of Wood Polymers: How Can They Be Overcome?* Appl. Microbiol. Biotechnol.*,* 2011. **91**: p. 1525-1536.

136   *Challenges of the Utilization of Wood Polymers: How Can They Be Overcome?* Appl Microbiol Biotechnol*,* 2011. **91**: p. 1525-1536.

137   Qiu, K., and Netravali, A.N., *A Review of Fabrication and Applications of Bacterial Cellulose Based Nanocomposites.* Polymer Reviews, 2014. **54**: p. 598-626.

138   Quiroz-Castañeda, R.E., and Folch-Mallol, J.L., *Hydrolysis of Biomass Mediated by Cellulases for the Production of Sugars.* 2013. p.

139   Ragauskas, A., 'Pretreatment Chemistry: What to Expect and Need', American Chemical Society, 2013), p. ENFL-116.

140   Ragauskas, A.J., Beckham, G.T., Biddy, M.J., et al., *Lignin Valorization: Improving Lignin Processing in the Biorefinery.* Science (Washington, DC, U. S.)*,* 2014. **344**: p. 709.

141   Ragauskas, A.J., and Huang, F., 'Chemical Pretreatment Techniques for Biofuels and Biorefineries from Softwood', in *Pretreatment Techniques for Biofuels and Biorefineries*, Springer, 2013), p. 151-179.

142   Ragnar, M., Lindgren, C.T., and Nilvebrant, N.-O., *Pka-Values of Guaiacyl and Syringyl Phenols Related to Lignin.* Journal of Wood Chemistry and Technology*,* 2000. **20**: p. 277-305.

143   Ramires, E.C., Megiatto, J.D., Gardrat, C., et al., *Valorization of an Industrial Organosolv–Sugarcane Bagasse Lignin: Characterization and Use as a Matrix in Biobased Composites Reinforced with Sisal Fibers.* Biotechnology and bioengineering*,* 2010. **107**: p. 612-621.

144   Rao, R.D., and Parikh, J.K., *Forecast and Analysis of Demand for Petroleum Products in India.* Energy policy*,* 1996. **24**: p. 583-592.

145   Reid, I.D., Bourbonnais, R., and Paice, M.G., 'Biopulping and Biobleaching', in *Lignin and Lignans*, CRC Press, 2010), p. 521-554.

146   Reina, L., Galetta, A., Vinciguerra, V., et al., *The Relationship between< I> Eucalyptus Grandis</I> Lignin Structure and Kraft Pulping Parameters.* Journal of Analytical and Applied Pyrolysis*,* 2014. **107**: p. 284-288.

147   Ruckelshaus, W.D., *Environmental Protection: A Brief History of the Environmental Movement in America and the Implications Abroad.* Envtl. L.*,* 1984. **15**: p. 455.

148   Russell, R.L., Johnson, K., Durbin, T., et al., 'Regulated Emissions from Liquefied Petroleum Gas (Lpg) Powered Vehicles', SAE Technical Paper, 2014).

149   Saadia, A., and Ashfaq, A., *Environmental Management in Pulp and Paper Industry.* J. Ind. Pollut. Control*,* 2010. **26**: p. 71-77.

150   Saadia, A., Ashfaq, A., and Khursheed, A., *Pollution Control Trends in Pulp and Paper Industry.* Environ. Pollut. Control J.*,* 2010. **13**: p. 43-46.

151   Sal'nikov, V.V., Rempel, S.I., Yur'eva, L.V., et al., *Effect of Ultrasound on Hydrolysis Lignin.* Tr. Ural'sk. Lesotekhn. Inst.*,* 1962. p. 9-21.

152   Samuel, R., Cao, S., Das, B.K., et al., *Investigation of the Fate of Poplar Lignin During Autohydrolysis Pretreatment to Understand the Biomass Recalcitrance.* RSC Adv.*,* 2013. **3**: p. 5305-5309.

153   Samuel, R., Foston, M., Jiang, N., et al., *Structural Changes in Switchgrass Lignin and Hemicelluloses During Pretreatments by Nmr Analysis.* Polym. Degrad. Stab.*,* 2011. **96**: p. 2002-2009.

154   Sanches, S., Penetra, A., Rodrigues, A., et al., *Nanofiltration of Hormones and Pesticides in Different Real Drinking Water Sources.* Separation and Purification Technology, 2012. **94**: p. 44-53.

155   Santos, A.J., Anjos, O., and Simoes, R., *Papermaking Potential of Acacia Dealbata and Acacia Melanoxylon.* Appita Journal: Journal of the Technical Association of the Australian and New Zealand Pulp and Paper Industry*,* 2006. **59**: p. 58.

156   Saratale, G.D., and Oh, S.E., *Lignocellulosics to Ethanol: The Future of the Chemical and Energy Industry.* Afr. J. Biotechnol.*,* 2012. **11**: p. 1002-1013.

157   Schorr, D., Diouf, P.N., and Stevanovic, T., *Evaluation of Industrial Lignins for Biocomposites Production.* Industrial Crops and Products*,* 2014. **52**: p. 65-73.

158   Schwanninger, M., Hinterstoisser, B., Gradinger, C., et al., *Examination of Spruce Wood Biodegraded by Ceriporiopsis Subvermispora Using near and Mid Infrared Spectroscopy.* Journal of near infrared spectroscopy*,* 2005. **12**: p. 397-410.

159   Sella Kapu, N., and Trajano, H.L., *Review of Hemicellulose Hydrolysis in Softwoods and Bamboo.* Biofuels, Bioproducts and Biorefining*,* 2014. p.

160   Sen, S., Sadeghifar, H., and Argyropoulos, D.S., *Kraft Lignin Chain Extension Chemistry Via Propargylation, Oxidative Coupling, and Claisen Rearrangement.* Biomacromolecules*,* 2013. **14**: p. 3399-3408.

161   *Kraft Lignin Chain Extension Chemistry Via Propargylation, Oxidative Coupling, and Claisen Rearrangement.* Biomacromolecules*,* 2013. **14**: p. 3399-3408.

162   Sevastyanova, O., Helander, M., Chowdhury, S., et al., 'Evaluation of Physico-Chemical Properties and Prediction of Spinning Parameters for High-Quality Lignins Produced by Ultra-Filtration of Industrial Kraft Liquor', American Chemical Society, 2013), p. CELL-278.

163   Shalaby, S., Horwitz, B., and Larkov, O., *Structure-Activity Relationships Delineate How the Maize Pathogen Cochliobolus Heterostrophus Uses Aromatic Compounds as Signals and Metabolites.* Mol Plant Microbe Interact*,* 2012. p.

164   Sharma, C., and Kumar, S., *Detection of Chlorophenolics in Effluents from Bleaching Processes of Rice-Straw Pulp.* J. Environ. Monit.*,* 1999. **1**: p. 569-572.

165   Shen, Q., Zhang, T., Zhang, W.-X., et al., *Lignin-Based Activated Carbon Fibers and Controllable Pore Size and Properties.* J. Appl. Polym. Sci.*,* 2011. **121**: p. 989-994.

166   Singh, A.K., Chaudhary, P., Macwan, A.S., et al., *Selective Loss of Lin Genes from Hexachlorocyclohexane-Degrading Pseudomonas Aeruginosa Itrc-5 under*

Different Growth Conditions. Appl. Microbiol. Biotechnol.*,* 2007. **76**: p. 895-901.

167   Sirotkina, M., Lyagin, I., and Efremenko, E., *Hydrolysis of Organophosphorus Pesticides in Soil: New Opportunities with Ecocompatible Immobilized His ₆-Oph.* International Biodeterioration & Biodegradation*,* 2012. **68**: p. 18-23.

168   Sjöström, E., *Wood Chemistry: Fundamentals and Applications*Gulf Professional Publishing, 1993).

169   Sjöström, E., and Alén, R., *Analytical Methods in Wood Chemistry, Pulping, and Papermaking*Springer, 1998).

170   Song, Y.-J., *Characterization of Aromatic Hydrocarbon Degrading Bacteria Isolated from Pine Litter.* Han'guk Misaengmul-Saengmyongkong Hakhoechi*,* 2009. **37**: p. 333-339.

171   Spain, J.C., *Biodegradation of Nitroaromatic Compounds.* Annual Reviews in Microbiology*,* 1995. **49**: p. 523-555.

172   Steinmann, Z.J., Venkatesh, A., Hauck, M., et al., *How to Address Data Gaps in Life Cycle Inventories: A Case Study on Estimating Co2 Emissions from Coal-Fired Electricity Plants on a Global Scale.* Environmental science & technology*,* 2014. p.

173   Sun, R., Sun, X.F., and Xu, X.P., *Effect of Ultrasound on the Physicochemical Properties of Organosolv Lignins from Wheat Straw.* J. Appl. Polym. Sci.*,* 2002. **84**: p. 2512-2522.

174   Tabata, M., Endo, R., Ito, M., et al., *The Lin Genes for Γ-Hexachlorocyclohexane Degradation in Sphingomonas Sp. Mm-1 Proved to Be Dispersed across Multiple Plasmids.* Biosci., Biotechnol., Biochem.*,* 2011. **75**: p. 466-472.

175   Thunga, M., Chen, K., Grewell, D., et al., *Bio-Renewable Precursor Fibers from Lignin/Polylactide Blends for Conversion to Carbon Fibers.* Carbon*,* 2014. **68**: p. 159-166.

176   Tolbert, A., Akinosho, H., Khunsupat, R., et al., *Characterization and Analysis of the Molecular Weight of Lignin for Biorefining Studies.* Biofuels, Bioprod. Biorefin.*,* 2014. p. Ahead of Print.

177   Umeanozie, A.O., Nduka, E.K., and Chukwu, J.O., *Subsidies and the Demand for Petroleum Products in Nigeria.* International Journal of Sustainable Energy and Environmental Research*,* 2014. **3**: p. 100-109.

178   Uraki, Y., *Utilization of Lignin Obtained by Separation of Wood Components.* Kami Pa Gikyoshi*,* 2012. **66**: p. 1120-1125.

179   Viola, E., Zimbardi, F., Cardinale, M., et al., *Processing Cereal Straws by Steam Explosion in a Pilot Plant to Enhance Digestibility in Ruminants.* Bioresour. Technol.*,* 2008. **99**: p. 681-689.

180   Walker, A.W., and Keasling, J.D., *Metabolic Engineering of Pseudomonas Putida for the Utilization of Parathion as a Carbon and Energy Source.* Biotechnol. Bioeng.*,* 2002. **78**: p. 715-721.

181   Wei, Q., Liu, H., Zhang, J.-J., et al., *Characterization of a Para-Nitrophenol Catabolic Cluster in Pseudomonas Sp. Strain Nyz402 and Construction of an Engineered Strain Capable of Simultaneously Mineralizing Both Para-and Ortho-Nitrophenols.* Biodegradation*,* 2010. **21**: p. 575-584.

182   Wells Jr, T., Kosa, M., and Ragauskas, A.J., *Polymerization of Kraft Lignin Via Ultrasonication for High-Molecular-Weight Applications.* Ultrasonics sonochemistry, 2013. p.

183   Wells Jr, T., and Ragauskas, A.J., *Biotechnological Opportunities with the B-Ketoadipate Pathway.* Trends in biotechnology, 2012. **30**: p. 627-637.

184   Wells, T., Jr., and Ragauskas, A.J., *Biotechnological Opportunities with the B-Ketoadipate Pathway.* Trends Biotechnol, 2012. **30**: p. 627-637.

185   Wells, T., Kosa, M., and Ragauskas, A.J., *Polymerization of Kraft Lignin Via Ultrasonication for High-Molecular-Weight Applications.* Ultrason. Sonochem., 2013. **20**: p. 1463-1469.

186   Wells, T., and Ragauskas, A.J., *Biotechnological Opportunities with the B-Ketoadipate Pathway.* Trends Biotechnol., 2012. **30**: p. 627-637.

187   Wells, T., Zhen, W., and Ragauskas, A., *Bioconversion of Lignocellulosic Pretreatment Effluent Via Oleaginous Rhodococcus Opacus Dsm 1069.* Biomass Bioenergy, 2014. p.

188   Willför, S., Sundberg, A., Pranovich, A., et al., *Polysaccharides in Some Industrially Important Hardwood Species.* Wood Science and Technology, 2005. **39**: p. 601-617.

189   Williams, P.A., and Kay, C.M., 'The Catabolism of Aromatic Compounds by Acinetobacter', Caister Academic Press, 2008), p. 99-117.

190   Wise, D.L., *Bioremediation of Contaminated Soils*CRC Press, 2000).

191   Wohlmann, B., and Stuesgen, S., 'Meltable Lignin Derivative for Production of Lignin Derivative Fiber Convertible to Carbon Fiber', Toho Tenax Europe GmbH, Germany . 2013), p. 56pp.

192   Xiong, X., Wang, X., and Chen, S., *Engineering of a Xylose Metabolic Pathway in Rhodococcus Strains.* Appl. Environ. Microbiol., 2012. **78**: p. 5483-5491.

193   Yin, Y., and Zhou, N.-Y., *Characterization of Mnpc, a Hydroquinone Dioxygenase Likely Involved in the Meta-Nitrophenol Degradation by Cupriavidus Necator Jmp134.* Current microbiology, 2010. **61**: p. 471-476.

194   Yoon, Y.-H., Yun, S.-H., Park, S.-H., et al., *Characterization of a New Catechol Branch of the B-Ketoadipate Pathway Induced for Benzoate Degradation in Acinetobacter Lwoffii K24.* Biochem. Biophys. Res. Commun., 2007. **360**: p. 513-519.

195   Yu, X., Zeng, J., Zheng, Y., et al., 'Simultaneous Saccharification and Fermentation of Lignocellulosic Biomass for Single Cell Oil Production by Oleaginous Microorganisms', Washington State University Research Foundation, USA . 2013), p. 34pp.

196   Yuan, T.-Q., He, J., Xu, F., et al., *Fractionation and Physico-Chemical Analysis of Degraded Lignins from the Black Liquor of Eucalyptus Pellita Kp-Aq Pulping.* Polym. Degrad. Stab., 2009. **94**: p. 1142-1150.

197   Zeinali, M., Vossoughi, M., and Ardestani, S.K., *Naphthalene Metabolism in Nocardia Otitidiscaviarum Strain Tsh1, a Moderately Thermophilic Microorganism.* Chemosphere, 2008. **72**: p. 905-909.

198   Zeyaullah, M., Ahmad, R., Naseem, A., et al., *Catechol Biodegradation by Pseudomonas Strain: A Critical Analysis.* Int. J. Chem. Sci., 2009. **7**: p. 2211-2221.

199   Zhang, J., Nieminen, K., Serra, J.A.A., et al., *The Formation of Wood and Its Control.* Current opinion in plant biology, 2014. **17**: p. 56-63.

200   Zhang, J., Xin, Y., Liu, H., et al., *Metabolism-Independent Chemotaxis of Pseudomonas Sp. Strain Wbc-3 toward Aromatic Compounds.* J. Environ. Sci. (Beijing, China), 2008. **20**: p. 1238-1242.

201   *Metabolism-Independent Chemotaxis of Pseudomonas Sp. Strain Wbc-3 toward Aromatic Compounds.* J. Environ. Sci. (Beijing, China), 2008. **20**: p. 1238-1242.

202   Zhang, L., Gellerstedt, G., Ralph, J., et al., *Nmr Studies on the Occurrence of Spirodienone Structures in Lignins.* Journal of Wood Chemistry and Technology, 2006. **26**: p. 65-79.

203   Zhang, S., Sun, W., Xu, L., et al., *Identification of the Para-Nitrophenol Catabolic Pathway, and Characterization of Three Enzymes Involved in the Hydroquinone Pathway, in Pseudomonas Sp. 1-7.* BMC Microbiol, 2012. **12**: p. 27.

204   Zhang, Y.-H.P., *Reviving the Carbohydrate Economy Via Multi-Product Lignocellulose Biorefineries.* Journal of industrial microbiology & biotechnology, 2008. **35**: p. 367-375.

205   Zhao, Z., Gong, Z., and Shen, H., 'Culture Medium for Culturing Oleaginous Microorganisms', Dalian Institute of Chemical Physics, Chinese Academy of Sciences, Peop. Rep. China . 2013), p. 13pp.

206   Zhu, H., Areskogh, D., Helander, M., et al., 'Investigation on Enzymatic Oxidative Polymerization of Technical Soda Lignin', American Chemical Society, 2012), p. CELL-168.

207   Zhu, W., Westman, G., and Theliander, H., *Investigation and Characterization of Lignin Precipitation in the Lignoboost Process.* Journal of Wood Chemistry and Technology, 2014. **34**: p. 77-97.